INFORMATION TO USERS

This manuscript has been reproduced from the microfilm master. UMI films the text directly from the original or copy submitted. Thus, some thesis and dissertation copies are in typewriter face, while others may be from any type of computer printer.

The quality of this reproduction is dependent upon the quality of the copy submitted. Broken or indistinct print, colored or poor quality illustrations and photographs, print bleedthrough, substandard margins, and improper alignment can adversely affect reproduction.

In the unlikely event that the author did not send UMI a complete manuscript and there are missing pages, these will be noted. Also, if unauthorized copyright material had to be removed, a note will indicate the deletion.

Oversize materials (e.g., maps, drawings, charts) are reproduced by sectioning the original, beginning at the upper left-hand corner and continuing from left to right in equal sections with small overlaps.

ProQuest Information and Learning
300 North Zeeb Road, Ann Arbor, MI 48106-1346 USA
800-521-0600

Université d'Ottawa • University of Ottawa

Investigation of the virus-host cell interactions involved in reovirus inclusion formation

Jean Lutamyo Mbisa

Thesis submitted to

The Faculty of Graduate Studies and Research

of

The University of Ottawa

in partial fulfilment of the requirements for the degree of Doctor of Philosophy

Department of Biochemistry, Microbiology and Immunology

Faculty of Medicine

January, 2002

ABSTRACT

Reovirus has a segmented dsRNA genome enclosed in a nonenveloped double capsid shell. Reovirus infection induces the formation of large cytoplasmic inclusions that serve as the major site for viral assembly. These inclusions contain the intermediate filament vimentin, in addition to viral proteins, RNA, mature and immature viral particles. However, the viral or host proteins involved in the formation of reovirus inclusions have not been identified, neither has the mechanism by which viral RNA and proteins are directed to these sites. In this study the reovirus M1 gene, which encodes the minor core protein μ2, was identified as the primary determinant of the rate of inclusion formation. Cellular localization studies of μ2 protein in cells infected with wild-type or *ts* mutants of reovirus as well as in M1 gene-transfected cells showed that μ2 protein may directly be involved in inclusion formation. Expression of μ2 protein in infected cells was shown to be strain-dependent with type 1 strain"Lang" (T1L) producing significantly more μ2 protein than type 3 strain "Dearing" (T3D). Protein stability was demonstrated to be partly responsible for the difference in μ2 protein expression between T1L and T3D, with T1L μ2 being more stable than T3D μ2. Degradation of μ2 protein was shown to occur via the ubiquitin-proteasome pathway (UPP). Ubiquitinated μ2 protein was present in reovirus inclusions together with components of the UPP making reovirus inclusions structurally similar to aggresomes and suggesting that reovirus may be using the UPP and aggresome formation pathway for inclusion formation. In keeping with this theory, it is shown that both reovirus inclusion formation and replication are inhibited when the cellular pool of free ubiquitin (Ub) is depleted by using proteasome inhibitor and that replication may be enhanced by mono-ubiquitination. Interestingly,

the most abundant ubiquitinated μ2 protein species was mono-ubiquitinated μ2 suggesting a role for mono-ubiquitinated μ2 in reovirus inclusion formation and viral assembly. In addition, the amino-terminal end of recombinant μ2 protein, which contains a potential E3 Ub-ligase motif, was shown to be important for protein complex formation. Most importantly reovirus inclusions, like aggresomes, were shown to impair the normal functioning of the UPP resulting in inhibition of Ub-dependent proteolysis which presumably contributes to cytopathology and disease in infected animals. This study is the first to show the use of the UPP in the replication of a nonenveloped or dsRNA virus.

DEDICATION

Dedicated to the memory of

Peter Meya Oniah (1936-1988)

and

Grace Mbisa (1941-2000)

ACKNOWLEDGEMENTS

This wonderful journey would not have been a success without the help of family and friends and I would like to take this opportunity to extend my sincere gratitude to them all. First and foremost to my mentor Dr. Earl Brown for believing in me and giving me the chance to pursue this exciting journey. Thanks for giving me the freedom to explore and yet not being far away to give me guidance when needed. My experience with you, in and out of the lab, will never be forgotten.

To my thesis advisory committee: Dr. Ken Dimock, Dr. Kathy Wright and Dr. Nathalie Chaly, for all the excellent suggestions and encouragement.

To all my co-workers (past and present) in Dr. Brown's lab: Celia Smeenk, Jane Bailly, Bogna Lasia, Kathyrn Slater, Liya Kelita, Laura Chang-Kit, Audrey Brewster, Quan Ngo and Kris Cunningham for creating such a wonderful atmosphere and for all your help.

To all the students and staff (past and present) in the department of BMI: "The Brat Pack" - Franco Pagotto, Stephane Bernatchez, Jason Szeto, Jason Tetro - for all the politically incorrect fun times and technical help; "Office mates" - David Alexander and Neil McKenna - for wonderful conversations and discussions; Sandra Ramirez and Hui Li - for making my lunch palatable; Dianne Sheppard, Julie Normand and Carol Anne Kelly for allowing me to pester you on a regular basis. A few additional words to Franco P., Jason T. and Kris C. - "Man United Forever!!!!!!"

To the many collaborators from whom I have learnt that "if you try to be a Jack of all trades you become a Master of nothing": Dr. T.S. Dermody, M.M. Becker, Dr. D.A. Gray, and

Dr. B. Sherry. Special thanks to Dr. Ken Tyler for assistance with statistical analysis of the reassortant data.

To my brothers and sisters: Jane, Meya, Yvonne and Akene - for your love and support, my only regret is that I have spent so much time away from you guys; The Doves - for welcoming me to Ottawa and making me feel at home; My late Aunt Theresa - for being such an inspiration; "The Outlaws" - The Warry family - for making me feel like one of their own.

My final thanks are reserved for the two most precious people in my life. My wonderful and beautiful wife George "Mavis", your love and support are second to none and I think you deserve a Ph.D. for all your sacrifices in the past five years. I know I don't say it as much but I love you dearly. And to my equally beautiful daughter Asante, you have made the last year a living fairy tale, love you too.

TABLE OF CONTENTS

LIST OF FIGURES

CHAPTER ONE

CHAPTER THREE

CHAPTER FOUR

CHAPTER FIVE

CHAPTER SIX

CHAPTER SEVEN

LIST OF TABLES

CHAPTER ONE

CHAPTER TWO

CHAPTER THREE

CHAPTER FOUR

CHAPTER FIVE

CHAPTER SIX

ABBREVIATIONS

ASFV	African swine fever virus
ATP	Adenosine triphosphate
ATPase	Adenosine triphosphatase
ATP-γ-S	Adenosine 5'-O-(3-thiotriphosphate)
BCIP	5-bromo-4-chloro-3-indolyl phosphate
bp	Base pair
BRAC1	Breast cancer 1 gene
BSA	Bovine serum albumin
cDNA	Complementary DNA
CMV	Cytomegalovirus
CPE	Cytopathic effect
DAPI	4',6-diamidino-2-phenylindole
dH_2O	Distilled water
ddH_2O	Double distilled water
DIC	Differential interference contrast
DNA	Deoxyribonucleic acid
DNase	Deoxyribonuclease
dNTP	Deoxyribonuclease triphosphate
ds	Double-stranded
DTT	Dithiothreitol
FITC	Fluorescein isothiocyanate
EBV	Epstein-Barr virus
EDTA	Ethylenediaminetetraacetic acid
EGF	Epidermal growth factor
EGTA	Ethylene glycol -bis(β-aminoethyl ether)-N,N,N',N'-tetraacetic acid
ER	Endoplasmic reticulum
FBS	Fetal bovine serum

GFP	Green fluorescent protein
HAUSP	Herpes virus-associated ubiquitin-specific protease
HECT	Homologous to the E6-accessory protein carboxy-terminus
HFV	Human Foamy virus
HIV	Human immunodeficiency virus
HPV	Human papilloma virus
Hsp-70	Heat shock protein-70
ISVP	Intermediate or infectious subviral particle
mAb	Monoclonal antibody
MEM	Minimum essential medium
MHC	Major histocompatibility complex
MOI	Multiplicity of infection
mRNA	Messenger RNA
mRNP	Messenger ribonucleoprotein
MTOC	Microtubule organizing center
NBT	Nitro blue tetrazolium
NES	Nuclear export signal
NLS	Nuclear localization signal
NTPase	Nucleotide triphosphatase
PAAP	Protein A-alkaline phosphatase
PBS	Phosphate buffered saline
PC	Proteolysis center
PCR	Polymerase chain reaction
PE	Phycoerythrin
PFU	Plaque forming unit
p.i.	Post-infection
PKR	dsRNA-activated protein kinase
PML	Promyelocytic leukemia
PMSF	Phenylmethylsulfonyl fluoride

PVDF	Polyvinyl diflurobenzene
RING	Really interesting new gene
RIPA	Radioimmunoprecipitation assay
RNA	Ribonucleic acid
RNase	Ribonuclease
RSV	Rous sarcoma virus
RT	Reverse transcription
SDS	Sodium dodecyl sulphate
SDS-PAGE	Sodium dodecyl sulphate-polyacrylamide gel electrophoresis
ss	Single-stranded
SV40	Simian virus-40
T1L	Reovirus type 1 prototype strain "Lang"
T2J	Reovirus type 2 prototype strain "Jones"
T3D	Reovirus type 3 prototype strain "Dearing"
TBS	Tris buffered saline
ts	Temperature-sensitive
Ub	Ubiquitin
UPP	Ubiquitin-proteasome pathway
VSV	Vesicular stomatitis virus
wt	Wild-type

Units

cm^2	Centimeter squared
^0C	Degrees centigrade
h	Hour
kDa	Kilodalton
µCi	Microrcurie
µCi/ml	Microcurie per milliliter
µg	Microgram

µg/ml	Microgram per milliliter
µl	Microliter
µl/ml	Microliter per milliliter
µm	Micrometer
µM	Micromolar
mg/ml	Milligram per milliliter
mM	Millimolar
ml	Milliliter
mm	Millimeter
min	Minute
M	Molar
ng	Nanogram
sec	Second
U	Unit
U/ml	Unit per milliliter
V	Volt
v/v	Volume per unit volume

CHAPTER ONE

GENERAL INTRODUCTION

The end point of a successful viral replication cycle is the assembly of its macromolecules into progeny viral particles. This is achieved by different viruses at a variety of distinct intracellular sites. These sites contain a high concentration of viral macromolecules to ensure efficient production of viral particles. Viruses depend on preexisting host cell intracellular transport and sorting mechanisms to accomplish delivery of their macromolecules to sites of virion assembly, and therefore must possess targeting signals similar to those of host cell components and organelles (reviewed by Hunter, 2001). Since this is achieved at the expense of normal host cell processes, it also usually results in deregulation of cellular metabolism and subsequent cell injury or death which in part is the basis of viral disease (reviewed by Knipe *et al.*, 2001). Understanding events leading to viral assembly would therefore contribute to the knowledge of pathogenic mechanisms of viruses. This might also help identify virus-specific processes that could become targets for anti-viral therapy.

The main aim of this project was to identify the viral and/or host proteins involved in the formation of reovirus inclusions, which are believed to be the major sites of reovirus assembly. Although viral inclusion formation is a common feature of all members of the *Reoviridae*, the viral and host proteins involved in their formation are yet to identified, except for the recruitment of kinky filaments identified as intermediate filaments (Francki and Boccardo, 1983; Sharpe *et*

al., 1982). Reovirus inclusions are synonymous with successful viral replication resulting in cytopathic effect (CPE) and disease in contrast to persistent infection which results in the establishment of a less cytopathic virus-host relationship and no or minor inclusion formation or disease. Identification of the viral and host proteins involved in reovirus inclusion formation would subsequently allow characterization of the mechanism behind their formation.

This chapter will focus on reovirus replication and biology. It also introduces the reader to the biology of intracellular targeting events and interactions of the ubiquitin-proteasome pathway. This pathway is not only involved in intracellular protein and RNA degradation but also plays a role in protein and RNA sorting, as well as in the assembly and maturation of some enveloped RNA and DNA viruses.

1.1 *REOVIRIDAE*

The common distinguishing feature of viruses belonging to the family *Reoviridae* is the possession of a multisegmented double-stranded (ds) RNA genome composed of 10 to 12 segments (reviewed in Nibert and Schiff, 2001). To date, nine recognized genera and more than 150 species make up the family *Reoviridae* (Table 1.1). The genome of *Reoviridae* viruses is enclosed in a nonenveloped icosahedral particle of about 60-85nm in diameter consisting of two to three concentric viral protein capsids. *Reoviridae* viral particles also package enzymes required for the synthesis of viral mRNA including an RNA-dependent RNA polymerase and 5' capping enzymes. The family has a diverse host range that includes some important human (rotavirus, colorado tick fever virus), animal (bluetongue virus), invertebrate (cytoplasmic

polyhedrosis virus) and plant pathogens.

Table 1.1 Genera of *Reoviridae* Family

Genus	No. of gene segments	Host range	Prototype viruses
Orthoreovirus	10	Mammals, birds	Reoviruses 1, 2, and 3; avian reoviruses
Orbivirus	10	Insects - primary host; Mammals - secondary host	Bluetongue virus 1
Rotavirus	11	Mammals	Group A and B human rotavirus; Simian rotavirus SA11
Coltivirus	12	Insects - primary host; Mammals - secondary host	Colorado tick fever virus
Aquareovirus	11	Fish	Golden shiner virus
Cypovirus	10	Insects	Bombyx mori cypovirus 1
Phytoreovirus	12	Plants	Wound tumour virus
Fijivirus	10	Plants; Insects	Fiji disease virus
Oryzavirus	10	Plants	Rice ragged stunt virus

1.2 MAMMALIAN REOVIRUS

Mammalian reovirus, commonly referred to as reovirus, is a prototype of the genus orthoreovirus (reviewed in Nibert and Schiff, 2001). Its genome is made up of 10 segments of dsRNA molecules surrounded by two radially concentric capsid shells. The gene segments are divided into three size classes; 3 large (L), 3 medium (M) and 4 small (S). Each gene segment encodes a single protein with the exception of S1 which is transcriptionally dicistronic and encodes two individual proteins in separate reading frames. Reoviruses were first identified in 1959 and wrongly classified as echoviruses belonging to the *Picornaviridae* family. They were

isolated from human respiratory and enteric tracts and were not associated with any known disease, hence the acronym - ***r***espiratory ***e***nteric ***o***rphan ***viruses***. There are three main serotypes of reovirus namely: type 1 prototype strain "Lang" (T1L) - which was a rectal swab isolate from a healthy child; type 2 prototype strain "Jones" (T2J) - an isolate from a child presenting with a diarrheal illness; and type 3 prototype strains "Dearing" (T3D) and "Abney" (T3A) - which were isolates from children presenting with diarrheal and upper respiratory tract illnesses respectively. The serotypes are morphologically identical and can exchange genome segments by reassortment upon co-infection of a host cell. These viruses can be differentiated by neutralization as well as by hemagglutination-inhibition tests. In addition, homologous genes and proteins can be distinguished by mobility differences on polyacrylamide gels. The different reovirus serotypes and strains also exhibit differing disease phenotypes and biological functions in animal models and cell culture. Cumulatively, this made reovirus one of the first animal viruses used to study the molecular and genetic basis of viral replication and pathogenesis.

The genus orthoreovirus also includes other viruses capable of infecting mammals and birds including isolates from a flying fox (Nelson Bay virus), baboon, python, rattlesnake, wild and domestic birds. A subgroup of these viruses are unusual in that they have a gene encoding a fusion-associated small transmembrane (FAST) protein which induces fusion of infected cells into large multinucleated syncytia (Shmulevitz and Duncan, 2000). Thus orthoreoviruses can be divided further into fusogenic and nonfusogenic groups with mammalian reovirus belonging to the latter group. The role for the atypical fusogenic property in nonenveloped viruses remains unclear.

1.3 THE REOVIRUS PARTICLE AND REOVIRUS PROTEINS

1.3.1 Structure of reovirus particle

First knowledge of the icosahedral structure of the reovirus particle and precise symmetrical arrangement of proteins within the capsids was obtained using negative-stain electron microscopy (Dales *et al.*, 1965; Luftig *et al.*, 1972; Mayor *et al.*, 1965; Vasquez and Tournier, 1962; Khaustov *et al.*, 1987; Metcalf, 1982). This has been improved upon by cryoelectron microscopy, as the structure of the reovirus particle is now known to 27Å resolution (Fig. 1.1; Dryden *et al.*, 1998; Dryden *et al.*, 1993; Metcalf *et al.*, 1991; Reinisch *et al.*, 2000). Eight of the 11 reovirus proteins are contained within the mature virus particle (Table 1.2).

Table 1.2 Reovirus Proteins

Protein	Gene	Mass (kDa)	Copy no./virion	Location in capsid
λ1	L3	137	120	Inner
λ2	L2	144	60	Outer
λ3	L1	142	12	Inner
μ1	M2	76	600	Outer
μ2	M1	83	18	Inner
μNS	M3	80	-	Non-structural
σ1	S1	49	36	Outer
σ1NS	S1	14	-	Non-structural
σ2	S2	47	150	Inner
σ3	S4	41	600	Outer
σNS	S3	41	-	Non-structural

Adapted from Nibert and Schiff, 2001.

Figure 1.1 Structure of the reovirus particle.

CryoElectron microscopy three-dimensional image reconstruction of reovirus particle (A), intermediate subviral particle (ISVP) (B) and core particle (C) viewed down a five-fold axis. (D-F) are cross-sectional diagrams of one five-fold axis region in reovirus particle, ISVP and core respectively. The major outer capsid proteins μ1 and σ3 are coloured blue while the major inner capsid proteins λ1, λ2 and σ2 are coloured green. The putative transcriptase complex made up of λ3, the RNA polymerase, and μ2, the RNA polymerase cofactor, is coluored red and positioned as has been proposed on the inner surface of the five-fold axis (Dryden *et al.*, 1998). The reovirus receptor-binding protein, σ1, is coloured black and is shown in its retracted conformation in the virus particle and in its extended form in ISVP as has been suggested for T1L and T3D strains (Dryden *et al.*, 1993).

(Images in panels A-C created by Stephan Spencer (University of Wisconsin) with IRIS Explorer from three-dimensional CryoElectron Microscopy datasets provided by Timothy S. Baker and colleagues (Purdue University) (Dryden *et al.*, 1993) and were extracted from:

http://www.bocklabs.wisc.edu/cryoEM.html)

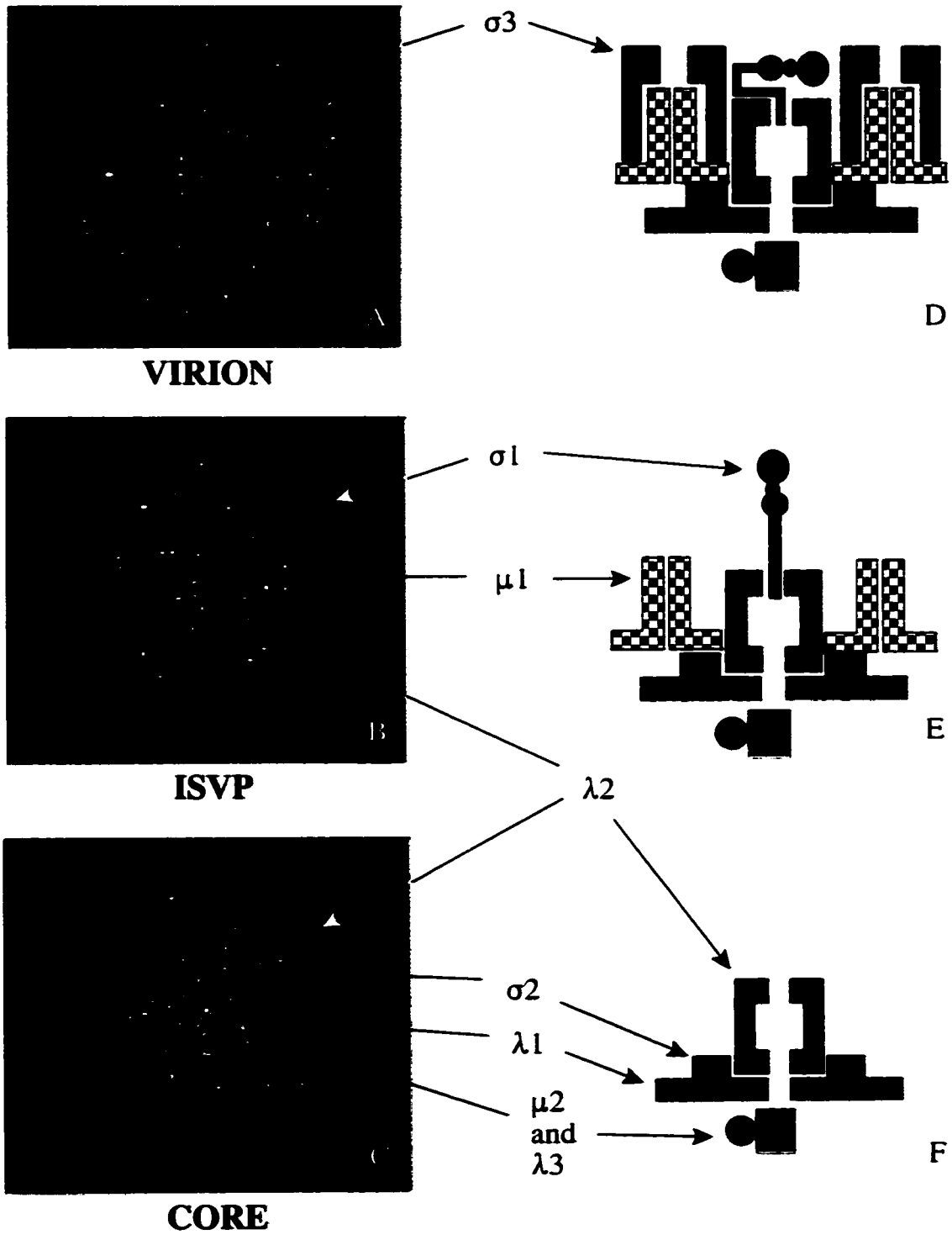
σ3
D
VIRION
σ1
μ1
E
ISVP
λ2
σ2
λ1
μ2
and
λ3
F
CORE

Inner capsid: The inner capsid, also called the core particle, is made up of five proteins namely, λ1, λ2, λ3, σ2, and μ2. These proteins are encoded by the L3, L2, L1, S2, and M1 gene segments respectively (Nibert and Schiff, 2001). There are 120 copies of λ1 protein arranged as dimers on a T=1 icosahedral lattice creating a radially directed channel at the 12 penta-coordinated positions (five-fold axes) with five λ1 dimers surrounding each five-fold axis. The λ1 layer is decorated on the outside by 150 copies of the σ2 protein. A pentamer of λ2 proteins form a turret-like structure surrounding each five-fold axis, creating a tunnel through which nucleotides pass into, and newly synthesized mRNA is extruded from, the core particle. The λ2 pentamers transverse both capsids and are in contact with core and outer capsid proteins in the virus particle. Thus λ2 protein is sometimes considered an outer capsid protein.

The core particle is the transcriptionally active part of the virus and contains a multi-enzyme transcriptase complex composed of at least two core proteins, the λ3 and μ2 proteins. λ3 is thought to be the main catalytic subunit because of its resemblance to other viral polymerases (Morozov, 1989; Bruenn, 1991) and because its expression in isolation elicited a limited poly(C)-dependent poly(G) polymerase activity (Starnes and Joklik, 1993), which also suggests the requirement of other core proteins. λ3 protein has also been shown to determine the pH optimum of the transcriptase (Drayna and Fields, 1982). μ2 protein is suspected of being one of the other core proteins involved in transcription because genetic studies have linked it to controlling the difference in temperature optimum of transcription and, together with λ3, the extent of transcription (Yin *et al.*, 1996). At least one copy each of λ3 and μ2 proteins are thought to be situated at the bottom of the λ2 pentameric vertices projecting inwards at the

fivefold axes. The other core proteins have also been associated with several enzymatic activities required for transcription of the reovirus genomic dsRNA and capping of mRNA. This includes guanyltransferase and methyltransferase activities associated with λ2 (Shatkin *et al.*, 1983; Cleveland *et al.*, 1986; Mao and Joklik, 1991; Seliger *et al.*, 1987), nucleoside triphosphatase (NTPase) activity associated with λ1 and μ2 (Bisaillon *et al.*, 1997; Noble and Nibert, 1997), helicase activity associated with λ1 (Bisaillon *et al.*, 1997) and dsRNA-binding activity associated with λ1, μ2 and σ2 (Lemay and Danis, 1994; Brentano *et al.*, 1998; Dermody *et al.*, 1991).

Outer Capsid: The outer capsid is made up of three proteins namely, μ1, σ3, and σ1 encoded by the M2, S4, and S1 gene segments respectively (Nibert and Schiff, 2001). The outer capsid subunits are arranged in a T=13 left-handed (laevo) skewed lattice made up of 600 molecules of μ1 organized in trimeric complexes creating radially directed channels at penta- and hexa-coordinated positions. The μ1 protein is replaced by the outward protruding λ2 protein pentamers at each of the 12 fivefold axes, with each λ2 protein occupying a space taken up by three μ1 proteins, thereby making a total of 780 molecules which fits the expected number of subunits in a classical T=13 structure (13X60). 600 copies of σ3 protein decorate the μ1 primary lattice with a trimer of σ1 proteins projecting outwards from the capsid at the fivefold axes. The σ1 protein is the hemagglutinin of reovirus and is involved in host cell receptor binding. As such, it is the key determinant of reovirus serotype and also a major player in reovirus infectivity and tropism. Most of the μ1 protein in the virion exists as a proteolytically cleaved fragment, called μ1C, missing 43 aa from the amino-terminal end. The μ1/μ1C polypeptide is thought to play an important role in reovirus penetration of the host cell membrane during virus entry. In addition

to its structural role, σ3 protein affects translation in infected cells. It is thought to achieve this through its ability to bind dsRNA thereby blocking activation of the interferon-induced and dsRNA-activated protein kinase, PKR (Schmechel *et al.*, 1997).

Other viral particle components: Apart from the eight structural proteins and dsRNA genome, the mature reovirus particle also contains oligonucleotides which make up about 25% of the RNA in purified virions and are thought to be products of abortive transcription during late stages of viral assembly. Reovirus particles are not known to contain any cellular proteins.

1.3.2 Nonstructural proteins

Reovirus has three proteins that are involved in the infection process but are not incorporated into the mature, infectious virion that is released from infected cells. These are μNS, σNS and σ1s proteins encoded by the M3, S3 and S1 genes respectively. The first two are present in large amounts in infected cells and are thought to play structural roles during replication and assembly of reovirus and reovirus particles (Antczak and Joklik, 1992; Zweerink *et al.*, 1976). σ1s is dispensable for reovirus growth in cell culture (Rodgers *et al.*, 1998).

1.3.3 Types of reovirus particles

Three main reovirus particles have been identified: these being the mature virion, and two distinct types of subviral particles, the intermediate (or infectious) subviral and core particles (Fig. 1.1). The mature virus particle is the predominant form released during infection and can be transformed into the two subviral particles following partial uncoating *in vivo* and *in vitro*.

These subviral particles play different roles during the reovirus replication cycle. The intermediate subviral particle (ISVP) is generated following the removal of outer capsid protein, σ3 and can directly infect cells by interacting with the lipid bilayer. Additional removal of the remaining core proteins, σ1 and μ1, results in the formation of core particles which are transcriptionally active and can synthesize viral mRNA.

A large proportion of viral particles isolated from infected cells contain markedly reduced quantities of dsRNA gene segments. However, they contain a full complement of viral proteins and have similar morphology to mature virions. They are called top component particles because they are less dense and migrate above mature viral particles in a caesium chloride (CsCl) gradient. They are not precursors of mature virions (Joklik, 1983) and although it is unclear what accounts for their formation they have been useful in the study of viral protein function (Hand annd Tamm, 1973; Lucia-Jandris *et al.*, 1993; Sharpe and Fields, 1981), viral particle morphology (Dryden *et al.*, 1998) and could yet prove useful in the study of viral assembly.

1.4 REOVIRUS M1 GENE

One of the three medium-sized gene segments, M1, encodes the μ2 protein, which is a minor component of the viral core and is believed to be a cofactor of the viral RNA polymerase. The μ2 protein is present in catalytic amounts at about 18 copies per virion (Coombs, 1998a) and is thought to be located on the interior surface of the viral core adjacent to the viral polymerase protein λ3 at the base of the icosahedral five-fold vertices (Fig. 1.1; Dryden *et al.*, 1998). The M1 genes of T1L and T3D are both 2304 nucleotides long and contain a single open reading

frame from nucleotide 14 to 2224 encoding a 736 amino acid long protein (Zou and Brown 1992). T1L and T3D M1 genes are well conserved differing at only 51 nucleotide positions which affect the coding at 10 aa positions, five of which are conservative aa substitutions (Wiener *et al.*, 1989; Zou and Brown 1992).

The 10 amino acid differences must account for the different molecular and biological functions attributed to the T1L and T3D μ2 proteins. Studies using reassortant reoviruses derived from reovirus strains T1L and T3D have demonstrated that the μ2-encoding M1 gene segregates with strain-specific differences in several biological properties including replication in myocardial cells (Matoba *et al.*, 1991), bovine aortic endothelial cells (Matoba *et al.*, 1993), and Madin-Darby canine kidney (MDCK) cells (Rodgers *et al.*, 1997). The M1 gene also segregates with strain-specific differences in the ability of reovirus to cause cytopathology in the liver (Haller *et al.*, 1995), and the heart which correlates with induction and sensitivity of reovirus to interferon (Sherry and Fields, 1989; Baty and Sherry, 1993; Sherry and Blum, 1994; Sherry *et al.*, 1998). Genetic studies employing T2J X T3D reassortants identified the M1 gene in modulating the extent of CPE and plaque size in L929 cells (Moody and Joklik, 1989).

In addition to its role in reovirus growth in cell culture and pathogenesis in mice, the μ2 protein has also been implicated as a cofactor in RNA synthesis. The M1 gene segment segregates with strain-specific differences in the temperature optimum of transcription as well as the extent of viral transcription, in conjunction with the λ3 protein, (Yin *et al.*, 1996). The M1 gene is also a genetic determinant of reovirus core NTPase activity (Noble and Nibert, 1997)

and recombinant μ2 protein binds both single-stranded (ss) and dsRNA (Brentano *et al.*, 1998). The M1 gene *ts* mutant, *tsH11.2*, is defective in dsRNA synthesis, which suggests that the μ2 protein is involved in genome replication (Coombs, 1996).

1.5 REOVIRUS GENETICS

Reovirus is an important viral system used to study the genetic basis of viral replication and pathogenesis. This is due to the segmented nature of its genome which makes it possible to generate genetic reassortants that have novel combinations of gene segments that are useful for studying the function of its individual genes. Reovirus dsRNA genomes can be resolved in polyacrylamide gels where they display unique migration patterns called electropherotypes. Homologous gene segments from two different strains have different characteristic electropherotypes and can be distinguished when run side by side in polyacrylamide gels. This is important because reassortment of gene segments between two different strains can occur upon co-infection of a host cell to produce reassortant progeny reoviruses that contain novel combinations of gene segments from both parents which can be differentiated when resolved in polyacrylamide gels. By using these reassortant reoviruses it is possible to analyze the gene segments involved in a particular phenotype or function if two reovirus strains differ in a given disease phenotype or biological function. Reassortant reoviruses have been used to identify the genetic and molecular basis of reovirus pathogenesis including different aspects of tissue tropism, disease, growth and apoptosis (Weiner *et al.*, 1980; Haller *et al.*, 1995; Sherry and Fields, 1989; Sherry and Blum, 1994; Sherry *et al.*, 1998; Matoba *et al.*, 1991; Matoba *et al.*, 1993; Rodgers *et al.*, 1997; Tyler *et al.*, 1995).

Mutant strains of reovirus are another tool used in the study of reovirus genetics. One such set of mutants that has proven useful and easy to use are the temperature sensitive (*ts*) mutants and were the first utilized to study reovirus genetics (Coombs, 1998). By definition, *ts* mutants are unable to replicate in cells when incubated at a slightly elevated temperature which is usually 39^{0}C or higher. This is in contrast to cold sensitive mutants which are unable to grow when cells are incubated at reduced temperatures. The first reovirus *ts* mutants were isolated after chemical mutagenesis and subsequently more were isolated following serial passage at high multiplicity of infection (MOI) or from persistently infected reovirus cultures. It has been possible to group these mutants by genetic analysis into 10 groups that correspond to each gene segment. Mutants can be grouped by a recombination assay that determines the ability of two different mutants to generate *ts*+ progeny where *ts* viruses of the same group fail to produce *ts*+ progeny. Alternatively, the mutant gene can be directly determined by genetic reassortment analysis using a *ts* mutant from a different strain with a *ts* lesion in another gene. Most of the *ts* mutations have also been mapped and the exact amino acid substitutions determined. The biologic characteristics of prototype *ts* mutants from each group have been characterized and are summarized in Table 1.3. Importantly, the morphology of the viral particles that are formed following infection with these mutants at a nonpermissive temperature have been identified and shed some light on the assembly of reovirus (discussed in detail in section 1.6.2).

Table 1.3 Reovirus temperature-sensitive mutants

Group	Clone	Gene	Protein	Synthesis (%)[a]			Particle morphology[b]
				ssRNA	Protein	dsRNA	
A	*tsA201*	M2	μ1	100	100	100	Normal virions
B	*tsB352*	L2	λ2	25-50	25	25-50	Core-like particles
C	*tsC447*	S2	σ2	5	5-10	0.1	Empty outer shells
D	*tsD357*	L1	λ3	5	10-20	0.1	Empty shells
E	*tsE320*	S3	σNS	5	5-10	1	None
F	*tsF556*	M3[c]	μNS	50-100	50-100	50-100	?
G	*tsG453*	S4	σ3	20	25	15-25	Core-like particles
H	*tsH11.2*	M1	μ2	50-100	1	0.1	None
I	*tsI138*	L3	λ1	ND	50-75	<1	None?
J	*tsJ128*	S1	σ1	ND	ND	ND	?

ND = not determined.
[a] Percentage synthesis of indicated component at nonpermissive temperature compared to synthesis at permissive temperature.
[b] At the nonpermissive temperature.
[c] Assumed, not definitively mapped.
Adapted from Coombs, 1998.

1.6 REOVIRUS REPLICATION AND VIRAL ASSEMBLY

1.6.1 Reovirus replication cycle

The initial step in reovirus infection involves the attachment of the virus to receptors on the cell surface through the virus attachment protein, σ1 (reviewed by Nibert and Schiff, 2001). To date, two distinct cell surface receptors have been described, an α-linked sialic acid which binds to the fibrous tail of T3D σ1 (Chappell *et al.*, 1997, 2000) and junction adhesion molecule (JAM) that binds the globular head of both T1L and T3D σ1 (Barton *et al.*, 2001). The fibrous tail of T1L σ1 binds a cell surface carbohydrate yet to be identified (Chappell *et al.*, 2000). Entry

of the viral particle into the cell is by receptor-mediated endocytosis which delivers the viral particle into vacuoles resembling endosomes and lysosomes. The reovirus particle is partially uncoated in the vacuoles in a pH-dependent process by proteolytic cleavage of μ1/μ1C protein and removal of σ3 protein. The mechanism by which the partially uncoated virus gains access into the cytoplasm is unclear. One possibility is that a fusion-like interaction between μ1, modified by a myristyl group, and the vacuole membrane results in the delivery of the transcriptionally active core particle into the cytoplasm (Nibert *et al.*, 1991). Direct infection of cells by ISVPs is believed to occur in a similar fashion with μ1 interacting with the cell's lipid bilayer. Uncoating of the virus particle to produce cores induces conformational changes in the particle which results in the activation of the transcriptase and the production of full length +ve strand transcripts from the 10 genomic dsRNA segments. The transcription of +ve strand RNA from input viral particles is termed primary transcription and the transcripts are capped and methylated at the 5' end but are not polyadenylated at the 3' end. The +ve strands are extruded from the core particle through channels made up of λ2 pentamers and serve as mRNA for translation of viral proteins. The mRNAs are also assembled into nascent virion particles, together with the newly synthesized viral proteins, and used as templates for replication of genomic dsRNA. The transcriptionally active progeny virions produce more mRNA in a process termed secondary transcription which is the major source of mRNA produced during infection (Skup *et al.*, 1980; Zarbl and Millward, 1983; Watanabe *et al.*, 1968). mRNA from secondary transcription is uncapped and is proposed to be preferentially translated at later times in infection although this remains controversial (Zarbl and Millward, 1983).

1.6.2 Viral assembly

The assembly of reovirus proteins and RNA into progeny viral particles is poorly understood, as is the nature of the protein and nucleoprotein complexes involved. The earliest ssRNA-containing structures termed "assortment" complexes are composed of σNS, μNS, σ3, and possibly μ1, λ1, and λ2 proteins (Antczak and Joklik, 1992). The recruitment of three core structural proteins not identified in assortment complexes, namely μ2 and λ3 (putative transcriptase complex), and σ2 results in the formation of "replicase" particles containing all the viral structural proteins as well as μNS (Zweerink *et al.*, 1976). These particles are transcriptionally active progeny subviral particles that synthesize dsRNA.

Additional knowledge on assembly of reoviruses has been gained from isolation of viral particles from cells infected with different *ts* mutants at the nonpermissive temperature that reveal different blocks in the viral assembly process resulting in the formation of atypical viral particles (Table 1.3). Viral or subviral particles have been isolated from all *ts* mutants except two, *tsE* and *tsH*, which are S3 and M1 gene mutants respectively (Coombs, 1998). This suggests that the σNS and μ2 proteins, the products of the S3 and M1 genes respectively, could play important roles in reovirus assembly. The other *ts* mutants show assembly restrictions resulting in either core-like or empty outer shell-like particles. In general, a *ts* mutation occurring in an outer capsid protein affects the assembly of the outer capsid and results in generation of core-like particles, whilst *ts* mutations in core proteins affect assembly of the core particle and dsRNA genome packaging producing empty double capsid shells or outer shells. This indicates that the two reovirus capsid shells can assemble independently of each other. In fact coexpression of

recombinant reovirus core proteins λ1, λ2, λ3, and σ2 in HeLa cells using vaccinia virus vectors resulted in the assembly of empty core-like particles containing at least λ1 and σ2, and in some cases all four proteins (Xu *et al.*, 1993). This confirms that λ1 and σ2 proteins are the major structural proteins of the reovirus core. Other studies have also shown that reovirus cores can be recoated using recombinant outer capsid proteins suggesting that reovirus assembly could initiate with the packaging of reovirus core proteins and RNA (Chandran *et al.*, 1999; Farsetta *et al.*, 2000). However, the outer capsid proteins have the potential to assemble into outer capsid shells as demonstrated in some *ts* mutants. The assembly of all reovirus structural proteins and RNA into progeny virions, or core proteins and RNA into core-like particles, has never been reported in an *in vitro* system suggesting that this requires a more highly organized and structured mechanism. The complexity of the system is made more daunting when you consider that the virus has to package 10, and only 10, different RNA species, a process requiring an unknown selection mechanism. It has been postulated that the nonstructural proteins, μNS and σNS, which both bind ssRNA, play a significant role in this process (Cross and Fields, 1972; Ito and Joklik, 1972; Mora *et al.*, 1987; Antczak and Joklik, 1992; Morgan and Zweerink, 1975).

1.6.3 Reovirus inclusions

The assembly of reovirus RNA and protein into progeny virion particles in infected cells is believed to occur at distinct cytoplasmic locations called viral inclusions containing a high concentration of reovirus macromolecules which enhances the efficiency of viral assembly. Reovirus inclusions, also termed viral "factories", are not enclosed by any membrane structures and are the primary sites of progeny virion localization, containing paracrystalline arrays of

mature and immature virions (Gomatos *et al.*, 1962; Spendlove *et al.*, 1963; Dales *et al.*, 1965; Fields *et al.*, 1971). Viral proteins and RNA are directed to inclusions that first appear as phase dense granules scattered in the cytoplasm before coalescing around the nucleus later in infection (Sharpe *et al.*, 1982; Gomatos *et al.*, 1962). Reovirus inclusions are detectable by a variety of light and electron microscopic techniques (Zarbl and Millward, 1983). They do not contain any ribosomes indicating that viral protein synthesis occurs outside the inclusions. Therefore, viral mRNA and/or proteins must be transported to and from the perinuclear inclusions to the cytoplasm where viral protein synthesis occurs.

The mechanism by which viral proteins and RNA are directed to the inclusions is unknown. However, it is believed that like other viruses, reovirus uses preexisting cellular transport mechanisms used to convey the cell's contents for the transport of its macromolecules. Knowledge of cellular transport and architecture has tremendously increased in the past two decades. The cell has been shown to have a highly ordered spatial organization and compartmentalization, and is no longer considered as a "bag of soup" with its contents moving around by Brownian diffusion. The cell cytoskeleton is made up of three types of filaments distinguished by their size, namely microtubules (25 nm in diameter), intermediate filaments (8-10 nm) and microfilaments (5-9 nm), which act as structural scaffolding by maintaining the integrity of the cell as well as being "highways" for the transport and anchoring of cellular contents (Kreis and Vale, 1999).

Host cytoskeletal proteins have been shown to play a role in the replication and morphogenesis of a number of viruses including reovirus (Luftig, 1982; Cudmore *et al.*, 1997; Ploubidou and Way, 2001). A number of reovirus proteins including σ1, σ3 and μNS have been shown to interact with the cell cytoskeleton (Babiss *et al.*, 1979; Mora *et al.*, 1987). Reovirus infection of CV-1 cells results in the disruption of the vimentin network, a type III intermediate filament, followed by its reorganization into a fibrous network within the viral inclusions (Sharpe *et al.*, 1982). The virus may be using this reconstituted vimentin filament network for viral replication and assembly. Microtubule and microfilament organization do not appear to be affected. However, microtubules have been shown to be covered with virions and viral proteins (Babiss *et al.*, 1979) and are believed to be involved in viral transport rather than morphogenesis, since colchicine treatment of reovirus infected cells, which depolymerizes microtubules, prevents development of the large perinuclear inclusions (Babiss *et al.*, 1979; Spendlove *et al.*, 1964).

1.7 UBIQUITIN-PROTEASOME PATHWAY AND VIRAL MORPHOGENESIS

1.7.1 Ubiquitin-proteasome pathway

The Ubiquitin-proteasome pathway (UPP) is the principal nonlysosomal system that controls the proteolysis of intracellular proteins. This pathway is complex, tightly regulated and is responsible for the degradation of misfolded, short-lived, regulatory and functionally critical proteins. Unsurprisingly, it has been shown to be important in a variety of cellular processes including DNA repair, cell cycle control, oncogenesis, antigen processing, ribosome biogenesis, transcription, programmed development, cell differentiation, stress response, apoptosis, signaling as well as viral infection (reviewed by Hochstrasser, 1996; Ciechanover, 1998). Protein

degradation by the UPP is a multistep process initiated by the covalent linkage of multiple ubiquitin (Ub) molecules to the target protein, a process called ubiquitination. Ub is a 76 aa heat-stable protein, with a molecular weight of approximately 8.5 kDa. The first Ub molecule is ligated to the target protein by an isopeptide bond between the C-terminal glycine of Ub and the ε-amine of a lysine (K) residue on the target protein. An alternative ubiquitination site to the internal lysine residue on the target protein in which the first Ub is conjugated linearly to the N-terminal residue has been reported for several proteins such as human papilloma virus (HPV) E7 oncoprotein, Epstein Barr Virus Latent Membrane Protein 1 (EBV-LMP1) and the nonviral myogenic transcription factor MyoD (Reinstein *et al.*, 2000; Aviel *et al.*, 2000; Breitschopf *et al.*, 1998). A polyubiquitin chain is then formed by the ligation of additional Ub molecules by covalent linkage of the C-terminal glycine of the new Ub to the ε-amine of K48 of the preceding Ub in successive rounds of ubiquitination. The polyubiquitin chain then acts as a recognition tag that leads to degradation of the tagged protein by the multi-subunit 26S proteasome in an ATP-dependent manner. A minimum of four Ub molecules is required for recognition by the 26S proteasome (reviewed by Pickart, 2000).

1.7.2 Ubiquitination enzymes

The covalent linkage of Ub to the target protein involves three sequential enzymatic reactions and is carried out by three distinct, hierarchical groups of enzymes, namely E1 (Ub-activating enzyme), E2 (Ub-conjugating enzyme) and E3 (Ub-protein ligase) (reviewed by Pickart, 2001). Covalent linkage of Ub to the target protein requires activation of the C-terminal carboxyl group of Ub, a reaction carried out by E1 enzyme in an ATP-dependent manner. It

activates the Ub molecule by linking the Ub C-terminal glycine to a cysteine residue on its active site via a high energy thioester bond. This is followed by the transfer of the activated Ub to any of a number of E2 enzymes in a similar thioester linkage. The E2 enzyme can either transfer the Ub molecule straight onto the target protein or it may require the presence of an E3 enzyme which binds to both the protein target and E2 forming a multiprotein complex. Most species have only a single E1 enzyme, a significant but limited number of E2 enzymes and multiple E3 enzymes. Specificity for protein recognition is therefore provided by the E2 and E3 enzymes, with the highest level of specificity conferred by the E2-E3-protein complex. The E2 and E3 enzymes recognize particular ubiquitination motifs or signals on the protein. All E2 enzymes contain a well conserved core domain approximately 150 aa long containing the active site cysteine residue which forms an intermediate thioester bond with Ub. The core domain is also thought to interact with the E1 enzyme. The N- and C-terminal extensions are not well conserved and are believed to facilitate specific interactions with target proteins or E3 enzymes.

On the other hand, E3 enzymes have two main domains, a protein interaction domain and a catalytic domain. There are numerous protein interaction domains for E3 enzymes, which provide substrate specificity, and they are linked to one of two catalytic domains. The first catalytic domain is called the HECT domain (**H**omologous to the **E**6-accessory protein **C**arboxy-**T**erminus) which is about 350 residues long and contains a conserved cysteine residue that forms an intermediate thioester bond with Ub during catalysis. The best characterized mammalian HECT domain Ub-ligase is E6-AP that forms a complex with the oncogenic HPV E6 protein which, when bound to p53, triggers the ubiquitination and degradation of this protein (Huibregtse

et al., 1991). In yeast the best studied HECT domain Ub-ligase is Rsp5 which is involved in degradation and endocytosis of a number of proteins and recognizes its substrate through its WW (tryptophan) domains (reviewed by Hicke, 1999). The human ortholog of Rsp5 is called Nedd4 and is also involved in ubiquitination and endocytosis of surface proteins such as the amiloride-sensitive sodium channel (EnaC) (reviewed by Staub *et al.*, 2000). The second type of catalytic domain of E3 enzymes is approximately 70 amino acids long and is called the **R**eally **I**nteresting **N**ew **G**ene (RING) finger which features a distinct spacing of cysteine and histidine residues forming two zinc binding domains. Eukaryotic cells contain over 200 RING finger proteins involved in a diverse array of cellular functions (Freemont, 2000; Saurin *et al.*, 1996), and some of them have been demonstrated to have Ub-protein ligase activity. RING finger proteins are often found in complex with other proteins including some that are essential for Ub-ligase activity, such as Skp1-Cullin-1-F-box (SCF) and Anaphase Promoting Complex (APC) or cyclosome, as well as putative ubiquitination protein substrates suggesting that they may act as molecular scaffolds. RING finger proteins shown to have Ub-ligase activity include the protein product from the breast cancer 1 gene (BRAC1) and c-Cbl which is involved in the Ub-dependent down regulation of the epidermal growth factor (EGF) receptor. The promyelocytic leukemia (PML) protein, the main constituent of nuclear domains called PML bodies, is a RING finger protein. However, a direct role for the PML protein in Ub ligation has not been demonstrated even though PML bodies themselves are believed to play a role in degradation of nuclear proteins (discussed in section 1.7.5).

Enzymes also exist for removal of Ub monomers from ubiquitinated proteins. They are called deubiquitinating enzymes (DUBs) or isopeptidases and fall into two classes namely **U**b C-terminal **h**ydrolases (UCHs) and **U**b-specific **p**roteases (UBPs). These enzymes are also responsible for proteolytic cleavage of Ub precursors, which are synthesized in a variety of distinct forms from different genes including a linear head to tail polyubiquitin precursor.

1.7.3 Proteasomes

The 26S proteasome also called the multicatalytic proteinase (MCP) is made up of three main components, the 20S core catalytic complex flanked on both sides by the 19S cap regulatory complexes (reviewed by DeMartino and Slaughter, 1999). The core 20S proteasome is a well conserved structure across all species emphasizing its central importance in all forms of life from the ancient archaebacteria up to humans. The 20S proteasome has a molecular weight of 700 kDa, is cylinder-shaped and consists of a stack of four rings, a pair of β rings in the middle and an α ring on either end. Each α and β ring is composed of seven distinct subunits (α1-7 and β1-7), for a total of 28 subunits, encoded by 14-17 different genes in humans. The multicatalytic protease activity resides within the centrally positioned β1, β2 and β5 subunits and is of three types; "chymotrypsin-like", "tryptic-like" and "post-glutamyl peptidyl hydrolytic-like" activities. The function of the other four β subunits are unknown. The α subunits have no catalytic role but stabilize the two β rings and act as a binding site for the 19S cap regulatory complexes. The 19S cap regulatory complex also known as PA700 is a 20 subunit complex that provides a recognition site for the polyubiquitin chain.

In addition to the 19S cap, the 20S proteasome can associate with a number of other complexes with the resulting multisubunit structures being involved not only in proteolysis but other biological functions. The proteasome activator PA28 or 11S regulator is one such complex which binds on either end of the 20S proteasome forming a structure that, unlike the 26S proteasome, digests only peptides and not ubiquitinated proteins. This structure is involved in the production of antigenic peptides for presentation by class I MHC molecules to T-cell receptors. Interestingly, expression of PA28 subunits is upregulated by γ-interferon, which also upregulates the expression of alternate catalytic β subunits of the 20S proteasome, such as LMP2 and LMP7, that are involved in peptide production (Fruh *et al.*, 1994; Ahn *et al.*, 1995; Realini *et al.*, 1994). The 20S proteasome also associates with mRNA in the non-translated state forming mRNP complexes (reviewed by Scherrer and Bey, 1994). 20S proteasomes that are associated with mRNA are referred to as "prosomes" to distinguish them from proteasomes when its proteinase activity is being addressed. Prosomes have ribonuclease (Petit *et al.*, 1997; Pouch *et al.*, 1995) and proteinase activity (Nothwang *et al.*, 1992) and are usually associated with intermediate and actin filaments suggesting that prosomes are involved in degradation as well as cytodistribution of mRNA (Grossi de Sa *et al.*, 1988; Olink-Coux *et al.*, 1992; De Conto *et al.*, 1997; Arcangeletti *et al.*, 1997). A recent study linked prosomes to cytodistribution of influenza mRNA including transport from the nucleus to the cytoplasm during infection (Arcangeletti *et al.*, 1997).

1.7.4 Proteolysis Centers

Ub-dependent proteolysis in the cytoplasm may occur at a specific, specialized perinuclear site called proteolysis center (PC). The PC is usually in a nuclear indentation in the vicinity of the microtubule organizing center (MTOC), next to the golgi and endoplasmic reticulum (ER) cisternae (Wojcik *et al.*, 1996). PCs contain protein aggregates rich in Ub and proteasomal antigens. Loading of viral antigenic peptides onto MHC class I molecules takes place in the ER and the closeness of the PC to the ER is thought to facilitate the delivery of peptides to MHC class I receptors (Lacaille and Androlewicz, 2000). PCs become more pronounced inclusion bodies when the production of aggregation-prone or misfolded proteins exceeds the cell's capacity to eliminate them or when the 26S proteasome is inhibited causing "cellular indigestion" (reviewed by Kopito and Sitia, 2000; Kopito, 2000). These protein aggregates or inclusion bodies are then called aggresomes. Aggresomes were first described as an accumulation of a misfolded cystic fibrosis transmembrane conductance receptor (CFTR) ΔF508 mutant, the most common cystic fibrosis causing allele, due to overexpression or treatment of cells with proteasome inhibitor (Johnston *et al.*, 1998). The distinguishing feature of aggresomes is the presence of a cage-like structure formed by vimentin which collapses from its normal fibrous cytoplasmic distribution (Johnston *et al.*, 1998). The function of the vimentin cage is unclear but is thought to play a stabilizing structural role. Nonetheless, the idea that vimentin itself might play a role in the formation of aggresomes can not be excluded. Like PCs, aggresomes are enriched in Ub, proteasomal antigens as well as molecular chaperones such as heat shock protein 70 (hsp70) (Johnston *et al.*, 1998; Garcia-Mata *et al.*, 1999; Wigley *et al.*, 1999). However, once formed the aggregates become resistant to proteolysis, in spite of the

presence of proteasomes. The formation of aggresomes is blocked by treatment of cells with drugs that depolymerize microtubules suggesting that aggresome formation is a microtubule-dependent event (Garcia-Mata *et al.*, 1999). The same study went on to show that the transport of aggregated proteins to aggresomes is by a dynein-dependent retrograde transport on microtubules by expression of dynactin protein p50 dynamitin, an inhibitor of dynein, which blocked aggresome formation.

Aggresome-like structures are also a pathological feature of several human diseases. For example, they are found in neurons and glia of individuals suffering from neurodegenerative diseases such as Parkinson's disease and amyotropic lateral sclerosis (ALS), forming what are called lewy and hyaline inclusion bodies respectively (Mayer *et al.*, 1989). The formation of aggresomes in Parkinson's disease and ALS results from the accumulation of abundant cytoplasmic proteins α-synuclein and superoxide dismutase (SOD1) respectively, due to missense mutations in the genes encoding these two proteins (Polymeropoulos *et al.*, 1997; Rosen *et al.*, 1993). It has recently been reported that the formation of aggresomes in these conditions impair the normal functioning of the UPP which results in cellular deregulation and cell death (Bence *et al.*, 2001).

1.7.5 Ub-dependent proteolysis of nuclear proteins

Degradation of nuclear proteins is also achieved by the UPP. PML bodies have been reported to be the equivalent of PCs in the nucleus. A mutated form of the influenza virus nucleoprotein (NP) that misfolds accumulates in PML bodies and MTOC resulting in its rapid

degradation by proteasomes that are recruited to both structures (Anton *et al.*, 1999). Interestingly, the treatment of cells not expressing the mutant NP protein with proteasome inhibitors resulted in the accumulation of proteasomal antigens and molecular chaperones at PML bodies and MTOC suggesting that both locations serve as proteasomal degradation sites. Similarly, examples of nuclear aggresome formation in neurodegenerative diseases exist, such as spinocerebellar ataxia type I, in which aggresome formation results from the accumulation of mutant ataxin-1 protein (Skinner *et al.*, 1997). These nuclear aggregates also contain PML, Ub, proteasomal antigens and molecular chaperones (Skinner *et al.*, 1997; Cummings *et al.*, 1998). The PML body is also dynamically associated with other UPP factors such as the herpes virus-associated Ub-specific protease (HAUSP) (Everett *et al.*, 1997).

PML bodies are proposed to also perform nonproteolytic functions although this remains controversial. They have been reported to function in transcription because they contain transcription factors and possibly RNA, while others hypothesize that they serve as storage depots for nuclear proteins until they are required for their respective functions (Hodges et al., 1998; Negorev and Maul, 2001). It has also been postulated that PML bodies play a role in anti-viral defence because a number of PML body-associated proteins are interferon-inducible. In addition PML bodies are targeted by a number of viral proteins during infection including the herpes simplex virus (HSV) regulatory protein ICP0 which has a RING finger and binds to HAUSP (Everett *et al.*, 1997), resulting in the disruption of PML body morphology. Other DNA and RNA viruses that alter or disrupt PML body architecture or encode proteins that translocate to PML bodies include adenovirus (Doucas *et al.*, 1996; Puvion-Dutilleul *et al.*, 1995). EBV

(Szekely *et al.*, 1996), cytomegalovirus (CMV) (Kelly *et al.*, 1995), hepatitis delta virus (Bell *et al.*, 2000) and arenaviruses (Borden *et al.*, 1998). The PML protein itself has been shown to inhibit influenza virus, vesicular stomatitis virus (VSV) and Human Foamy virus (HFV) replication (Chelbi-Alix *et al.*, 1998; Regad *et al.*, 2001). This suggests that the PML body and the UPP play important roles in viral replication.

1.7.6 Nonproteolytic roles of ubiquitination

Accumulating evidence shows that modification of proteins by Ub conjugation performs other roles apart from protein degradation. The best studied of these is the conjugation by a single Ub monomer called mono-ubiquitination (reviewed by Hicke, 2001). Mono-ubiquitination has been shown to be involved in the endocytosis of receptors and surface proteins following conjugation of Ub to their cytoplasmic tails. For example, following activation of the EGF receptor at the plasma membrane, the c-Cbl Ub-ligase associates and mono-ubiquitinates the EGF receptor cytoplasmic tail leading to its down regulation and degradation in lysosomes (Ettenberg *et al.*, 2001; de Melker *et al.*, 2001). Recent studies also suggest that mono-ubiquitination could be involved in subcellular localization and sorting of proteins. It has been shown that Ub modification resulting in down regulation of receptors is coupled with protein sorting in the multivesicular body pathway (Katzmann *et al.*, 2001). In addition, the Fanconi anaemia protein FANCD2 is mono-ubiquitinated following DNA damage, and is subsequently targeted to nuclear foci where it interacts with BRAC1 protein which is involved in DNA repair (Garcia-Higuera *et al.*, 2001). Mono-ubiquitination also plays important roles in histone

regulation and the budding of some enveloped viruses (Hicke, 2001). Polyubiquitination chains can also be made through other Ub lysine residues, in addition to K48. Ubiquitination *in vivo* can proceed via four of the seven lysine residues present in Ub, these being K11, K29, K48 and K63. The formation of a polyubiquitin chain via K63 has been shown to be involved in DNA repair and not proteolysis (Dubiel and Gordon, 1999). Functions for the polyubiquitin chains linked via K11 and K29 have not been demonstrated yet.

1.7.7 Role of UPP in viral morphogenesis

Evidently, the UPP plays a critical role in cellular metabolism and it is therefore not surprising that recent studies have linked it to the replication, assembly and budding of a number of viruses.

Enveloped RNA viruses: Ub has been shown to function during budding of enveloped retroviruses such as Rous sarcoma virus (RSV) and Human immunodeficiency virus (HIV). The Gag polyproteins of the two viruses are structurally involved in virus assembly and undergo ubiquitination (Ott *et al.*, 1998; Putterman *et al.*, 1990). Virus budding is inhibited at a late stage in RSV- or HIV-infected cells following treatment with proteasome inhibitors which reduce the levels of the cellular pool of free Ub molecules (Schubert *et al.*, 2000; Patnaik *et al.*, 2000). Regions within Gag polyproteins called late assembly (L) domains are required for the efficient separation of assembled virions from host cell plasma membrane. Recent evidence shows that the L domains achieve this through the recruitment of a Ub-ligase activity (Strack *et al.*, 2000). L domains contain a proline-rich motif which interacts with specific WW domains of the Nedd4

Ub-ligase family. Similarly, the VSV and rabies matrix (M) proteins, and VP40 protein, the putative matrix protein of Ebola virus, all possess similar proline-rich motifs which have been demonstrated to interact with Nedd4 Ub-ligases (Craven *et al.*, 1999; Harty *et al.*, 1999; Harty *et al.*, 2000; Harty *et al.*, 2001). All three proteins are involved in the budding stages of their respective viruses. It has been postulated that these viruses are using the endocytosis-promoting activity of Ub to accomplish their budding process. Furthermore, the presence of ubiquitinated Gag, as well as free Ub, has been demonstrated in mature virions of some retroviruses (Ott *et al.*, 1998; Putterman *et al.*, 1990).

Enveloped DNA Viruses: The assembly of large cytoplasmic DNA viruses such as poxviruses, iridoviruses and African swine fever virus (ASFV) is similar to that of reovirus in that it occurs at distinct cytoplasmic inclusion bodies. These inclusion bodies contain all the components required for viral assembly including viral proteins, DNA and amorphous cellular membranous material. Recently they have been compared to aggresomes not only structurally but also because of their mode of formation (Heath *et al.*, 2001). Both complexes have been shown to have a perinuclear location and to be situated in the vicinity of the MTOC. They both recruit mitochondria and cellular chaperones such as hsp70 and their formation results in the rearrangement of the intermediate filament, vimentin, which collapses into a characteristic cage around both complexes. The formation of both structures also requires a functional retrograde microtubule transport system dependent on dynein/dynactin motors. Given these similarities it has been proposed that assembly of these viruses exploits the aggresome formation pathway to concentrate their structural proteins at sites of viral assembly. To date, the UPP has never been

shown to play a role in the replication, assembly or morphogenesis of nonenveloped or dsRNA viruses such as reovirus.

1.8 GOALS OF THE PROJECT

1.8.1 Relevance of the project

The project has the potential to make contributions in three main areas:

1. The knowledge gained from this study will contribute to the understanding of reovirus pathogenesis and morphogenesis, thereby helping to identify new and novel therapeutic targets for dsRNA-containing viruses. This includes important human pathogens such as rotavirus which is the most common cause of severe diarrhoea worldwide and a major cause of mortality in the developing world. Rotavirus accounts for up to one million deaths each year which is approximately 25% of all deaths attributed to diarrhoea illnesses and 6% of all deaths among children under five years of age (Cook *et al.*, 1990).
2. Because of its segmented genome, diverse cell tropism and no apparent link to any significant disease, reovirus has the potential for development into an expression vector for *in vitro* expression of foreign genes or for gene therapy. Preliminary work in our laboratory was unsuccessful in introducing a foreign gene into reovirus. It was therefore postulated that a better understanding of events leading to assembly of reovirus RNA and protein into progeny viral particles would help in this endeavour. The recent introduction of a chloramphenicol acetyl transferase (CAT) gene into reovirus has given credence to the idea that reovirus could be used as an expression vector (Roner and Joklik, 2001).

3. It has long been known that reovirus grows better in transformed and tumour cell lines compared to normal cells (Hashiro *et al.*, 1977; Duncan *et al.*, 1978). This has led to the development of reovirus as an oncolytic agent and is now in clinical trials as an anti-cancer agent in humans (Coffey *et al.*, 1998; Norman and Lee, 2000; Wilcox *et al.*, 2001). The molecular basis of reovirus oncolysis is believed to stem from the activation of the Ras signaling pathway in tumour and transformed cell lines (Strong *et al.*, 1998). This inhibits the phosphorylation of the dsRNA-activated protein kinase, PKR. Phosphorylation of PKR results in the inhibition of protein translation and therefore inhibition of viral growth. However, it is also possible that conditions in tumour and transformed cell lines are favourable for other aspects of reovirus replication and morphogenesis, such as inclusion formation, resulting in the killing of host cells. Therefore, this study may also contribute to the understanding of the nature and basis of reovirus oncolysis which would result in the design of better reovirus-based anticancer therapies.

1.8.2 Hypothesis

Two different studies have shown that reovirus T1L and T3D form inclusions at different rates. Rhim *et al.*, (1962) observed that T1L-infected monkey kidney epithelial cells require 54 hours for inclusions to form in 75% of cells while Gomatos *et al.*, (1962) report that it took 17 hours for maximal inclusion formation in T3D-infected L929 cells. It is therefore hypothesized that by using T1L X T3D reassortant reoviruses it should be possible to identify the gene(s) involved in determining the rate of viral inclusion formation using the technique of indirect

immunofluorescence. It is further hypothesized that characterizing the biology and function of the protein(s) encoded by the identified gene(s) using immunological and molecular techniques will provide insight into host proteins involved as well as the mechanism behind reovirus inclusion formation. In summary, the goals of the project are as follows:

1. Identification of the viral protein(s) involved in the rate of reovirus inclusion formation using reassortant and *ts* mutant reoviruses.
2. Characterization of the biology, expression and interactions with host proteins of the viral protein(s) involved in the rate of inclusion formation.
3. Having identified viral and host proteins involved in reovirus inclusion formation, characterize the mechanism behind the formation of these structures.

CHAPTER TWO

GENERAL MATERIALS AND METHODS

2.1 Cells and viruses

Mouse fibroblast L929 cells, Human cervical carcinoma HeLa cells, African green monkey kidney Cos-1 cells and monkey kidney CV-1 cells were propagated in adherent culture in minimum essential medium (MEM) (Gibco BRL Life Technologies, Burlington, ON) supplemented to contain 5% VSP neonate bovine serum (Biocell Laboratories, Carson, CA), 2 mM glutamine, 100 U/ml penicillin and 100 μg/ml streptomycin sulfate. Reovirus strains T1L and T3D were laboratory stocks initially obtained from B.N. Fields. The *ts* mutants, *tsC447*, *tsG453*, and *tsH11.2* were provided by K. Coombs (University of Manitoba). The T1L X T3D reassortant viruses were produced previously (Brown *et al.*, 1983). All reoviruses were passaged in adherent L929 cells (~5×10^7 plaque-forming units (PFU)/25 cm^2 culture) and released by three freeze-thaw cycles. The recombinant vaccinia virus vTF7.3 that expresses the T7 RNA polymerase was a kind gift from K. Dimock (University of Ottawa) and was grown in CV-1 cells. 150 μl of vaccinia virus stock was trypsinized by adding 2.35 ml of MEM (without FBS) and 250 μl of 0.5% trypsin followed by incubation at 37°C for 15 min. The sample was then used to infect one T75 flask for 1 h and the media was changed to MEM plus FBS and incubated till CPE was pronounced (48 to 72 h). The vaccinia virus was harvested by centrifugation (300g for 5 min) and the pellet was resuspended in MEM without FBS (2.5 ml for each T75 flask). The virus was released by three freeze-thaw cycles and sonication. Reoviruses and vaccinia virus were

titrated by plaque assay in L929 cells as described previously (Zou and Brown, 1992).

2.2 Antibodies

The primary antibodies used in this study are listed in Table 2.1. Prior to use for indirect

Table 2.1 Primary antibodies

Antibody	Source	Working dilution
Rabbit anti-T1L	E.G. Brown	1:1000 (IB)[a]; 1:500 (IF)[b]
Rabbit anti-T3D	E.G. Brown	1:1000 (IB); 1:500 (IF)
Rabbit anti-T1L μ2	E.G. Brown	1:1000 (IB); 1:500 (IF)
Rabbit anti-T1L μ2	M. Nibert (Harvard University, MA)	
Rabbit anti-σNS	T.S. Dermody (Vanderbilt University, TN)	1:1000 (IB); 1:500 (IF)
monoclonal anti-μ1/μ1C protein (clone 8H6)	T.S. Dermody (Vanderbilt University, TN)	10 μg/ml (IF)
monoclonal anti-σNS protein (clone 3E10)	T.S. Dermody (Vanderbilt University, TN)	10 μg/ml (IF)
monoclonal anti-α-tubulin (clone B-5-1-2)	Sigma, St. Louis, MO	1:2000 (IF)
monoclonal anti-β-tubulin (clone DM1B)	Amersham, Baie d'Urfe, Que	1:1000 (IB)
Goat anti-vimentin	P. Traub (Max-Planck-Institut fur Zellbiologie, Germany)	1:1500 (IF)
Goat anti-vimentin	Sigma, St. Louis, MO	1:40 (IF)
Rabbit anti-ubiquitin	DAKO diagnostics, Mississauga, ON	1:600 (IB); 1:100 (IF)
Rabbit anti-20S proteasome	Calbiochem-Novabiochem Corp., San Diego, CA.	1:10000 (IB); 1:100 (IF)
monoclonal anti-heat shock protein 70 (clone BRM-22)	Sigma, St. Louis, MO	1:100 (IF)
monoclonal anti-γ-tubulin (clone GTU-88)	Sigma, St. Louis, MO	1:100 (IF)

[a] immunoblot
[b] immunofluorescence

immunofluorescence the rabbit polyclonal against T1L, T3D or μ2 protein were adsorbed to acetone-fixed L929 or HeLa cell extract to block unspecific binding to host cell proteins.

Secondary antibodies used were FITC-conjugated goat anti-rabbit IgG (Sigma); FITC-conjugated donkey anti-goat, Cy3-conjugated donkey anti-rabbit and Cy3-conjugated donkey anti-mouse (Jackson ImmunoResearch Laboratories, Inc., West Grove, PA). The dsDNA-specific fluorescent dyes 4',6-diamidino-2-phenylindole (DAPI) (Sigma) and pico green (Molecular Probes, Inc., Eugene, OR) were used to detect the nucleus at dilutions of 1 μg/ml and 2 μg/ml respectively. Protein A conjugated to alkaline phosphatase (PAAP) and goat anti-rabbit conjugated to alkaline phosphatase were obtained from Sigma.

2.3 Indirect Immunofluorescence

L929 or HeLa cells seeded on 22x22 mm glass coverslips (Corning Inc., Big Flats, NY) in 6 well plates were either mock-infected or infected with reovirus at an MOI of 10 PFU/cell. Prior to staining, the cells were fixed in prechilled acetone for 5 min. After rinsing in PBS (3 x 5 min), 90μl of an appropriate dilution of primary antibody was applied and incubated in a humidified chamber at room temperature for 30 min. The coverslips were then rinsed in PBS (3 x 5 min) and reacted with the appropriate dilution of a fluorophore-conjugated secondary antibody. After another 30 min incubation period at room temperature the coverslips were rinsed in PBS (3 x 5 min). For double immunolabeling the cells were similarly reacted with the second primary and secondary antibodies. After the last PBS rinse the cells were incubated with DAPI for 2 min and rinsed in PBS (2 x 5 min) and once in ddH_2O, and mounted on glass slides in

Gel/Mount (Biomeda Corp., Foster City, CA) or ProLong Antifade (Molecular Probes). All antibody dilutions were done in PBS/3%BSA. The samples were visualized using a Zeiss microscope equipped with epifluorescence and a 63X or 100X, 1.40 NA PlanApo objective. The images were collected using Image One Metamorph software (Universal Imaging Corporation, West Chester, PA) and a Hamamatsu chilled charge-coupled digital camera (model C5985) (Hamamatsu Corporation, Bridgewater, NJ). Confocal microscope images were captured using a Zeiss confocal fluorescence microscope (Carl Zeiss, New York, NY), and the images were processed and coloured using Adobe Photoshop (Adope Systems, Inc., San Jose, CA) or Image Tool (University of Texas, San Antonio, TX).

2.4 Immunoblotting

Infected or transfected cell monolayers were lysed in SDS sample buffer (62.5 mM Tris-HCl pH 6.8, 10% glycerol, 2% SDS, 0.05% bromophenol blue and 5% 2-mercaptoethanol (2-ME) freshly added). The proteins were separated by sodium dodecyl sulphate-polyacrylamide gel electrophoresis (SDS-PAGE) (Laemmli, 1970) and electroblotted on to PVDF membrane (Immobilon-P, Millipore Corp., Mississauga, ON) at 25V overnight at 4°C. The dried membrane was blocked with 5% skim milk in PBS for 1 h at RT. This was followed by the addition of primary antibody in fresh milk and incubation for 2 h at 4°C. The membrane was then washed three times in PBS and once in TBS (150 mM NaCl, 50 mM Tris-HCl pH 7.5) to remove phosphate and incubated in 5% milk in TBS containing 1 μg/ml PAAP. Finally the membrane was washed 4X in TBS before reaction with chromogenic substrate, nitro blue tetrazolium (NBT) (33 μl/ml) plus 5-bromo-4-chloro-3-indolyl phosphate (BCIP) (3.3 μl/ml), in alkaline

phosphatase buffer (100 mM NaCl, 5 mM $MgCl_2$ and 100 mM Tris-HCl pH 9.5). If the blot was to be reacted with the phosphofluorescent reagent Attophos™ (Promega, Madison, WI), the blocking was done in Casein blocking buffer (0.5% Hammerstein casein, 0.1% Tween 20, 0.01% sodium azide in TBS) and the washes (3 x 10 min) were done in Casein wash buffer (0.1% Hammerstein casein, 0.01% Tween 20, 0.01% sodium azide in TBS), with all the reactions performed at room temperature. The blot was then reacted with Attophos reagent on a clean overhead acetate sheet. The blot was visualized using a Storm 860 PhosphoImager equipped with ImageQuant software (Molecular Dynamics, Sunnyvale, CA) or AlphaImager™ 1220 Documentation and Analysis System (Alpha Innotech Corp., San Leandro, CA). For quantification purposes known amounts of appropriate reference protein were run in parallel to ensure that the readings were within the linear range of analysis by the phosphoimager.

2.5 Transfection

L929, HeLa or Cos-1 cells were seeded in 6 well plates for immunoblot analysis or in 6 well plates containing 22x22 mm glass coverslips (Corning) for immunofluorescent staining. The cells were transfected with DNA using either lipofectin reagent (Gibco-BRL) or Effectene (Qiagen Inc., Mississauga, ON) when they were at 80-85% confluence using the manufacturer's protocol. For lipofectin reagent, 5μg of DNA and 15μl of lipofectin and 1 ml MEM without FBS were used for each transfection reaction. After a 5 h incubation period the cells were infected with the recombinant vaccinia virus vTF7.3, at an MOI of 0.5 to 1 followed by incubation in complete MEM. For Effectene reagent, 1 μg of DNA, 100 μl Buffer EC, 6.4 μl of Enhancer and 8 μl of Effectene were used for each transfection reaction in complete MEM. After 2 to 3 h

incubation the cells were infected with recombinant vaccinia virus as for lipofectin reagent. The cells were then incubated for 24 or 48 h before immunofluorescent staining or immunoblot analysis as described above. No vaccinia virus was used if Cos-1 cells were transfected with pcDNA3 constructs since they can drive transcription through the mammalian CMV promoter and have an SV40 origin of replication for replication of plasmid to high copy number.

2.6 Screening and preparation of plasmid DNA

The boiling method (Holmes and Quigley, 1981) was used for small scale plasmid DNA preparation (minipreps). Single colonies from LB plates or frozen bacterial stock were picked into 2 ml LB broth cultures (1% tryptone, 0.5% yeast extract and 0.5% NaCl plus 200 μg Ampicillin) and grown overnight at 37°C. 1.5 ml of the culture was decanted into a microfuge tube and centrifuged at 12000g for 30 sec at 4°C. The bacterial pellet was resuspended in 350 μl of STET (0.1 M NaCl, 10 mM Tris-HCl pH 8.0, 1 mM EDTA pH 8.0 and 5% Triton X-100) followed by addition of 5 μl of lysozyme at 50 mg/ml in Tris-HCl pH 8.0. Samples were mixed by vortexing for 3 sec and boiled for 40 sec in a boiling water bath followed by centrifugation at 12000g for 10 min at room temperature. The pellet of bacterial debris was removed using a sterile toothpick and the DNA was precipitated with 40 μl of 2.5 M sodium acetate (pH 5.2) and 420 μl of isopropanol. The sample was mixed by vortexing and stored at room temperature for 5 min followed by recovery of the DNA pellet by centrifugation at 12000g for 5 min at 4°C. The DNA pellet was rinsed once in 1 ml 70% ethanol, dried and resuspended in 50 μl TE (pH 7.6) containing DNase-free pancreatic RNase (20 μg/ml) and could be analyzed on agarose gel immediately or stored at -20°C.

For medium-scale DNA preparation (midipreps), the Wizard *Plus* Midipreps DNA purification system from Promega was used according to manufacturer's protocol. Between 200 to 300 μg of plasmid DNA could be obtained from 100 ml of an overnight bacterial culture. The amount of DNA obtained was quantified by spectrophotometry (1 OD_{260} = 50 μg/ml of dsDNA) and the DNA was stored at -20°C.

2.7 Cell fractionation

Infected or transfected cell monolayers were washed with cold PBS, lysed in lysing buffer (10 mM Pipes, pH6.8, 100 mM NaCl, 300 mM sucrose, 3 mM $MgCl_2$, 1 mM EGTA, 4 mM vanadyl riboside complex, 0.5% Triton X-100, and 1.2 mM Phenylmethylsulfonyl fluoride (PMSF) freshly added) for 5 min at 4°C and scraped into microfuge tube. To collect the cytoplasmic and nuclear fractions, a modification of the procedure described by He *et al* (1990) was used. Briefly, the samples were centrifuged (600g for 3 min at 4°C) and the supernatant was decanted (cytoplasmic fraction), and the pellet was rinsed with RSB buffer (10 mM Tris pH 7.4, 10 mM NaCl, 1.5 mM $MgCl_2$ and 1 mM PMSF) and resuspended in SDS sample buffer (nuclear fraction). The samples were then separated by SDS-PAGE and electroblotted on to a PVDF membrane before immunoblotting as described above.

CHAPTER THREE

REOVIRUS M1 GENE DETERMINES STRAIN-SPECIFIC DIFFERENCES IN THE RATE OF VIRAL INCLUSION FORMATION IN L929 CELLS

3.1 Introduction

In association with the production of nucleic acid and protein, reovirus infection of permissive cells involves the reorganization of cellular architecture to generate sites that facilitate viral assembly. All members of the *Reoviridae* induce cytoplasmic inclusions (Francki and Boccardo, 1983) that contain fibrillar constituents. In the case of orthoreoviruses, these filamentous structures have been identified as intermediate filament proteins (Sharpe *et al.*, 1982). Insect reoviruses (cypoviruses) encode a polyhedrin protein that forms the matrix of inclusions (Payne and Mertens, 1983). However, viral proteins that mediate inclusion formation have not been identified for vertebrate reoviruses.

Experiments were conducted to identify the genetic basis for inclusion formation in reovirus. Although inclusion formation is a hallmark of productive reovirus infection it has not been addressed as a defined molecular process that is controlled by viral and cellular components. Following the observation that T1L and T3D differ in the rate of viral inclusion formation, reassortant reoviruses were used to identify viral genes that control this phenotype. The M1 gene encoding the μ2 protein was identified as the primary determinant in the rate of inclusion formation with a secondary role for the S3 gene encoding the nonstructural protein, σNS. The

cellular localization of μ2 protein was monitored by fluorescent microscopy in cells infected with wild type (wt) or *ts* mutants as well as M1 gene-transfected cells. The results suggest that the μ2 protein plays a crucial role in formation of reovirus inclusions, perhaps indirectly by influencing the rate of RNA synthesis or by directly being involved in the process of inclusion formation and viral assembly.

3.2 Materials and Methods

3.2.1 Transfections and plasmid constructs

All transfections in this chapter were carried out using lipofectin as described in section 2.5. The M1 DNA constructs used were pCMV-M1CN (clones T1-7 and T3-13) and pGEM-M1 (clones T1-7 and T3-18) both under control of a bacteriophage T7 RNA polymerase promoter (Zou and Brown, 1996b).

3.2.2 Statistical analyses

The association of reovirus gene segments with the rate of inclusion formation was determined by using *t* test (parametric) and Mann-Whitney (MW) test (non-parametric) statistical techniques. The contributions of individual genes was analyzed further by parametric linear regression. Stepwise linear regression analysis was performed for all combinations of genes found to be statistically significant. Statistical analyses were performed by using the Minitab (release 8) statistical software package (Addison-Wesley, Reading, MA).

3.3 Results

3.3.1 Reovirus exhibits strain-specific differences in the rate of inclusion formation in L929 cells

To determine whether T1L and T3D differ in kinetics of inclusion formation in L929 cells, indirect immunofluorescence was used to assess the relative proportion of antigen-positive cells that formed cytoplasmic inclusions. Cells were infected with either T1L or T3D at an MOI of 10 PFU/cell. The cells were then fixed in acetone at varying times after infection and stained with strain-specific rabbit antisera followed by Cy3-conjugated donkey anti-rabbit. Viral inclusions were seen as local concentrated areas of staining within the cytoplasm relative to generalized cytoplasmic staining (Fig. 3.1 A, thin and heavy arrows, respectively). Cells showing intermediate staining patterns were scored as inclusion-negative. Immunofluorescent staining showed that viral antigen was diffusely distributed in the cytoplasm in the majority of T1L-infected cells at 12 and 24 hours (h) post infection (p.i.) but was seen to localize into inclusions by 48 h p.i. (Fig. 3.1 A, C, and Table 3.1). In contrast, inclusion formation in T3D-

Table 3.1 Rate of inclusion formation in T1L- or T3D-infected L929 cells

Time post-infection	Percent Inclusions[a]	
(hours)	T1L (n)[b]	T3D (n)
15	4 ± 2 (328)	46 ± 2 (35)
20	7 ± 8 (79)	67 ± 15 (37)
24	11 ± 9 (219)	66 ± 4 (84)
48	63 ± 10 (251)	nd

[a] average of 2 to 3 experiments
[b] n = number of antigen-positive cells counted.
nd = not done

Figure 3.1 Cellular localization of reovirus proteins in infected cells showing the difference in the rate of inclusion formation between reovirus T1L and T3D.

L929 cells were either infected with T1L and labeled with rabbit anti-T1L antiserum at 24 (A) and 48 (C) h p.i., or with T3D and labeled with rabbit anti-T3D antiserum at 24 (B) and 48 (D) h p.i. Infections were done at an MOI of 10 PFU/cell. The secondary antibody used was Cy3-conjugated donkey anti-rabbit. Images were obtained using an epifluorescence microscope. An antigen-positive cell without inclusions is indicated with a heavy arrow and a cell with inclusions is indicated with a thin arrow in panel (A). The bar represents 10 μm.

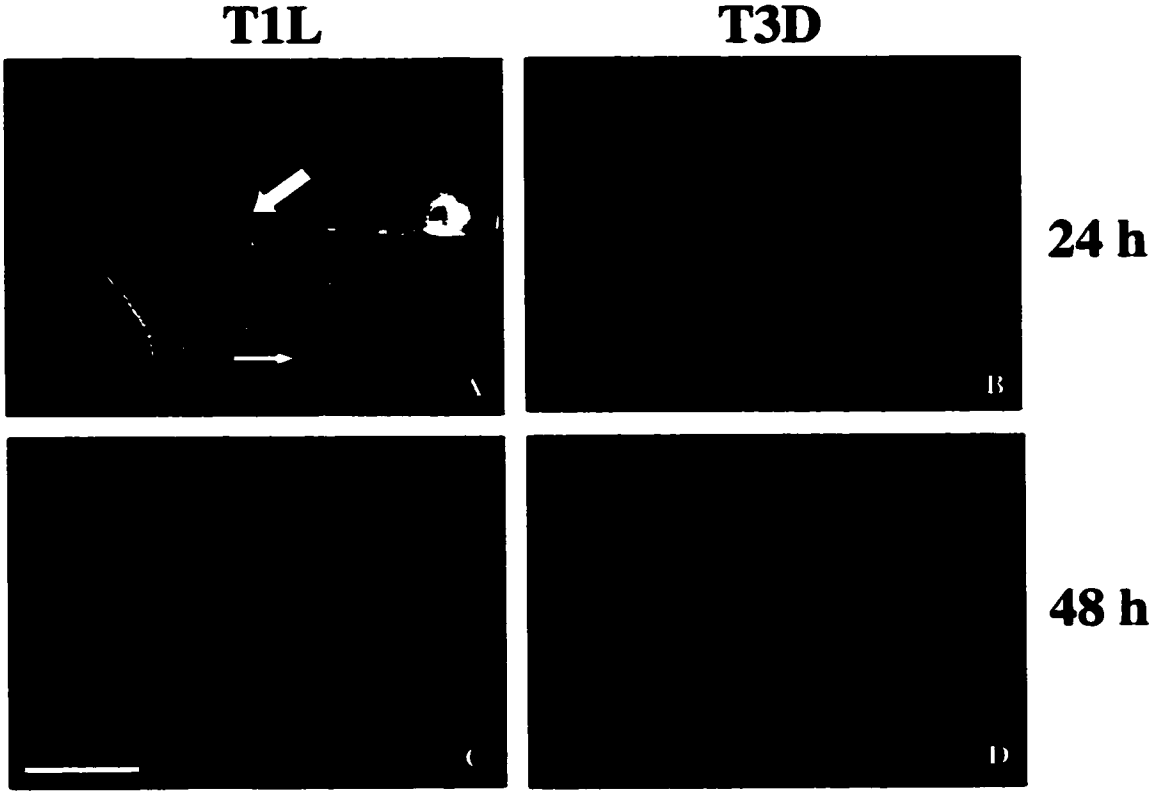
T1L
T3D
24 h
48 h

infected cells was observed at much earlier time points, with a majority of cells showing inclusions by 20 h p.i. (Fig. 3.1 B, D and Table 3.1). T1L and T3D differed strikingly in the rate of inclusion formation with median times of 39 and 18 h, respectively. These results demonstrate that reovirus strains T1L and T3D differ in the rate of inclusion formation in L929 cells.

3.3.2 Strain-specific differences in the rate of reovirus inclusion formation are determined primarily by the M1 gene

To identify viral genes that segregate with differences in the kinetics of inclusion formation exhibited by T1L and T3D, 15 T1L X T3D reassortant reoviruses were tested for the rate of inclusion formation in L929 cells by immunofluorescent staining at 24 h p.i. (Table 3.2). This time point was chosen because it demonstrated the maximum difference in the extent of inclusion formation by T1L and T3D in infected L929 cells (Table 3.1). Those reassortant reoviruses that produced the greatest percentage of infected cells with inclusions at 24 h p.i. possessed a T3D M1 gene, while those that produced the least contained a T1L M1 gene. Reassortant reoviruses containing a T3D M1 gene and a T1L S3 gene produced inclusions with faster kinetics than the T3D parent. The rate of inclusion formation of reassortant reoviruses containing a T1L M1 gene was however not influenced by the allelic nature of the S3 gene. The association of the M1 gene with the rate of inclusion formation was highly statistically significant (*t* test, $p < 0.0001$; Mann-Whitney (MW) test, $p < 0.001$). The remaining genes were not significantly associated with the rate of inclusion formation in these experiments (*t* test and MW test, $p > 0.05$). Parametric stepwise linear regression analysis was used to determine the individual contribution of genes to the rate of inclusion formation. This analysis showed that

Table 3.2 Rate of inclusion formation exhibited by T1L X T3D reassortant reoviruses in infected L929 cells

	Parental origin of genome segments											
Virus	L1	L2	L3	M1	M2	M3	S1	S2	S3	S4	percent inclusion formation (n)[a]	Rank
EB129	3	3	3		3	1	3	1		3	96.2 (157)	17
G16	1	1	1		1	1	1	3		1	88.4 (69)	16
EB123	3	3	1		3	3	3	3		3	79.4 (160)	15
EB146	1	1	1		1	1	1	1		3	76.3 (97)	14
EB88	3	3	3		1	3	3	3	3	3	65.4 (162)	13
T3D	3	3	3		3	3	3	3	3	3	65.5 (84)	12
EB96	1	3	1		1	1	1	1	3	1	64.8 (88)	11
EB28	3	3	1		3	3	3	1	3	3	64.1 (167)	10
EB86	1	3	3		3	1	3	3	3	1	46 (174)	9
EB31	1	1	1		1	1	1	3	3	1	38.2 (110)	8
H60	3	3	1	1	3	3	3	3	3	1	29.6 (81)	7
H15	1	3	3	1	3	3	3	3	3	1	27 (89)	6
EB39	1	3	3	1	3	3	3	3	3	3	19.3 (88)	5
EB47	1	3	1	1	1	1	1	1	1	1	14.5 (124)	4
T1L	1	1	1	1	1	1	1	1	1	1	10 (219)	3
H17	3	3	1	1	3	3	1	3	3	1	7.6 (92)	2
EB73.1	1	3	1	1	3	3	3	3	3	3	6.5 (124)	1

[a] n = total number of antigen-positive cells counted by immunofluorescent staining with rabbit polyclonal anti-T1L and T3D antiserum.

89.8% ($p = 0.027$) of the variability in inclusion formation is accounted for by the 10 reovirus genes with 86% contributed by the M1 gene ($p < 0.001$), with minor and less statistically significant roles for the S3 gene (7%, $p = 0.169$) and the S1 gene (4%, $p = 0.649$). There was no detectable contribution by the other viral genes to this phenotypic difference. These results indicate that M1 is the only viral gene that independently contributes to the rate of reovirus inclusion formation. When only those reassortant reoviruses containing a T3D M1 gene ($n = 10$) were analyzed, the S3 was the only gene significantly associated with the rate of inclusion formation (*t* test, $p = 0.004$; MW test, $p = 0.014$). These results indicate that the rate of viral inclusion formation is due primarily to the M1 gene, which encodes the μ2 protein, and is modulated by the S3 gene, which encodes the nonstructural protein, σNS.

3.3.3 Colocalization of μ2 and other reovirus proteins in cytoplasmic inclusions

The observation that the M1 gene is the primary determinant of strain-specific differences in the rate of viral inclusion formation led to examination of the cellular localization of μ2 protein with respect to other reovirus proteins during infection of L929 cells. A monoclonal antibody (8H6) specific for μ1/μ1C (Virgin IV *et al.*, 1991), a reovirus outer-capsid protein, was used to identify reovirus inclusion bodies, and rabbit anti-T1L-μ2 polyclonal antiserum was used to detect μ2 protein. The polyclonal rabbit anti-T1L-μ2 antiserum demonstrated equivalent reactivity with both T1L and T3D μ2 proteins, which are 98.6% identical in amino acid sequence, by both immunoprecipitation (Zou and Brown, 1996b) and immunoblot (data not shown). To determine the subcellular distribution of μ2 relative to other reovirus proteins during infection, double immunofluorescence labeling of cells infected with either T1L or T3D was performed

using confocal laser scanning microscopy. T3D μ2 protein was primarily concentrated in inclusions, whereas T1L μ2 protein had a more diffuse distribution (Fig. 3.2 C and G). However, in cells infected with either strain, μ2 and μ1/μ1C proteins colocalized in cytoplasmic inclusions (Fig. 3.2 B, C, D, F, G and H). In addition μ2 protein localized to the nucleus in both T3D- and T1L-infected cells (Fig. 3.2 C and G). The presence of μ2 protein in the nucleus was confirmed by costaining with the nucleus-specific marker, ToPro3 (Fig. 3.2 D and H). Occasionally, μ2 protein was observed to accumulate in small cytoplasmic foci that were not associated with μ1/μ1C staining (Fig. 3.2 H). These results indicate that μ2 localizes to sites of viral assembly and also is distributed in the nucleus.

3.3.4 μ2 protein localization in cells infected with reovirus *ts* mutants

Reovirus *ts* mutants that are defective in viral assembly were used to further examine the role of μ2 protein in inclusion formation. The *ts* mutant, *tsH11.2*, does not replicate at nonpermissive temperature (39.5°C) due to a conditionally defective μ2 protein (Coombs, 1996). Progeny virions are not observed in *tsH11.2*-infected cells due to a defect in viral assembly. Infection of L929 cells with *tsH11.2* at permissive temperature (33°C) resulted in normal inclusions with colocalization of μ2 and μ1/μ1C proteins (data not shown). Infection of L929 cells with *tsH11.2* at nonpermissive temperature resulted in accumulation of μ1/μ1C protein in subcellular structures that did not contain μ2 protein and were generally smaller than inclusions observed in cells infected with wt virus (Fig. 3.3 J and L). Instead, μ2 protein had a diffuse cytoplasmic and nuclear localization (Fig. 3.3 K and L). These results demonstrate that subcellular structures that resemble inclusions by differential interference contrast (DIC)

Figure 3.2 Cellular localization of reovirus μ2 and μ1/μ1C proteins in cells infected with reovirus strains T1L or T3D.

L929 cells were infected with either T1L (A-D) or T3D (E-H) at an MOI of 10 PFU/cell. Following adsorption, cells were incubated at 37°C for 18 h. Cells were stained for μ1/μ1C using μ1/μ1C-specific mAb 8H6 (B and F) and for μ2 using a μ2-specific rabbit polyclonal antiserum (C and G) as primary antibodies followed by goat anti-mouse Alexa488 and goat anti-rabbit Alexa546 as secondary antibodies. The μ1/μ1C protein is coloured green, and the μ2 protein is coloured red. ToPro3, a dsDNA-specific dye, was incubated with the secondary antibodies and is coloured blue (D and H). Images were obtained using a confocal laser scanning microscope. A DIC image of each field is shown in panels (A and E) and the fluorescent images in (B, C, F and G) are overlaid on the respective DIC image. In the overlay images, colocalization of μ2 and μ1/μ1C is indicated by the yellow colour, and colocalization of μ2 and ToPro3 is indicated by the pink colour.

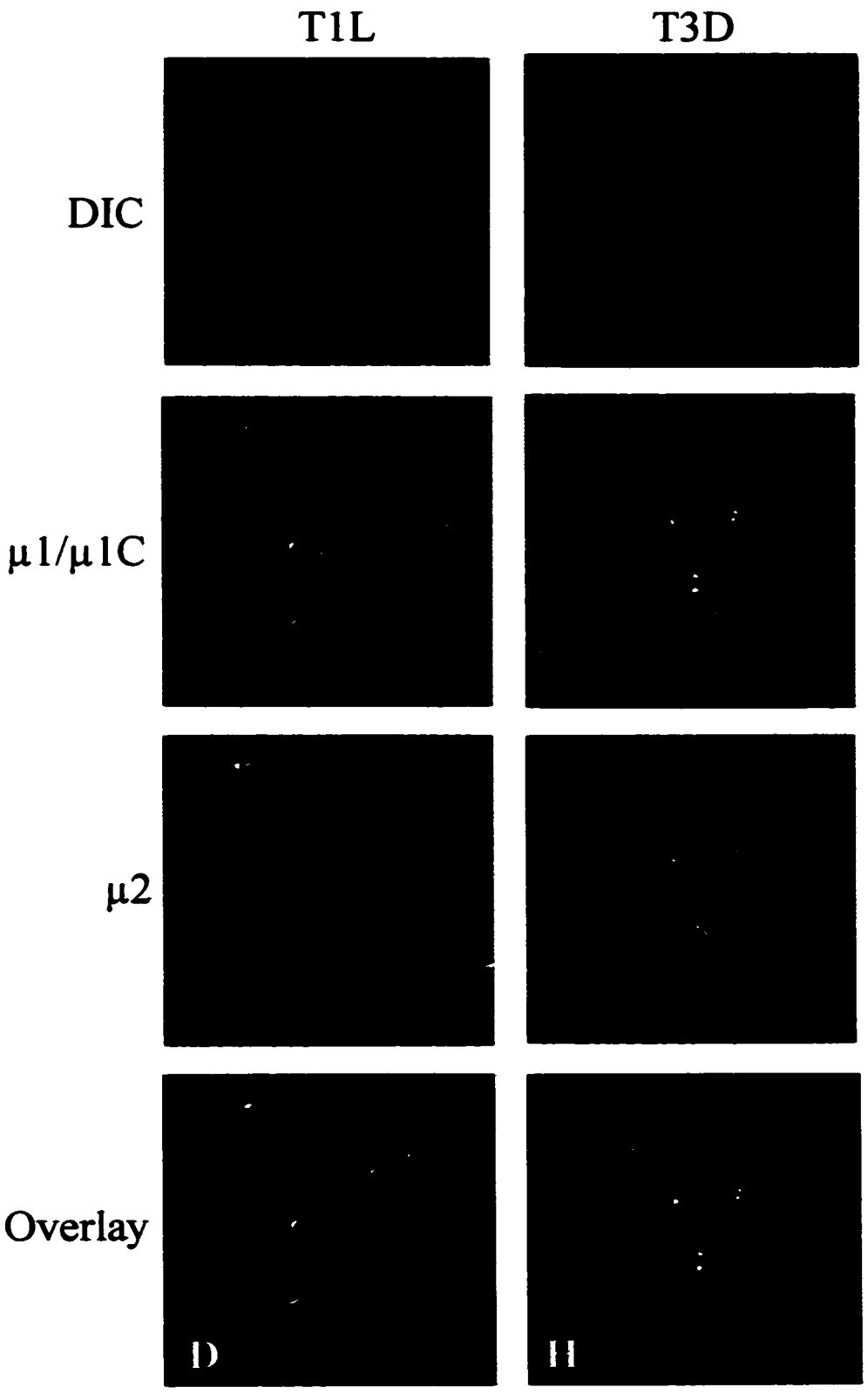
T1L
T3D
DIC
μ1/μ1C
μ2
Overlay
D
H

Figure 3.3 Cellular localization of reovirus μ2 and μ1/μ1C proteins in cells infected with *ts* mutant reoviruses *tsH11.2*, *tsC447*, or *tsG453*.

L929 cells were infected with either *tsC447* (A-D), *tsG453* (E-H), or *tsH11.2* (I-L) at an MOI of 10 PFU/cell. Following adsorption, cells were incubated at 39.5°C for either 24 (*tsC447* and *tsH11.2*) or 36 h (*tsG453*). Cells were stained for μ1/μ1C using μ1/μ1C-specific mAb 8H6 (B, F and J) and for μ2 using a μ2-specific rabbit polyclonal antiserum (C, G and K) as primary antibodies followed by goat anti-mouse Alexa488 and goat anti-rabbit Alexa546 as secondary antibodies. The μ2 protein is coloured red, and the μ1/μ1C protein is coloured green. ToPro3, a dsDNA-specific dye, was incubated with the secondary antibodies and is coloured blue (D, H and L). Images were obtained using a confocal laser scanning microscope. A DIC image of each field is shown in panels (A, E and I) and the fluorescent images in (B, C, F, G, J and K) are overlaid on the respective DIC image. In the overlay images, colocalization of μ2 and μ1/μ1C is indicated by the yellow colour, and colocalization of μ2 and ToPro3 is indicated by the pink colour.

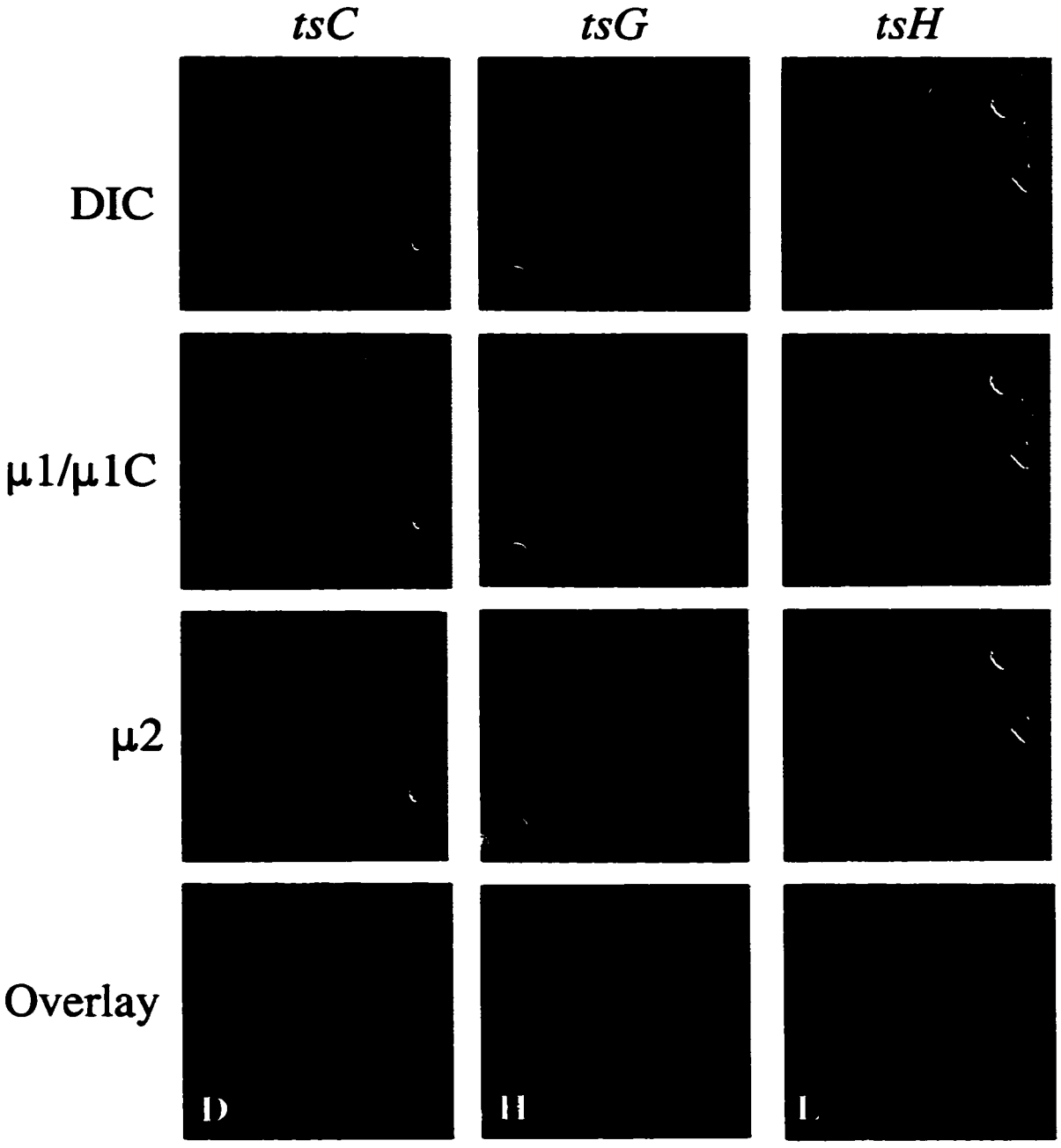
tsC
tsG
tsH
DIC
μ1/μ1C
μ2
Overlay
D
H
L

microscopy can form without μ2 protein, however, these do not result in viral particle formation.

To determine whether viral inclusion formation was affected by defects in other viral genes, two other *ts* mutants, *tsC447* and *tsG453*, with mutations in the σ2-encoding S2 and σ3-encoding S4 genes respectively, were used to infect L929 cells. Infection with either *ts* mutant resulted in the accumulation of μ1/μ1C protein in subcellular structures that did not stain for μ2 protein (Fig. 3.3 B, D, F, and H). In contrast to *tsH11.2*, infection with *tsC447* and *tsG453* resulted in the accumulation of μ2 in small protein complexes seen as punctate cytoplasmic staining adjacent to subcellular structures containing μ1/μ1C protein, in addition to having diffuse nuclear staining (Fig. 3.3 C, D, G, and H). Occasionally, μ2 protein was also seen to accumulate in discrete structures in the nucleus (Fig. 3.3 H). Unlike *tsH11.2*, infection with tsC447 and tsG453 result in subviral particle formation suggesting that μ2 protein complex formation is important for viral particle formation.

3.3.5 Recombinant T1L and T3D μ2 proteins form nuclear and cytoplasmic complexes at different rates

Genetic analysis of the rate of reovirus inclusion formation indicated that this property is linked to the μ2-encoding M1 gene. Accumulation of μ2 in protein complexes independent of μ1/μ1C protein was also observed in cells infected with either wt viruses or *ts* mutants (Fig. 3.2 H, 3.3 D, and 3.3 H). These observations suggested that μ2 would be capable of forming protein complexes in cells independent of other viral proteins. To examine this possibility, recombinant μ2 protein was expressed in L929 cells by transfection with either T1L or T3D M1

gene-containing plasmids under control of a bacteriophage T7 RNA polymerase promoter. Immunoblot analysis of transfected cells showed high levels of μ2 protein expression 24 h post-transfection for both the T1L and T3D M1 gene constructs. This is in contrast to μ2 protein expression during infection, when expression of T1L μ2 was more robust than T3D μ2 at 24 h p.i. (Fig. 3.4).

M1 gene-transfected cells were stained for μ2 protein at 24 and 48 h after transfection. The μ2 protein of both T1L and T3D formed complexes in the absence of the other reovirus proteins (Fig. 3.5 C, D, E, and F). The rate of complex formation did, however, vary in a strain-specific manner. The median time of complex formation by T3D μ2 protein was 22 h post-transfection compared to 43 h post-transfection for cells expressing T1L μ2 protein (Table 3.3; Fig. 3.5 B, C, E, and F). These differences in the rate of complex formation exhibited by T1L and T3D μ2 proteins paralleled that of inclusion formation in reovirus-infected cells. Recombinant μ2 protein formed complexes in both the nucleus and cytoplasm (Fig. 3.5 D). Although the μ2 protein complexes formed with similar strain-dependent kinetics to reovirus inclusions, they did not co-localize with the intermediate filament vimentin to the same extent as reovirus inclusions. In reovirus-infected cells the vimentin filament network is reorganized and colocalizes with μ2 protein in reovirus inclusions, whereas in M1 gene-transfected cells most of the vimentin localizes to a perinuclear site (Fig. 3.6). Since poxvirus infection results in perinuclear inclusion bodies that contain vimentin, such a structure in M1 gene-transfected cells probably represents a vaccinia virus inclusion body. However, some vimentin is present in the μ2 protein complexes suggesting that the μ2 protein complexes could be similar to

Figure 3.4 Immunoblot analysis of μ2 protein expression in infected and transfected L929 cells.

L929 cells were infected with T1L or T3D, or transfected with T1L or T3D M1 gene. Cell lysates were collected 24 h p.i or post-transfection, resolved by SDS-PAGE and immunoblotted with anti-T1L-μ2 antiserum followed by PAAP. The blot was then reacted with the chromogenic substrate NBT/BCIP. Lane annotation left to right: Infection: M = mock-infected, T1 = T1L-infected, T3 = T3D-infected. Transfection: T1 = pCMV-M1CN T1-7, T3c = pCMV-M1CN T3-13, T3g = pGEM-M1 T3-18, pc = pcDNA3 vector control and pg = pGEM7Zf(+) vector control. In the lower panel the same samples stained with Coomassie blue showing a host cell protein of approx. 120 kDa, as a loading control.

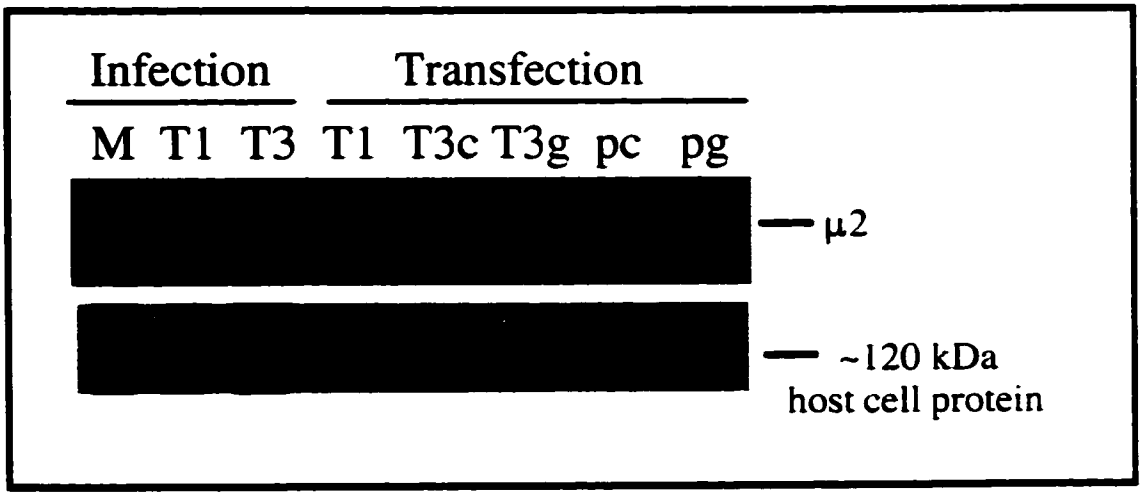
Infection
Transfection
M T1 T3 T1 T3c T3g pc pg
μ2
~120 kDa
host cell protein

Figure 3.5 Cellular localization of recombinant μ2 protein in transfected cells.

L929 cells were transfected with control vector (pcDNA3) (A), pCMV-M1CN clone T1-7 expressing the T1L M1 gene (B, E), or transfected with pCMV-M1CN clone T3-13 expressing the T3D M1 gene (C, F). Following incubation for either 24 (A, B, C) or 48 h (E, F) cells were stained for μ2 using μ2-specific rabbit polyclonal antiserum followed by FITC-conjugated goat anti-rabbit. (D) Higher magnification of cells transfected with pGEM-M1 clone T3-18 expressing the T3D M1 gene, stained for μ2 at 24 h post-transfection showing nuclear and cytoplasmic complexes of μ2. The bars represent 10 μm.

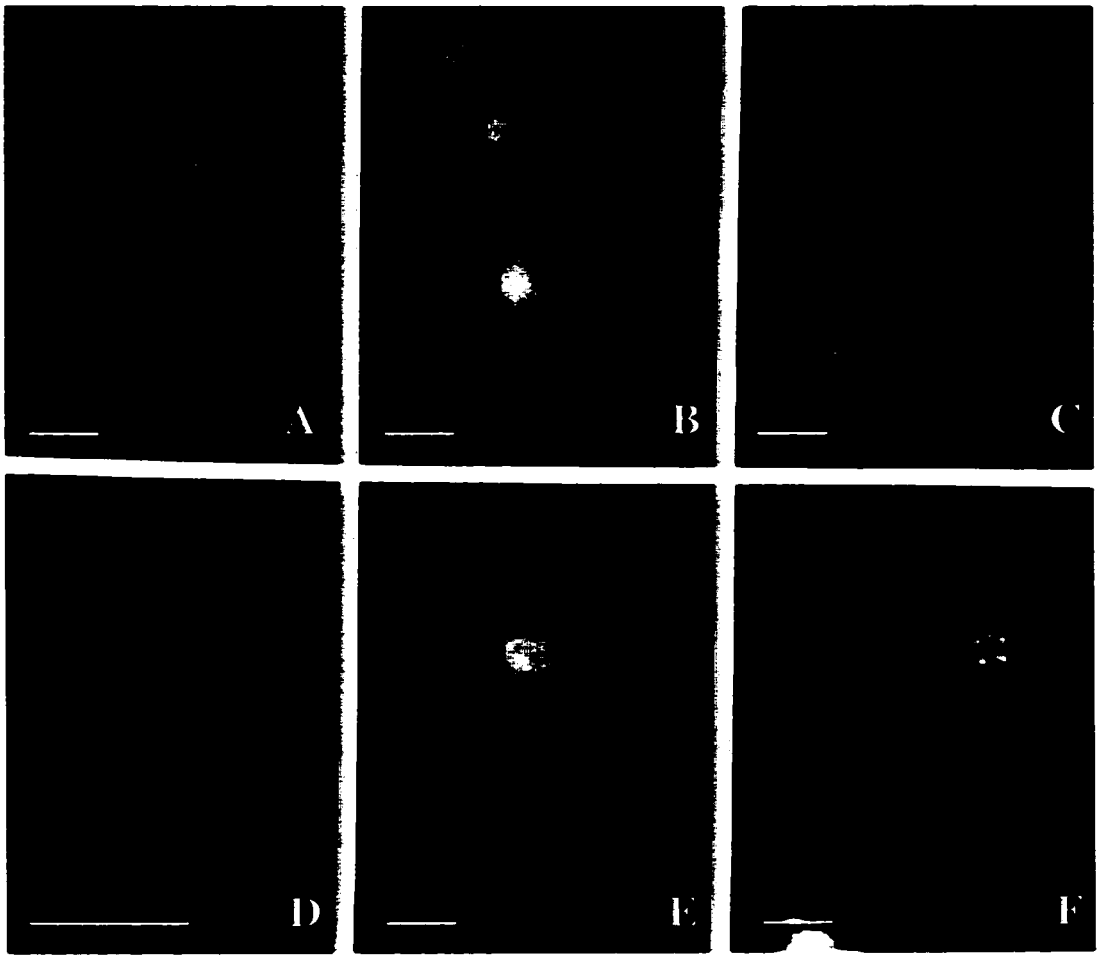
A
B
C
D
E
F

Figure 3.6 Cellular localization of μ2 protein and vimentin in reovirus-infected and M1 gene-transfected cells.

HeLa cells were either infected with T3D (A-C) at an MOI of 10 PFU/cell or transfected with a T3D M1 gene construct (pGEM-M1 clone T3-18) (D-F). Cells were stained at 24 h p.i. or post-transfection for μ2 using a μ2-specific rabbit polyclonal antiserum (A and D) and for vimentin using a goat anti-vimentin polyclonal antiserum (B and E) as primary antibodies followed by Cy3-conjugated donkey anti-rabbit and FITC-conjugated donkey anti-goat as secondary antibodies. The μ2 protein is coloured red and the vimentin is coloured green. The cells were also incubated with DAPI, a dsDNA-specific fluorescent dye to stain the nuclei and is coloured blue (C and F). In the overlay images, colocalization of μ2 and vimentin is indicated by the yellow colour. The bar represents 10 μm.

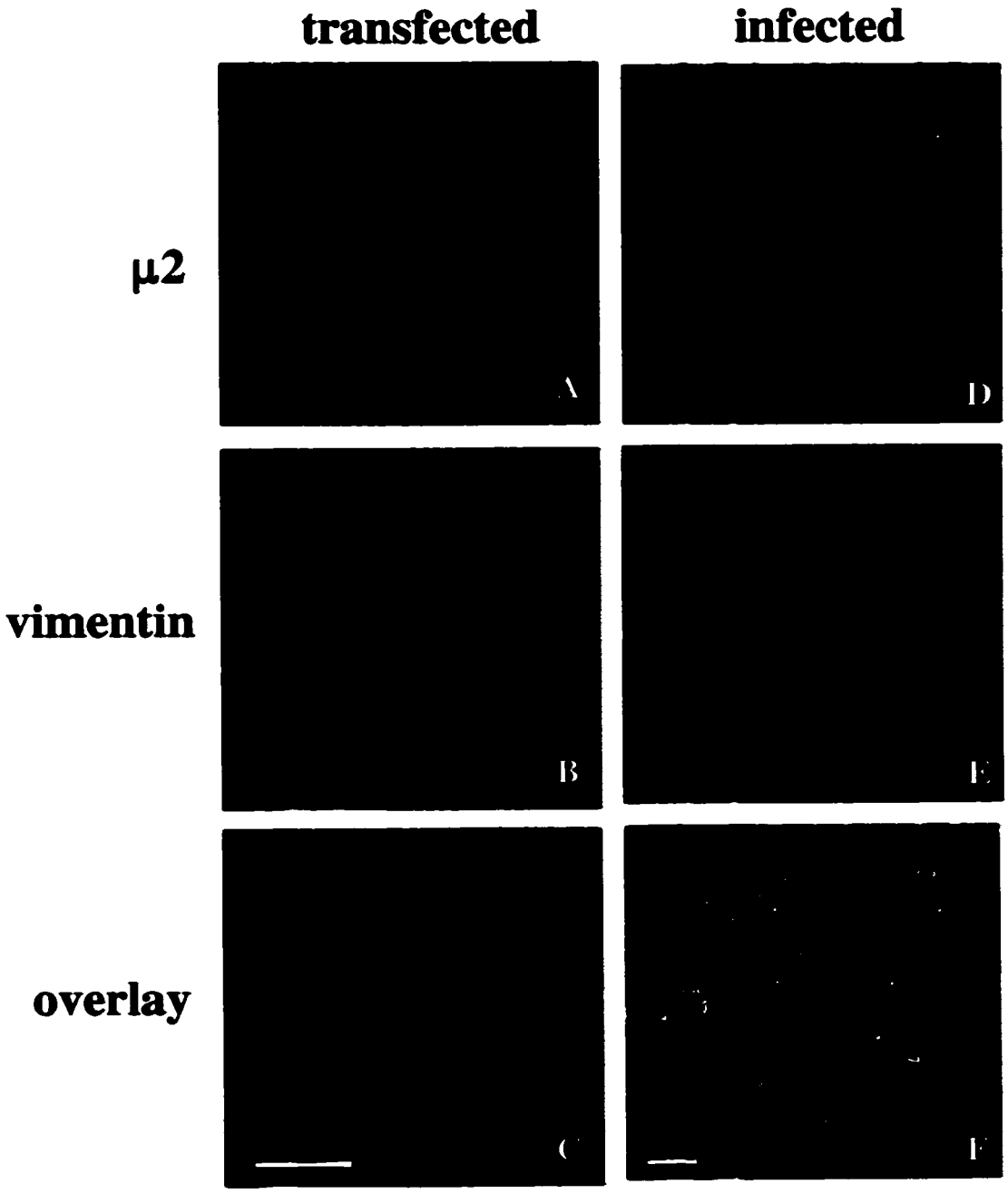
transfected
infected
μ2
vimentin
overlay
A
D
B
E
C
F

reovirus inclusions.

Expression of recombinant *tsH11.2* μ2 protein resulted in complex formation at both permissive (17 ± 9 % of antigen-positive cells) and nonpermissive (7 ± 7 % of antigen-positive cells) temperatures at 48 h post-transfection (data not shown). The number of cells containing μ2 complexes after transfection with *tsH11.2* μ2 at both permissive and nonpermissive temperatures was significantly less than that after transfection with wt μ2 protein (17 ± 9 % and 7 ± 7 % vs 56 ± 8 % for T1L μ2; *t* test, $p < 0.00001$). This finding suggests that the M1 mutation in *tsH11.2* has an effect on the capacity of *tsH11.2* μ2 to form protein complexes.

Table 3.3 Rate of inclusion formation in L929 cells transfected with the T1L or T3D M1 cDNA

Time post-transfection (h)	Percent cells with protein complex formation[a]	
	T1L M1 (n)[b]	T3D M1 (n)
24	15 ± 10 (132)	61 ± 11 (88)
48	56 ± 8 (115)	98 ± 5 (26)

[a] average of 2 to 4 experiments (at least one with pGEM and pcDNA3)
[b] n = number of antigen-positive cells counted by immunofluorescent staining with rabbit polyclonal anti-T1L μ2 antiserum.

3.4 Discussion

These experiments show that reovirus strains T1L and T3D differ in the rate of inclusion formation in L929 cells. This finding is consistent with early studies of the rate of inclusion

formation by T1L and T3D (Rhim *et al.*, 1962; Gomatos *et al.*, 1962). Genetic analysis using T1L X T3D reassortant reoviruses showed that the M1 gene is the primary determinant of strain-specific differences in kinetics of inclusion formation. Since T1L synthesizes several-fold more μ2 protein and other reovirus proteins than T3D (Fig. 3.4; Schmechel *et al.*, 1997; Matoba *et al.*, 1991) and yet forms inclusions at a slower rate, it is likely that an intrinsic biological difference in T1L and T3D μ2 proteins influences the rate of inclusion formation in reovirus-infected cells.

The S3 gene modulated the rate of inclusion formation in conjunction with the M1 gene such that pairing of a T1L S3 gene with a T3D M1 gene in T1L X T3D reassortant reoviruses resulted in a faster rate of inclusion formation than for the parental strain T3D. This finding suggests that the T3D S3 gene attenuates the rate of inclusion formation by the cognate T3D M1 gene. The strain of origin of the S3 gene did not affect kinetics of inclusion formation when paired with the T1L M1 gene, suggesting that the T1L μ2 protein differs from T3D μ2 in its interactions with σNS. It is possible that the σNS protein modulates the rate of inclusion formation by direct interactions with μ2 and/or host factors.

In addition to controlling the rate of inclusion formation, μ2 protein may play a direct physical role in the inclusion formation process. This hypothesis is supported by expression of recombinant μ2 protein in L929 cells which resulted in formation of protein complexes. Although these μ2 complexes were not associated with other viral proteins and did not colocalize with vimentin to the same extent as reovirus inclusions, they were formed with kinetics that reflect the parental origin of the M1 gene. This observation may be relevant to the inclusion

formation process since the activity parallels the rate of inclusion formation during infection. However, μ2 protein is probably not the only reovirus protein involved in inclusion formation. Infection of L929 cells with *ts* mutant reoviruses *tsH11.2*, *tsC447* and *tsG453* resulted in formation of subcellular structures that resembled reovirus inclusions but did not contain μ2 protein. In addition, at least one other reovirus protein, μ1/μ1C, has been shown to form protein complexes when expressed alone (Yue and Shatkin, 1996). The σ1 protein also has been shown to have either a uniform cytoplasmic distribution or to accumulate in punctate foci in different studies using different cell lines for transfection (Banerjea *et al.*, 1988; Belli and Samuel, 1991). Inclusion formation may thus be a concerted function of several reovirus proteins with μ2 protein controlling the rate of formation. Alternatively, μ2 could coordinate the formation of a subset of protein complexes that serve as a prerequisite for mature viral inclusion formation along with other viral and/or host proteins.

In addition to localizing to cytoplasmic inclusions, μ2 localizes to the nucleus in cells infected with wt and *ts* mutant reoviruses as well as M1-gene-transfected cells. The localization of the protein to the nucleus was unanticipated considering that reovirus replication is thought to be entirely cytoplasmic. It is possible that μ2 protein localizes to the nucleus to influence cellular events required for reovirus replication, including inclusion formation. The μ2 protein is not the only reovirus protein that localizes to the nucleus. The σ3 protein accumulates in the nucleus of both infected and transfected cells (Yue and Shatkin, 1996; Schmechel *et al.*, 1997), and σ1s, a nonstructural protein encoded by the S1 gene, localizes to the nucleolus (Belli and Samuel, 1991; Rodgers *et al.*, 1998).

The μ2 protein did not accumulate in protein complexes in cells infected with *tsH11.2*, and although complexes were observed in cells expressing high levels of recombinant *tsH11.2* μ2 protein they were formed less efficiently than wt T1L μ2 protein. These findings suggest that the mutations in *tsH11.2* μ2 protein affect the accumulation of μ2 in complexes. The *tsH11.2* M1 gene has two mutations resulting in two amino acid substitutions that are 11 residues apart, $M^{399}\rightarrow T$ and $P^{414}\rightarrow H$ (Coombs, 1996). Constitutive expression of wt μ2 protein in L929 cells complements the M1 defect of *tsH11.2* at nonpermissive temperature (Zou and Brown, 1996a). Expression of μ2 proteins containing either single mutation is capable of partially complementing the *tsH11.2* defect, which indicates that both mutations contribute to the *ts* phenotype (Zou, Brown, and Coombs unpublished; Coombs, 1998b). The P^{414}-H mutation resides in a region with partial homology to the A motif of known ATPases (Noble and Nibert, 1997). This observation raises the possibility that μ2 protein either mediates the rate of inclusion formation directly by an ATP- or other nucleotide-dependent event or indirectly through an ATP-dependent interaction with host regulatory proteins. Consistent with this idea, the M1 gene, in addition to the L3 gene, influences NTPase activity of reovirus cores (Noble and Nibert, 1997).

Reovirus assembly is poorly understood, but the earliest ssRNA-containing structures termed "assortment" complexes are composed of σNS, μNS, σ3, and possibly μ1/μ1C, λ1 and λ2 (Antczak and Joklik, 1992). Progeny subviral particles also acquire three other proteins that were not identified in assortment complexes namely μ2, λ3, and σ2. This results in the formation of replicase particles containing all the viral structural proteins as well as μNS (Zweerink *et al.*, 1976). These particles are transcriptionally active progeny subviral particles that synthesize

dsRNA. It is possible that ssRNA-containing complexes associate with another complex containing μ2, λ3, and σ2 and that μ2 protein controls the formation of this complex at the site of inclusion formation. Since the M1 gene determines the rate of inclusion formation, the formation of this complex could be the rate limiting step.

The secondary role of the S3 gene in kinetics of inclusion formation suggests that σNS influences the rate of formation of the ssRNA-containing complex. Alternatively, σNS might directly interact with μ2 to form replicase particles. Such an association could be modulated by the different M1 and S3 genes to affect the rate of inclusion formation. This model predicts that μ2 protein does not associate with μ1/μ1C-containing complexes in either *tsC447*- or *tsG453*-infected cells that express mutant σ2 and σ3 proteins, respectively. The absence of μ2 in μ1/μ1C-containing complexes in cells infected with these *ts* mutants could result from failure of μ2 protein to recognize the aberrant structures produced during these infections due to mutations in σ2 and σ3 resulting in the accumulation of μ2 in an intermediate complex and the formation of either core-like or empty outer shell particles respectively. The crucial role played by the M1 and S3 genes in inclusion formation and viral assembly is elaborated further by *ts* mutants of the two genes, namely *tsH11.2* (M1 gene) and *tsE320* (S3 gene). *tsH11.2* and *tsE320* are the only reovirus *ts* mutants identified to be completely defective in virion assembly where capsid structures do not form at nonpermissive temperature (Table 1.3; reviewed by Coombs, 1998b). Cells infected with *tsH11.2* show accumulation of σNS protein in protein complexes but diffuse distribution of μ2 protein while infection with *tsE320* results in accumulation of μ2 protein in punctate foci but diffuse distribution of σNS protein (Becker *et al.*, 2001). This indicates that

even though protein complexes do form in *tsE320*- and *tsH11.2*-infected cells at nonpermissive temperature, viral assembly can not proceed without either a functional μ2 or σNS protein, suggesting that interaction between the two proteins or with host factors is crucial for inclusion formation and viral assembly. Taken together, these data further support the hypothesis that virion assembly and inclusion formation are functionally linked and that μ2 and σNS proteins play important roles in both processes.

CHAPTER FOUR

STRAIN- AND CLONE-DEPENDENT DIFFERENCES IN EXPRESSION AND STABILITY OF REOVIRUS μ2 PROTEIN

4.1 Introduction

Both the kinetics and extent of protein expression are ways in which a virus can regulate protein function. The results in the previous chapter showed a significant difference in expression of μ2 protein between T1L and T3D at 24 h p.i., suggesting that the extent of protein expression might play a role in the biological functions of the protein including the rate of inclusion formation. μ2 protein is present in catalytic amounts on the interior surface of the core particle which is in keeping with its proposed enzymatic functions during RNA synthesis. Previous studies of μ2 protein expression of T3D-infected cells have shown that it is expressed at very low levels, compared to other reovirus proteins (Gaillard and Joklik, 1985; Roner *et al.*, 1989), which correlates with its low requirement in virions. However, these studies were hindered because μ2 protein comigrates with the abundant reovirus structural protein, μ1C, on SDS-PAGE (McCrae and Joklik, 1978) and also because most reovirus antisera have poor reactivity for μ2. Some previous studies comparing overall reovirus protein expression in T1L- and T3D-infected cells, have shown that T1L-infected cells produce significantly more viral protein than T3D-infected cells (Schmechel *et al.*, 1997), whereas others have reported similar levels of viral protein expression between the two strains (Munemitsu and Samuel, 1984). This suggests the possibility of clonal differences in protein expression among reovirus strains.

The amount of reovirus protein produced during infection is regulated at both the level of transcription and translation. The amount of each species of reovirus mRNA produced during transcription is inversely proportional to gene size i.e. there is more S (small) segment mRNA produced than M (medium) segment and more M than L (large) segment (Banarjee and Shatkin, 1970; Joklik, 1981). mRNA degradation does not play a role because reovirus transcripts have been shown to have similar stabilities (Furuichi *et al.*, 1977). The translation efficiencies of reovirus mRNA, defined as the amount of protein synthesized per unit of mRNA, have been shown to vary significantly for each species of mRNA (Gaillard and Joklik, 1985). Several factors play a role in controlling the amount of protein translated from each individual mRNA species, including the sequence context of the initiation codon (Kozak, 1981; Munemitsu and Samuel, 1988; Roner *et al.*, 1989; Belli and Samuel, 1993), mRNA secondary structure and protein elongation (Doohan and Samuel, 1992; Belli and Samuel, 1993), as well as host translation factors that respond to inhibitors such as the interferon inducible PKR (Belli and Samuel, 1993; Bischoff and Samuel, 1989; Samuel and Brody, 1990).

The M1 mRNA has been reported to be one of the two least efficiently translated reovirus transcripts *in vivo*, being translated 100-fold less frequently than the most efficiently translated S4 mRNA (Gaillard and Joklik, 1985). The reason for the low translation efficiency of M1 mRNA is unknown. The initiation codon of the M1 mRNA at position 14 possesses a very good Kozak sequence context (Brown, 1998; Zou and Brown, 1996b). *In vitro* translation of the M1 mRNA is comparable to other reovirus mRNAs, leading to the hypothesis that translation, *in vivo*, is probably influenced by negative regulatory factors in the host cell (Roner *et al.*, 1993).

In this chapter, expression levels of μ2 protein were analyzed in cells infected with different plaque-purified clones of T1L and T3D. μ2 protein was found to be expressed to high levels that are comparable to that of the abundant major structural protein μ1C, especially in T1L-infected cells. The relatively low level expression of μ2 protein in T3D-infected cells was shown to be due to a combination of lower mRNA expression and decreased stability of T3D μ2 protein compared to T1L μ2 protein.

4.2 Materials and Methods

4.2.1 Viruses

Reovirus T1L and T3D clones A, B, and C were plaque-purified from their respective laboratory stocks (referred to as T1L-O and T3D-O for original clone) after four high titer passages (~$5x10^7$ PFU/$25cm^2$ culture). Stocks were made by two passages in L929 cells.

4.2.2 Extraction of cellular RNA

Monolayers of L929 cells in 60 mm dishes were infected with either T1L or T3D at an MOI of 10 PFU/cell and incubated at 37°C for various intervals. To extract the cellular RNA the monolayers were washed twice with PBS and lysed in 0.5 ml of STE (100 mM NaCl, 10 mM Tris-HCl pH7.4 and 1 mM EDTA) containing 1% SDS and freshly added 0.1 M vanadium ribonucleoside complex and 25 μg Protease K. T1L and T3D samples were then mixed and incubated for 30 min at 37°C. This was followed by extraction in a 3:1 (v/v) mixture of phenol and chloroform and a further extraction in chloroform. The RNA was then precipitated with 0.3 M sodium acetate and 2.5 volumes ethanol overnight at -20°C. Following centrifugation the

pelleted RNA was washed with cold 70% ethanol, vacuum-dried and resuspended in RNase-free ddH_20.

4.2.3 Competitive RT-PCR assay

This RT-PCR assay has previously been shown to accurately reflect the initial relative concentrations of two nearly identical PCR products (Bailly and Brown, 1998; Cottrez *et al.*, 1994). The total infected cellular RNA isolated as described above was mixed with 100 ng of negative sense segment-specific oligonucleotide primers M1 - 1697 and S4 - 1001 (see Appendix two) and reverse transcribed with dNTP (1 mM each), 10 mM DTT, 0.5 U/µl RNAguard RNase Inhibitor (Amersham Pharmacia Biotech, Inc., Baie d'Urfe, Que), RT buffer (Gibco BRL) and 200 U of Moloney Murine Leukemia Virus (M-MLV) reverse transcriptase (Gibco BRL) for 1 h at 37°C. PCR amplification was carried out using 1 µl of RT product in the presence of 100 ng of segment-specific negative and positive sense oligonucleotide primers, one of which was end-labeled with $\gamma[^{32}P]$-ATP (Amersham Pharmacia Biotech, Inc.) using T4 polynucleotide kinase (Amersham Pharmacia Biotech, Inc.) and purified by chromatography through G-50 sephadex (Amersham Pharmacia Biotech, Inc.). Negative sense primers used were as above and positive sense primers used were M1+1133 and S4+174 (see Appendix two). The PCR reactions included dNTPs (200 µM each), 1.5 mM $MgCl_2$, 0.1% NP40, PCR buffer (Gibco BRL) and 1 U Ultratherm *Taq* DNA polymerase (Bio/Can Scientific, Mississauga, ON) in a final volume of 100 µl. The samples were incubated for 4 min at 94°C and subjected to 30 cycles of 94°C for 30 sec; 42°C for 30 sec; 72°C for 30 sec followed by a final incubation of 7 min at 72°C. To generate strain-specific fragments, the PCR product was digested with Hae III, overnight at

37°C. The digested products were resolved by SDS-PAGE, and the gel was fixed, dried and autoradiographed before the bands were excised and quantified by scintillation counting.

4.2.4 Protein stability assays

L929 cell monolayers grown in 30 mm dishes were infected with T1L or T3D at an MOI of 10 PFU/cell and incubated at 37°C. At 20 h p.i. the monolayer was washed with PBS and pulse labeled for 4 h by addition of 0.5 ml of methionine/cysteine-free Dublecco's Modified Eagle Medium (Gibco BRL) containing 50 μCi/ml [^{35}S]met, [^{35}S]cys (NEN, Boston, MA). After radiolabeling the cell monolayer was washed twice with PBS and fresh MEM containing 100 μg/ml cycloheximide was added. Samples were collected after pulse-labeling and every 8 h thereafter by washing the monolayer with cold PBS twice and lysing in 250 μl of lysing buffer on ice for 5 min. The lysed cells were then scrapped into a microfuge tube and pelleted at 600g to remove the insoluble fraction. The supernatant was then mixed with 5 μl of μ2-specific rabbit polyclonal antiserum and 200 μl of 10% protein-A sepharose slurry at 4°C for 1 to 4 h. The sepharose beads were sedimented in a microfuge for 20 sec followed by 3 washes with cold washing buffer (100 mM Tris-HCl pH8-9, 500 mM LiCl, 1% 2ME) and a final wash with TE (10 mM Tris-HCl pH7.6, 1 mM EDTA). The beads were resuspended in 2X SDS sample buffer and the precipitated proteins were separated by SDS-PAGE and the gel was fixed, dried and processed for autoradiography.

For immunoblot analysis, cycloheximide (100 μg/ml) was added to the medium at 24 h p.i. Samples were collected at 0 h and every 12 h thereafter by washing the monolayer in cold

PBS twice and lysing in 500 µl of SDS sample buffer. The proteins were separated by SDS-PAGE and subjected to immunoblot analysis as described in section 2.4.

4.3 Results

4.3.1 Expression level of µ2 protein in L929 cells infected with different clones of reovirus T1L or T3D

To investigate the expression level of µ2 protein in infected cells, L929 cells were infected with different plaque-purified clones of T1L or T3D. Clones of T1L and T3D were obtained from our laboratory strains (T1L-O and T3D-O) after four serial passages in L929 cells and plaque purification. Cells were infected at an MOI of 10 PFU/cell and analyzed at 24 h p.i. by SDS-PAGE and immunoblot using a µ2-specific rabbit polyclonal antiserum (Zou and Brown, 1996b). The expression levels were found to be similarly high in all T1L clones but varied in T3D clones (Fig. 4.1 A). As a result all T1L experiments in this study were done using T1L clone O (T1L-O).

To determine whether the difference in µ2 protein expression in T3D clones was due to different expression kinetics, a time course was done for T1L-O, and two T3D clones that differed in expression of µ2 protein, T3D-O and T3D-A, a low and a high µ2-expressing clone, respectively. Samples were collected at different time points over a 72 h infection period and analyzed by immunoblot (Fig. 4.1 B). The absolute amount of protein at each time point was determined by comparing it to known amounts of TrpE-µ2 fusion protein (Zou and Brown, 1996b), which was initially determined by comparison to known quantities of bovine serum

Figure 4.1 Expression of μ2 protein in L929 cells infected with different plaque-purified clones of T1L or T3D.

(A) L929 cell monolayers were infected with T1L clones O, A, B, C or T3D clones O, A, B, C at an MOI of 10 PFU/cell for 24 h and the samples were resolved by SDS-PAGE and immunoblotted with a polyclonal rabbit anti-T1L μ2 antibody and PAAP followed by reaction with NBT/BCIP. M = mock-infected. The panel below is an L929 cell protein from the same samples stained with coomassie blue, as a loading control.

(B) Immunoblot of time course of μ2 protein expression in L929 cells infected with T1L-O, T3D-O or T3D-A. L929 cell monolayers were infected with T1L-O, T3D-O or T3D-A at an MOI of 10 PFU/cell. Cell lysates were collected at different times as indicated and the samples were resolved by SDS-PAGE and immunoblotted with a polyclonal rabbit anti-T1L μ2 antibody and PAAP followed by reaction with NBT/BCIP. M = mock-infected. The bottom panel is a representative immunoblot of Trp-E μ2 fusion protein serial dilution run in parallel with every blot to obtain absolute values and to ensure quantification readings were within linear range of detection of the phosphoimager.

(C) Bar graph showing quantification of μ2 protein expression in L929 cells infected with T1L-O, T3D-O or T3D-A by immunoblot analysis using a phosphoimager. Absolute values were obtained by comparison with known quantities of TrpE-μ2 fusion protein run in parallel as shown in panel (B) above. Error bars denote the standard error of the mean of 2 to 3 separate experiments. * = not done.

A

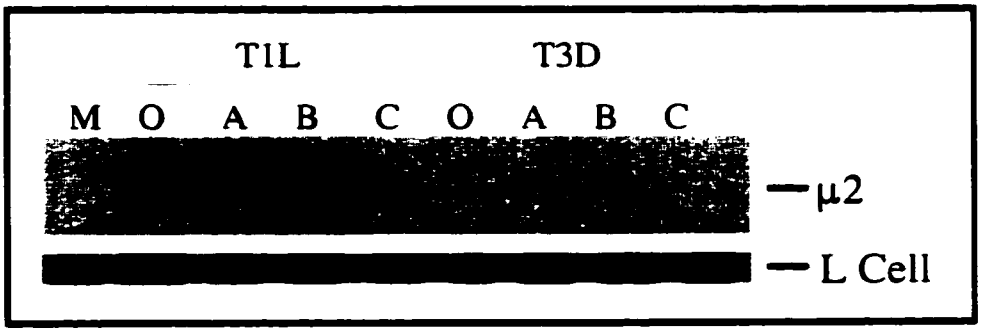
T1L
T3D
M O A B C O A B C
μ2
L Cell

B

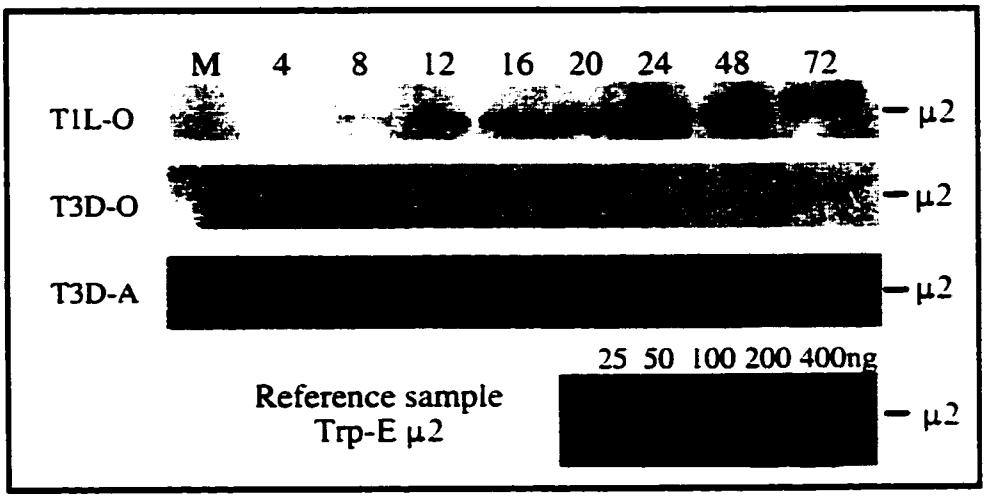
M 4 8 12 16 20 24 48 72
T1L-O
μ2
T3D-O
μ2
T3D-A
μ2
25 50 100 200 400ng
Reference sample
Trp-E μ2
μ2

C

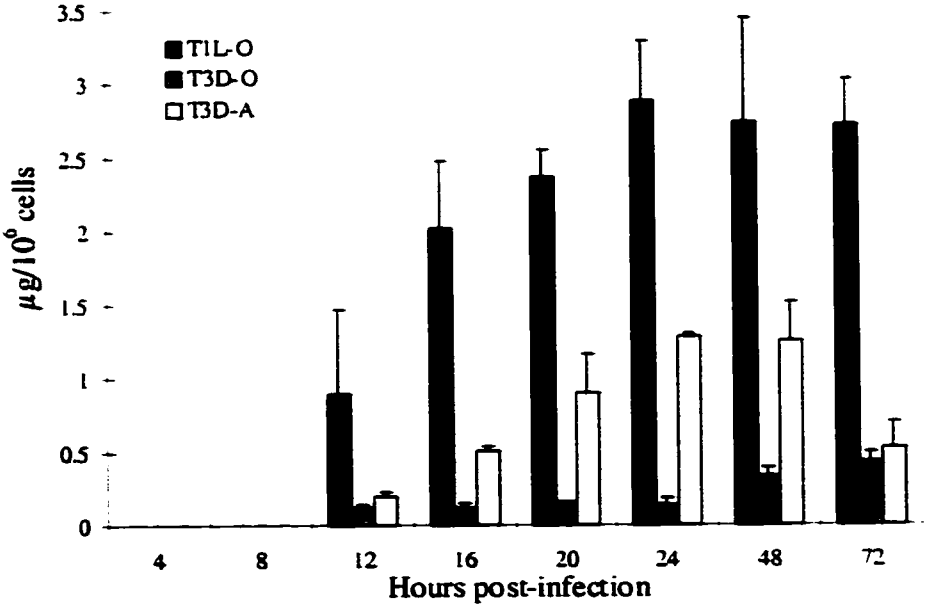
T1L-O
T3D-O
T3D-A
μg/10^6 cells
3.5
3
2.5
2
1.5
1
0.5
0
4 8 12 16 20 24 48 72
Hours post-infection

albumin (BSA) by densitometry (data not shown). For every experiment serial dilutions of the TrpE-μ2 fusion protein were run in parallel to ensure that μ2 protein readings were within the linear range of detection of the phosphorimager or densitometer. These data showed that there was significantly more μ2 protein produced during the course of reovirus T1L infection than either clone of reovirus T3D (Fig. 4.1 B). Quantification of the immunoblots showed that the production of μ2 protein in T1L-O- and T3D-A-infected cells peaked at 24 h p.i. (Fig. 4.1 C). T1L μ2 protein expression at this time point was approximately 20-fold and 2-fold more than that produced in T3D-O- and T3D-A-infected cells respectively. In contrast, the expression of μ2 protein in T3D-O-infected cells peaked much later, at 72 h p.i., when it was similar to T3D-A-infected cells but was still less than that in T1L-infected cells (6-fold less). In summary, these findings show that μ2 protein expression in reovirus-infected cells is dependant on the virus strain (T1L vs T3D) as well as the clonal origin in T3D.

4.3.2 Expression level of other reovirus proteins in T1L or T3D-infected L929 cells

The expression level of other reovirus structural proteins was investigated to determine whether the difference in μ2 protein expression between high μ2-expressing T1L-O and T3D-A and low μ2-expressing T3D-O was protein specific. L929 cells were infected with either T1L-O, T3D-A or T3D-O in parallel and samples were collected at 8, 16, 24 and 48 h p.i. The samples were analyzed by immunoblot using a combination of T1L and T3D antisera to ensure equal detection of both T1L and T3D proteins as shown in figure 4.2 for defined quantities of purified T1L and T3D virions (determined by spectrophotometer, 1 OD_{260} = 184.5 μg/ml of virus). T1L-O- and T3D-A-infected cells produced similar amounts of viral proteins during the course of

Figure 4.2 Viral protein expression in L929 cells infected with T1L-O, T3D-O or T3D-A.

(A) L929 cell monolayers were infected with either T1L-O, T3D-O or T3D-A at an MOI of 10 PFU/cell. Cell lysates were collected at different times as indicated and the samples were resolved by SDS-PAGE and immunoblotted with an equal mixture of rabbit anti-reovirus T1L and T3D antibodies and PAAP followed by reaction with NBT/BCIP. End lanes contain 1 μg of purified T1L or T3D viruses as determined by spectrophotometry.

(B) Immunoblot showing specificity of anti-reovirus and anti-μ2 antibodies. Mock-infected L929 cells (M), T1L-infected L929 cells at 48 p.i. (I), Purified T1L virus (V), Trp-E μ2 fusion protein (T) and recombinant μ2 protein expressed in baculovirus (R) were resolved by SDS-PAGE and immunoblotted with either rabbit polyclonal anti-T1L or anti-T1Lμ2 antibody and PAAP followed by reaction with NBT/BCIP.

A

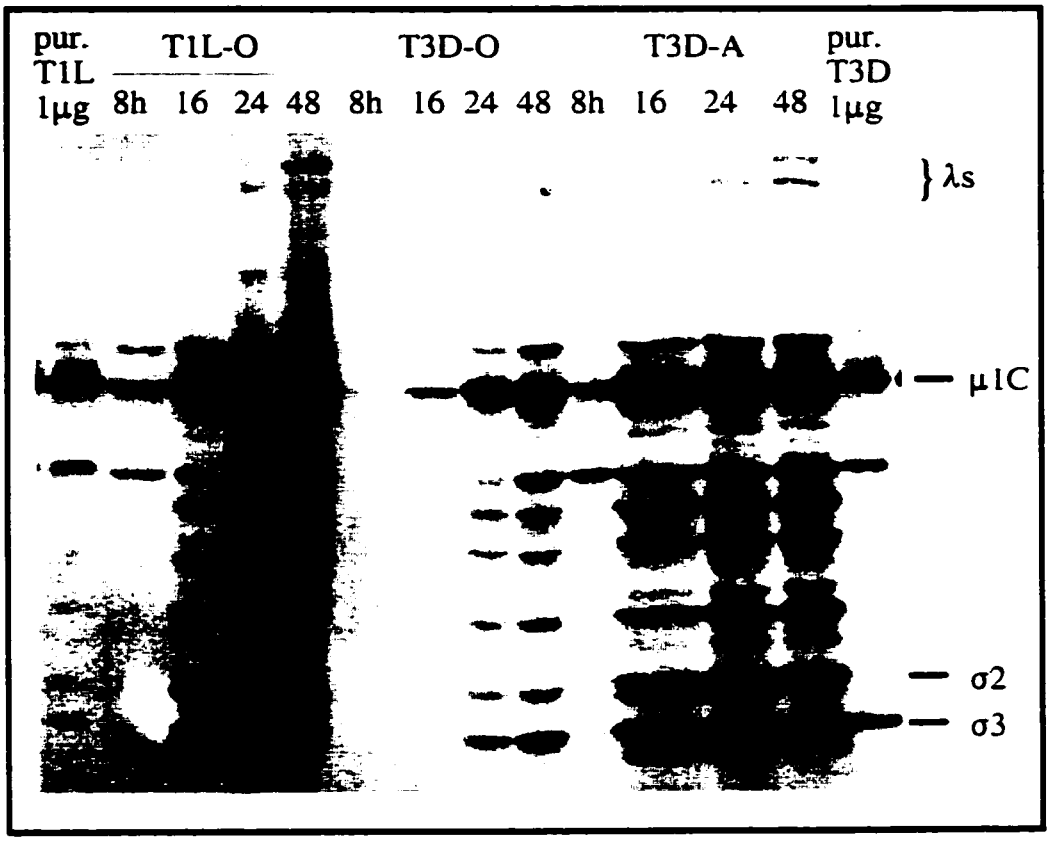
pur. T1L 1μg
T1L-O
8h 16 24 48
T3D-O
8h 16 24 48
T3D-A
8h 16 24 48
pur. T3D 1μg
} λs
— μ1C
— σ2
— σ3

B

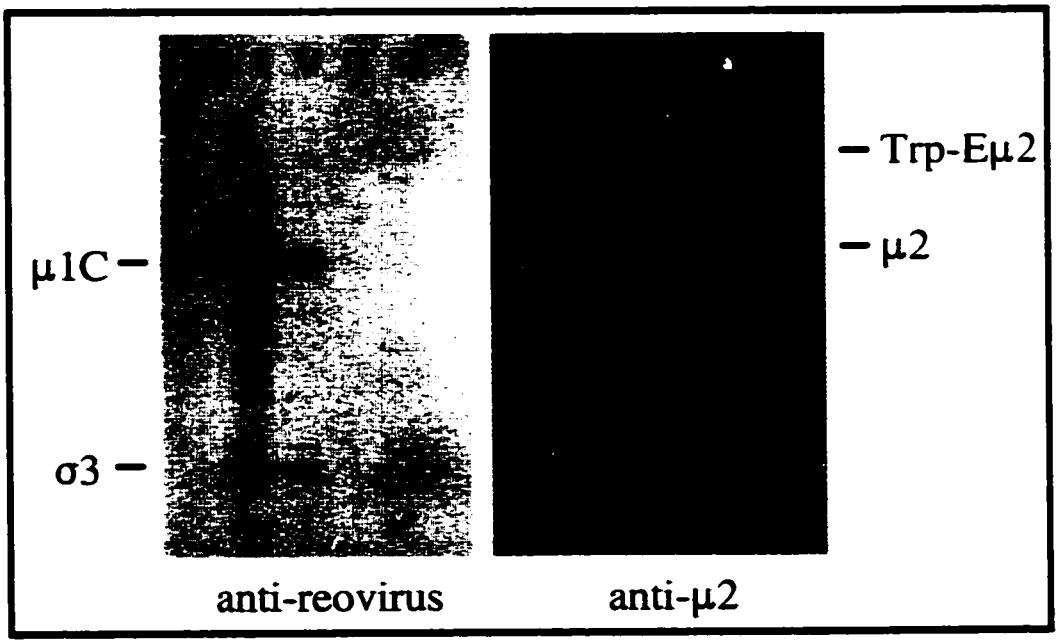
μ1C —
σ3 —
— Trp-Eμ2
— μ2
anti-reovirus
anti-μ2

infection even though the relative proportion of μ2 protein was reduced for T3D-A as determined by comparison of figures 4.1 and 4.2. In contrast, T3D-O-infected cells produced significantly less protein than T1L-O and T3D-A.

The expression of outer capsid proteins μ1C and σ3 was quantified over a 72 h infection period in L929 cells infected with either T1L-O or T3D-O. The samples were collected at different times, resolved by SDS-PAGE and immunoblotted using strain-specific reovirus antiserum. Although μ1C and μ2 proteins co-migrate there is no contribution of μ2 reactivity with the μ1C band since the anti-viral antiserum did not detect μ2 protein (Fig. 4.2 B). Quantification of μ1C and σ3 protein expression was done using a phosphorimager and known quantities of purified reovirus with the amount of μ1C and σ3 proteins determined by comparison with known quantities of BSA by densitometry (data not shown). Serial dilutions of the reference sample were run in parallel for each analysis to ensure that the readings were within the linear range. The data was then expressed as the ratio of T1L-O/T3D-O for both μ1C and σ3 proteins and compared to the ratio of μ2 proteins. These data showed that there was more T1L-O protein produced than T3D-O for both μ1C and σ3 throughout the infection period (Fig. 4.3 A - ratio T1L-O/T3D-O greater than 1). However, the ratio T1L-O/T3D-O protein was highest in μ2 peaking at 24 h p.i. at 20.5, in contrast to that for μ1C which peaked at 5.2 at 12 h p.i. and for σ3, at 12.6 at 16 h p.i. This suggests that μ2 protein expression in T3D-O was reduced relative to other viral proteins compared to T1L. This experiment also showed that the amount of μ2 protein produced in T1L-O-infected cells is comparable to that of μ1C protein, while in T3D-O-infected cells μ2 protein expression is significantly lower than that of μ1C protein (Fig.

Figure 4.3 Comparison of μ2, μ1C and σ3 protein expression in T1L-O- and T3D-O-infected L929 cells.

L929 cell monolayers were infected with either T1L-O or T3D-O at an MOI of 10 PFU/cell. Cell lysates were collected at different times as indicated and the samples were resolved by SDS-PAGE and immunoblotted with either rabbit polyclonal anti-T1Lμ2, anti-reovirus T1L or anti-reovirus T3D sera followed by PAAP. The amount of expression for each protein was determined by comparing the intensity of the band to that of reference proteins, Trp-E-μ2 fusion protein for μ2 protein expression and purified virus for μ1C and σ3 proteins, using a phosphorimager.

(A) Comparison of protein expression between T1L-O and T3D-O for μ2, μ1C and σ3 proteins expressed as the ratio T1L-O/T3D-O.

(B) Comparison of absolute amounts of μ2 and μ1C proteins expressed in T1L-O- or T3D-O-infected cells. * = not done.

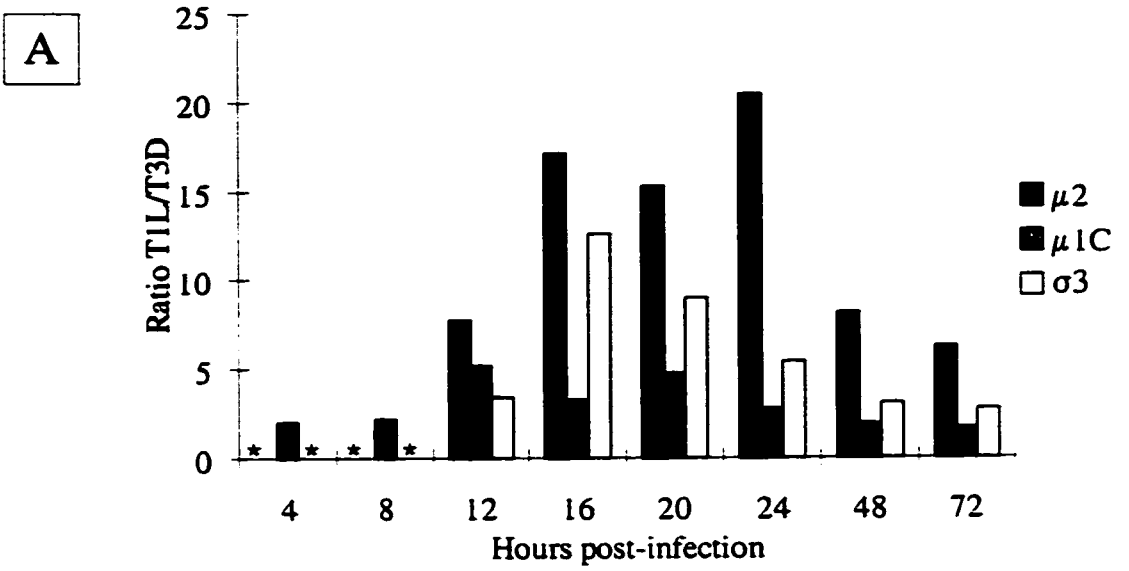
A
25
20
15
10
5
0
Ratio T1L/T3D
μ2
μ1C
σ3
4
8
12
16
20
24
48
72
Hours post-infection

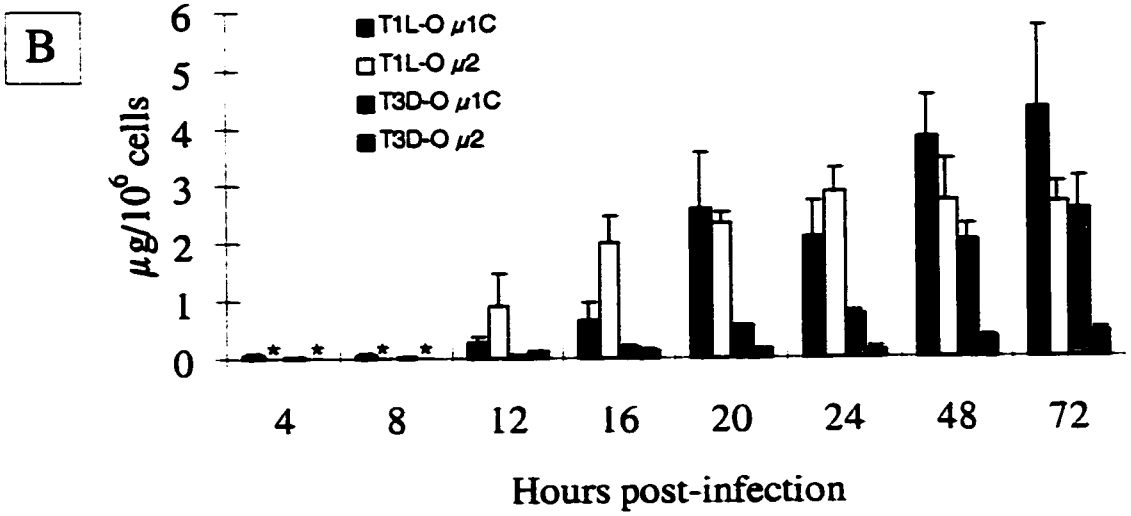
B
6
5
4
3
2
1
0
μg/10^6 cells
T1L-O μ1C
T1L-O μ2
T3D-O μ1C
T3D-O μ2
4
8
12
16
20
24
48
72
Hours post-infection

4.3 B).

In summary, infection of L929 cells resulted in higher protein expression with T1L-O than T3D-O, and of the three proteins quantified, the greatest difference in protein expression was in μ2 protein that was reduced in the T3D relative to T1L. Furthermore expression of μ2 protein in T1L-O-infected cells was very high, being comparable to that of the abundant major structural protein μ1C.

4.3.3 Relative quantification of M1 and S4 mRNA

One explanation for the difference in protein expression level of T1L-O relative to T3D-O is that they differ in the extent of transcription, producing different amounts of mRNA. To test this theory the relative amounts of M1 and S4 mRNA produced during infection of L929 cells with either T1L-O or T3D-O was quantified using a competitive RT-PCR assay. This assay makes use of unique restriction sites to differentiate particular T1L and T3D gene segments as has been used in other systems (Bailly and Brown, 1998; Lin *et al.*, 1991; Becker-Andre and Halbrook, 1989). Control experiments using cDNA from the same gene segment of two different viral strains showed that the mixing of defined quantities of cDNA accurately determines the ratios of cDNA mixtures at the start of the PCR reaction (data not shown; Bailly and Brown, 1998; Cottrez *et al.*, 1994). L929 cells were infected in parallel with either T1L-O or T3D-O at an MOI of 10 PFU/cell, subsequently lysed and immediately mixed in the same tube for each of the different time points. Total RNA was then purified and cDNA was made for each gene segment using negative sense primers complementary to regions of complete sequence homology

between T1L and T3D gene segments. The cDNA was then amplified using the same negative sense primer as above and a plus sense primer also directed to a region of complete sequence homology between T1L and T3D gene segments. One of the primers was radioactively end-labeled and the PCR products were subsequently digested using the strategy outlined in figure 4.4, resolved by SDS-PAGE and exposed for autoradiography (Fig. 4.5 A). The quantity of each T1L and T3D PCR product was determined by excision and scintillation counting. The results were expressed as the ratio of T1L mRNA/T3D mRNA and compared to the corresponding protein ratios. These experiments showed that the majority of the difference in the amount of μ2 protein expressed is accounted for by the difference in the relative amount of M1 mRNA produced by the two viruses (Fig. 4.5 B). However, a fraction of the difference in expression could result from factors independent from transcription such as a better translation efficiency of the T1L M1 mRNA or stability of the T1L μ2 protein. In contrast, the difference in σ3 protein expression is more than accounted for by the difference in the amount of S4 mRNA produced by the two viruses (Fig. 4.5 C). In fact, the S4 mRNA ratio is slightly higher than the σ3 protein ratio suggesting a contribution from other factors independent of transcription that may affect the ratio of σ3 protein.

4.3.4 Difference in stability of T1L and T3D μ2 proteins

To assess whether protein degradation, in addition to mRNA expression, plays a role in the amount of μ2 protein expressed in T1L- or T3D-infected cells, the stability of T1L and T3D μ2 proteins in infected cells in the absence of protein synthesis was investigated. Two methods were used to assess μ2 protein stability in infected cells. The first method involved

Figure 4.4 Restriction digestion strategy for discriminating T1L from T3D M1 and S4 mRNA coamplified by RT-PCR.

PCR products were digested with HaeIII to generate strain-specific restriction fragments. Radioactively labeled fragments are indicated with stars. The positions of restriction sites and nucleotide positions of each amplicon are numbered (in bp).

M1 Gene

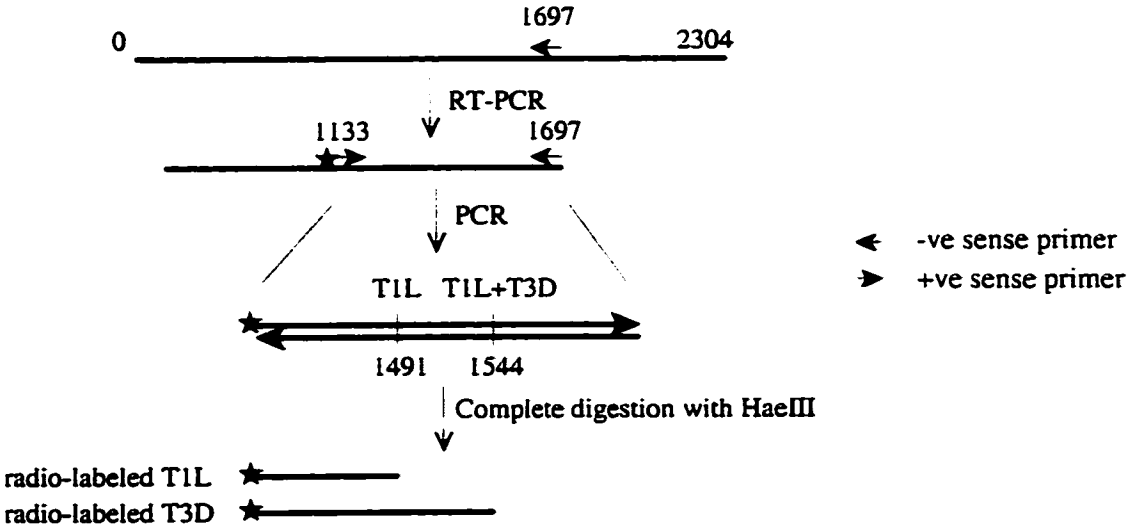

S4 Gene

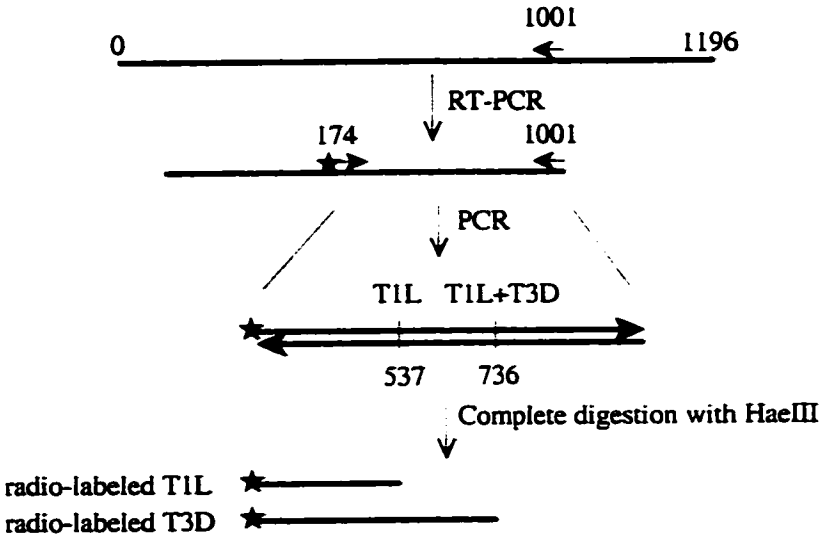

Figure 4.5 Relative levels of M1 and S4 mRNA expression in T1L-O- and T3D-O-infected L929 cells.

(A) Gel electrophoresis of radioactively end-labeled cDNA following RT-PCR and restriction digestion of M1 mRNA from L929 cells infected with T1L-O or T3D-O. L929 cell monolayers were infected with either T1L-O or T3D-O at an MOI of 10 PFU/cell. Total mRNA was extracted at 8, 16, 24 or 48 h p.i. and same time point samples from the two strains immediately mixed in the same tube. cDNA was made by reverse transcription using segment specific primers and amplified by PCR with one of the primers radioactively end-labeled. This was followed by restriction digest using HaeIII to yield strain-specific gene segments which were resolved by SDS-PAGE. The gel was then processes for autoradiography.

(B) Bar graph comparing the ratios of mRNA and protein expression of the M1 gene between T1L-O and T3D-O.

(C) Bar graph comparing the ratios of mRNA and protein expression of the S4 gene between T1L-O and T3D-O.

mRNA ratios were calculated by excision of the bands from the gel and scintillation counting. Protein ratios were calculated from the data in Fig. 4.1 and 4.3. * = not done.

A

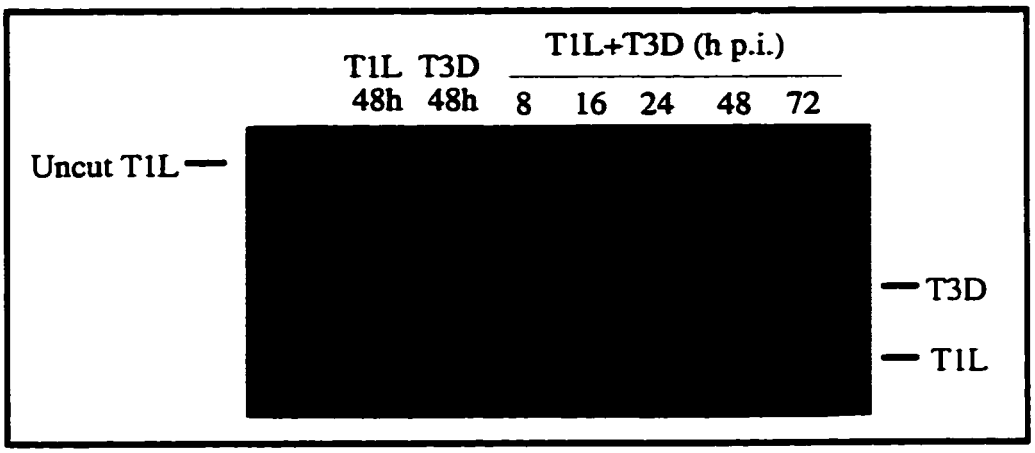
T1L 48h
T3D 48h
T1L+T3D (h p.i.)
8
16
24
48
72
Uncut T1L
T3D
T1L

B

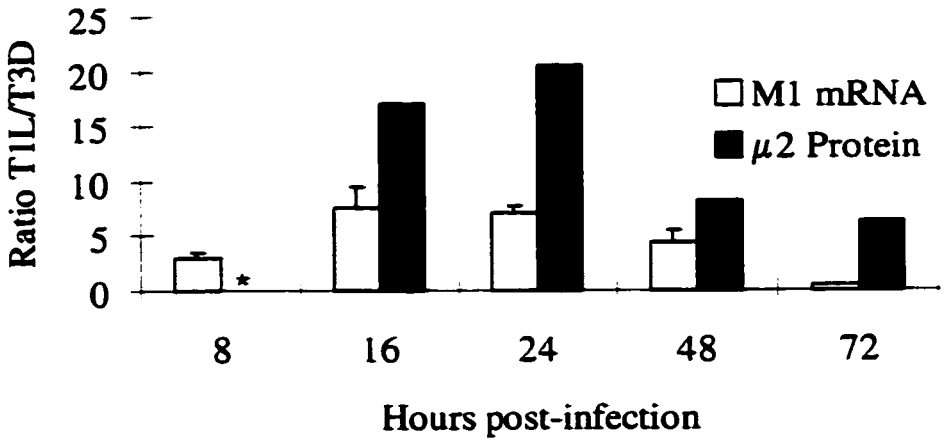
Ratio T1L/T3D
25
20
15
10
5
0
M1 mRNA
μ2 Protein
*
8
16
24
48
72
Hours post-infection

C

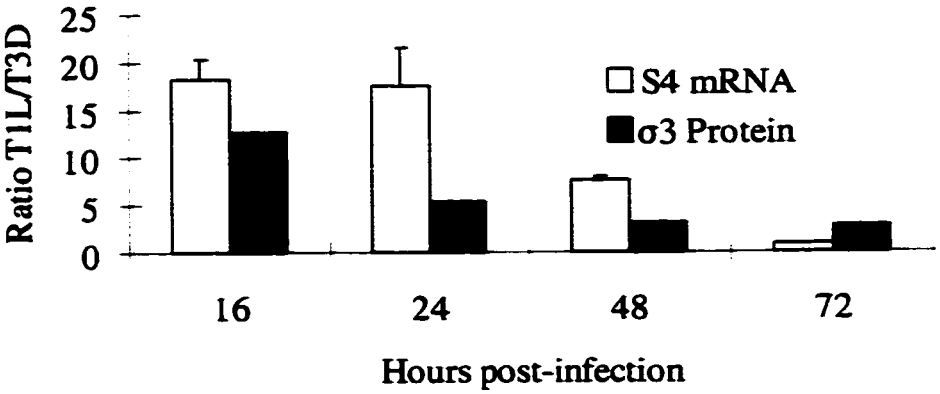
Ratio T1L/T3D
25
20
15
10
5
0
S4 mRNA
σ3 Protein
16
24
48
72
Hours post-infection

radioimmunoprecipitation assay (RIPA) of the nonionic detergent soluble cellular fraction of the protein. This excludes the insoluble fraction of μ2 protein that localizes to the nucleus or viral inclusions because the nuclei and, to some extent, viral inclusions are resistant to detergent extraction (Gomatos, 1967; Mora *et al.*, 1987; Capco *et al.*, 1982; He *et al.*, 1990). L929 cells were infected with either T1L-O or T3D-A for 20 h before pulse radiolabeling for 4 h and chased in the presence of cycloheximide (100 μg/ml) to inhibit protein synthesis. Samples were taken at this time (T=0) and subsequently every 8 h until 40 h after cycloheximide treatment (*i.e.* 64 h p.i.). The samples were immunoprecipitated using rabbit anti-μ2 polyclonal antiserum, resolved by SDS-PAGE and processed for autoradiography. The amount of soluble T3D-A μ2 protein decreased faster than that of soluble T1L-O μ2 protein in infected cells (Fig. 4.6 A). Quantification by excision of the bands and scintillation counting gave a half-life of 7.6 h for T3D-A μ2 compared to 38.0 h for T1L-O μ2. The decrease in μ2 protein in T3D-infection was not due to cell loss because 92 ± 4.2 % of cells were still present compared to 98 ± 6.3 % of cells in T1L-infected cells, 24 h after cycloheximide treatment. The cell recovery was measured by quantifying the amount of a stable cellular protein after cycloheximide treatment in both T1L and T3D-infected cells (Fig. 4.6 B, lower panel). The half-life of T3D-O μ2 protein was 9.2 h which was similar to that of T3D-A μ2 protein. These results suggest that T3D μ2 protein has either decreased stability and/or localizes to the insoluble fraction faster compared to T1L μ2 protein.

To investigate this further the stability of μ2 protein was assessed using an immunoblot assay that quantifies total μ2 protein in infected cells. Cells were infected with T1L-O or T3D-A for 20 h and then chased in the presence of cycloheximide for various times up to 60 h. The

samples were resolved by SDS-PAGE and immunoblotted using rabbit anti-μ2 polyclonal antiserum (Fig. 4.6 B). Following quantification by phosphorimaging, the T3D μ2 protein was found to be less stable compared to T1L μ2 protein with half-lives of 27.6 h and ~60.0 h, respectively. The half-life of total T3D μ2 protein was longer than that of the soluble fraction indicating that the soluble half-life is in part due to movement of μ2 into the insoluble fraction, as well as protein degradation. Taken together these results suggest that not only is T3D μ2 protein less stable but it also translocates into the insoluble fraction more rapidly than T1L μ2 protein.

Consistent with this, fractionation of T1L- and T3D-infected cells into soluble and insoluble fractions at 24 h p.i. showed that a higher proportion of T3D μ2 protein is present in the insoluble fraction than T1L μ2 protein (Fig. 4.6 C). Quantification by phosphorimaging showed that 7-fold more μ2 is present in the insoluble fraction compared to the soluble fraction in T3D-infected cells whereas in T1L-infected cells only 2-fold more μ2 is present in the insoluble fraction compared to the soluble fraction (Table 4.1). The amount of T1L μ2 protein present in the insoluble fraction increases further by 48 h p.i. whilst that of T3D μ2 protein had peaked at 24 h p.i. This further supports the concept that T3D μ2 protein translocates to the insoluble fraction faster than T1L μ2 protein.

Figure 4.6 Analysis of μ2 protein stability in T1L- and T3D-infected L929 cells by RIPA and immunoblot assay.

(A) RIPA: L929 cell monolayers were infected with either T1L-O or T3D-A at an MOI of 10 PFU/cell and radioactively labeled at 20 h p.i. for 4 h followed by addition of cycloheximide to block protein synthesis and chased for the period of times indicated. The samples were immunoprecipitated using polyclonal rabbit anti-T1L μ2 antibody, resolved by SDS-PAGE and processed for autoradiography.

(B) Immunoblot assay: L929 cell monolayers were infected with either T1L-O or T3D-A at an MOI of 10 PFU/cell and cycloheximide was added to the growth media at 20 h p.i. to block protein synthesis and μ2 protein was chased for the period of times indicated. The samples were resolved by SDS-PAGE and immunoblotted using polyclonal rabbit anti-T1L μ2 antibody and PAAP followed by reaction with the phosphofluorescent substrate Attophos. The blot below shows a stable L929 cell protein chased for the same period of time and stained with coomassie blue as a control for cell viability.

(C) Immunoblot showing μ2 protein in the soluble and insoluble fractions of T1L- or T3D-infected cells. L929 cells were infected for 24 or 48 h and fractionated into soluble and insoluble fractions by nonionic detergent treatment and sedimentation. The samples were resolved by SDS-PAGE and immunoblotted using polyclonal rabbit anti-T1L μ2 antibody and PAAP followed by reaction with Attophos.

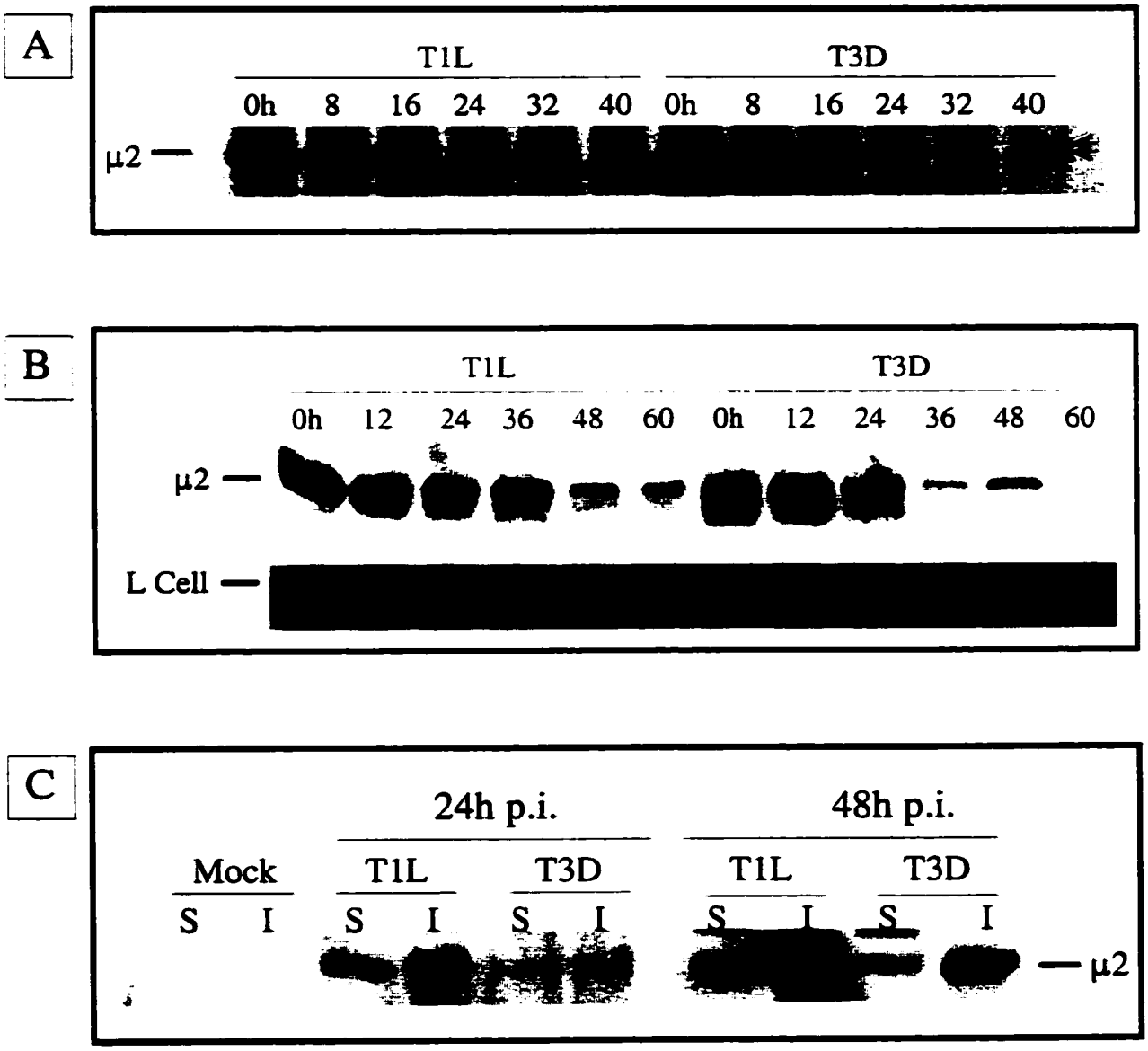
A
T1L
T3D
0h 8 16 24 32 40 0h 8 16 24 32 40
μ2
B
T1L
T3D
0h 12 24 36 48 60 0h 12 24 36 48 60
μ2
L Cell
C
24h p.i.
48h p.i.
Mock
T1L
T3D
T1L
T3D
S I S I S I S I S I
μ2

Table 4.1 Quantification of the amount of μ2 protein in soluble and insoluble fractions of T1L- and T3D-infected cells

Virus strain	Time (h p.i.)	Percentage of protein in soluble fraction	Percentage of protein in insoluble fraction	Ratio (insoluble/ soluble)
T1L	24	31.3 ± 2.1	68.7 ± 2.1	2.2
	48	14.9 ± 8.6	85.1 ± 8.6	5.7
T3D	24	12.25 ± 1.25	87.75 ± 1.25	7.2
	48	15.7 ± 0.1	84.3 ± 0.1	5.4

4.3.5 Rate of viral inclusion formation and viral yield is independent of viral protein expression

In the previous chapter it was shown that the M1 gene controls the difference in the rate of viral inclusion formation between T1L and T3D, with T3D having a faster rate. To test whether differences in extent of viral protein expression correlate with rate of viral inclusion formation, inclusion formation in T1L-O-, T3D-O- and T3D-A-infected HeLa cells was investigated by indirect immunofluorescence staining of μ2 protein at 24 h p.i. It was shown in Chapter three that μ2 protein localizes to viral inclusions together with other viral proteins and that 24 h p.i. is the point of maximal difference in the rate of viral inclusion formation between T1L- and T3D-infected cells. Immunofluorescent staining showed that both T3D clones were similar in their rapid rate of viral inclusion formation and cellular localization of the μ2 protein (Fig. 4.7 C and D). The rate of viral inclusion formation in both T3D clones was faster than

Figure 4.7 Viral protein expression is not directly related to rate of viral inclusion formation and yield.

HeLa cells were either mock-infected (A) or infected with T1L-O (B), T3D-A (C) or T3D-O (D) at an MOI of 10 PFU/cell for 24 h and fixed in acetone. The cells were stained with polyclonal rabbit anti-T1Lμ2 antibody and Cy3-conjugated donkey anti-rabbit and visualized using an epifluorescence microscope. The bar represents 10 μm.

(E) L929 cell monolayers were infected with either T1L-O, T3D-O or T3D-A at an MOI of 10 PFU/cell. Virus was harvested at different times as indicated by three freeze-thaw cycles and titrated in L929 cells. Error bars denote the standard error of the mean of at least two different experiments.

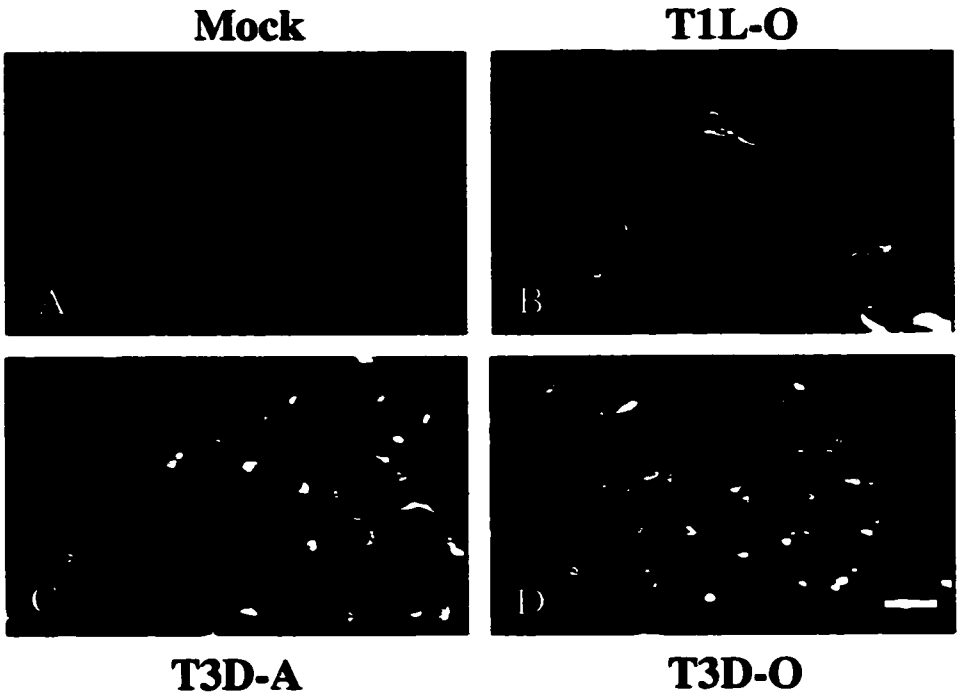
Mock
T1L-O
A
B
C
D
T3D-A
T3D-O

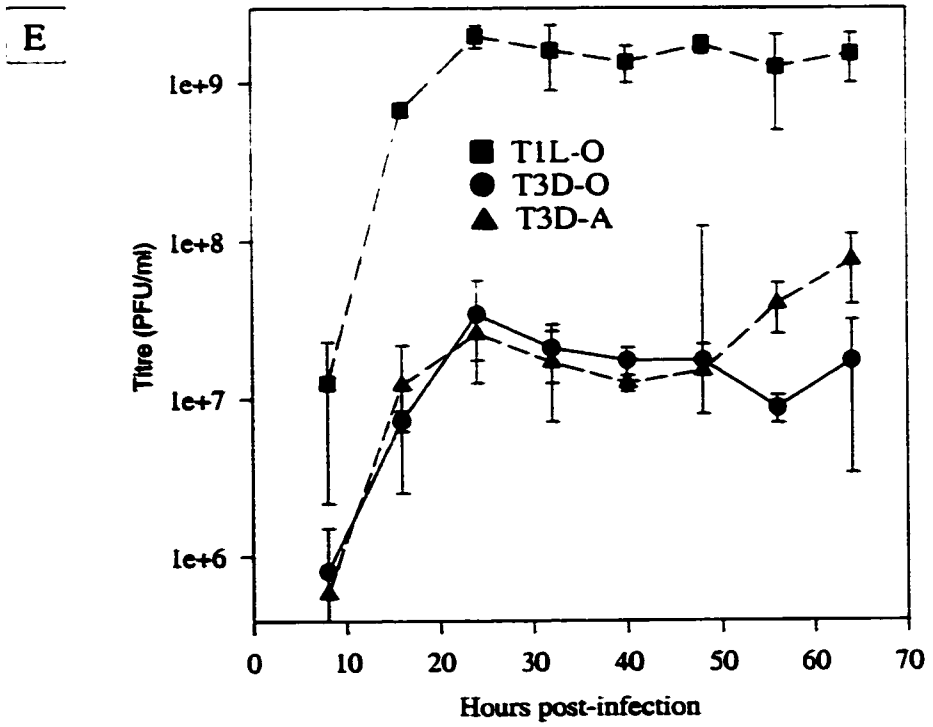
E
1e+9
1e+8
1e+7
1e+6
Titre (PFU/ml)
T1L-O
T3D-O
T3D-A
0
10
20
30
40
50
60
70
Hours post-infection

T1L-O which showed minimal inclusion formation at 24 h p.i. (Fig. 4.9 B).

The growth of the three viruses in infected L929 cells was also assessed by plaque assay. This showed that T1L-O grew to greater than 10-fold higher titer compared to both T3D clones (fig. 4.7 E). Comparison of the two T3D clones showed that T3D-A grew to a significantly higher titer than T3D-O, approximately 5-fold more at 64 h p.i. However, the two T3D clones were similar in growth at earlier times up to 48 h p.i. Since T1L-O and T3D-A produced about the same amount of protein which was significantly higher than that of T3D-O, these results indicate that viral yield as well as inclusion formation is not directly dependant on extent of protein expression.

4.4 Discussion

Analysis of the role of the M1 gene in the formation of viral inclusion bodies in Chapter three, indicated that the laboratory virus strains of reovirus T1L and T3D differed in their ability to express the M1 gene-encoded μ2 protein. That finding was extended in this chapter by characterizing the level of expression of the minor capsid protein μ2 in comparison with the most abundant outer capsid proteins μ1C and σ3 among clonal isolates of the above prototype strains obtained after four serial passages in mouse L cells. These experiments show that μ2 protein is expressed at more than catalytic amounts in infected cells, especially in T1L-infected cells and that expression of μ2 protein in reovirus-infected cells is strain- and clone-dependent.

The most abundant reovirus capsid proteins are μ1C and σ3 that are present at 600 copies/virion, 30 times greater than the amount of μ2 protein (18 copies/virion) (Coombs, 1998). Experiments in this chapter demonstrate that μ2 is expressed during T1L infection at very high levels that are similar to the most highly expressed outer capsid protein μ1C where large amounts are needed for virion production. The high level expression of μ2 protein is in contrast to previous reports (Gaillard and Joklik, 1985; Roner *et al.*, 1989). The reason for high expression of such a minor structural protein is unclear but it suggests that high levels of the protein may be required for other functions during the reovirus replication process, in addition to its structural and catalytic roles in the virus particle. The high expression level of μ2 protein opens the possibility of stoichiometric interactions with other viral or host structures during reovirus replication including the process of assembly of viral inclusion bodies.

Even though the expression level of μ2 protein was consistently high in all cells infected with different clones of T1L, it was significantly lower and varied in cells infected with different clones of T3D. In addition, the relative amount of μ2 protein expressed in T3D clones was uniformly lower than that of μ1C and σ3 proteins compared to T1L. For example, in clone T3D-A that produced levels of viral proteins that were high and comparable to T1L, the level of μ2 was reduced by 2- to 3-fold relative to T1L (Fig. 4.1 and 4.2). Since T3D μ2 protein is linked to a faster rate of inclusion formation than T1L μ2 protein this suggests that the T3D μ2 may have enhanced activity relative to the T1L μ2 and as a result more T1L μ2 protein is required to accomplish the same function compared to T3D μ2 protein. Recombinant T3D μ2 protein also forms protein complexes at a faster rate than T1L μ2 protein in M1 gene-transfected cells (see

Chapter three).

mRNA expression level was shown to be the main factor accounting for differences in protein expression between T1L-O and T3D-O. However, protein stability was also shown to play an additional role in μ2 protein expression levels. It was shown that T3D μ2 protein is less stable than T1L μ2 protein with the former having a half-life of 27.6 h and the latter of >60.0 h. This indicates that one of the reasons for the low expression of T3D μ2 protein is its accelerated degradation and that this may influence the difference in μ2 protein accumulation between T1L and T3D relative to the other viral proteins. Interestingly, it is inherently more difficult to constitutively express T3D μ2 protein than T1L μ2 protein, which is consistent with the reduced stability of T3D μ2 (Zou and Brown, 1996a). The proposed higher specific activity of T3D μ2 protein could also be a determining factor for its accelerated degradation compared to T1L μ2 protein where its removal may be a mechanism for modulating its overall activity level. The protein levels and activities of several important cellular regulatory proteins are controlled by Ub modification and degradation by the multi-subunit 26S proteasome (Hochstrasser, 1996; Ciechanover, 1998). The appearance of slower migrating bands in addition to the μ2 protein band at regular intervals following pulse-chase and immunoprecipitation with μ2-specific antibody (Fig. 4.8 A arrows) resembles Ub conjugation. T1L and T3D μ2 proteins are very conserved differing at only ten amino acid (aa) positions out of 736 (Wiener *et al.*, 1989; Zou and Brown 1992). One or more of the ten aa substitutions between T1L and T3D μ2 proteins could be critical for the stability of the protein.

Interestingly, the half-lives of the soluble fraction of the μ2 proteins were shorter, especially for T3D μ2 protein, 7.6 h compared to 38.0 h for T1L μ2. Since the soluble fraction excludes the protein present in viral inclusions and the nucleus, these results suggest a faster localization of T3D μ2 protein to viral inclusions and/or nucleus. Comparison of the amount of μ2 protein in the soluble and insoluble fractions in T1L- and T3D-infected cells showed that 1/8 of T3D μ2 protein was present in the soluble fraction at 24 h p.i. compared to 1/3 for T1L μ2 protein. The proportion of T1L μ2 protein in the soluble fraction decreased to 1/6 at 48 h p.i. being similar to that of T3D μ2 protein. The greater relative abundance of T3D μ2 protein in the insoluble fraction thus could be a combined function of greater degradation of soluble μ2 protein and faster translocation to the viral inclusions. A faster rate of localization of the T3D μ2 to viral inclusions is consistent with the faster rate of viral inclusion formation for T3D compared to T1L.

The biological heterogeneity of T3D clones with respect to gene expression is cause for concern with respect to comparing data from different laboratories. However, it was reassuring to observe that clones that differed markedly in gene expression, clones T3D-O and T3D-A were similar in the biological properties of growth and ability to rapidly form viral inclusion bodies. When the viral yield of the two clones was compared in L929 cells, it was shown that they both had similar yields at earlier times during infection. Difference in yield was seen late in infection, after 48 h p.i. with T3D-A producing up to 5-fold more virus than T3D-O. This indicates that the extent of protein synthesis was not limiting at early times. Interestingly, both T3D clones formed viral inclusions at a faster rate than T1L. Taken together these results indicate that viral growth, in addition to the rate of viral inclusion formation, is not primarily influenced by the level

of viral protein expression but is more a function of viral protein activities. It will be interesting to determine the basis for the difference in viral protein expression between the T3D clones. Possible explanations include differences in transcription as well as interactions with host defense mechanisms such as interferon induction and sensitivity that has implicated the M1 and L1 genes (Sherry *et al.*, 1998). The biological heterogeneity of T3D relative to T1L mirrors the differences in genetic stability seen for these two strains on serial undiluted passage where clones of T3D readily formed defective interfering populations that accumulated deletion mutants and established persistent infections whereas T1L clones did not (Brown *et al.*, 1983).

The biological effect of a given gene product is a function of its specific activity, expression level as well as factors that influence bio-availability such as cellular localization. The extent and timing of viral protein expression in virus-infected cells is a controlled process to ensure that proteins are expressed at the right times and in adequate amounts for the viral replication cycle. Expression level and cellular localization in infected cells may be critical aspects of regulating μ2 protein functional activity during infection.

CHAPTER FIVE

ROLE OF THE UBIQUITIN-PROTEASOME PATHWAY (UPP) IN μ2 PROTEIN DEGRADATION AND REOVIRUS INCLUSION FORMATION

5.1 Introduction

The data in the last two chapters shows that μ2 protein controls the rate of viral inclusion formation and that its expression in infected cells is strain-dependent. One of the factors contributing to the difference in μ2 protein expression between T1L and T3D is protein stability. T3D μ2 protein which forms inclusions at a faster rate than T1L μ2 protein, was shown to be less stable than T1L μ2 protein. The mechanism behind μ2 protein degradation is unknown, neither is the mechanism involved in reovirus inclusion formation. It is hypothesized that reovirus, like other viruses, uses preexisting cytoskeleton-dependent cellular mechanisms to transport its macromolecules. Reovirus would therefore be predicted to possess targeting signals similar to those of host cell components. Correspondingly, degradation of reovirus μ2 protein is possibly accomplished by normal cellular protein degradation mechanisms.

The principal intracellular nonlysosomal system for protein degradation is the Ub-proteasome pathway (UPP). This system has also been shown to play a role in assembly and budding of a number of enveloped RNA and DNA viruses. In this chapter, it is shown that μ2 protein is ubiquitinated and degraded by the 26S proteasome and that the nonenveloped reovirus uses the UPP for reovirus inclusion formation and viral assembly. It is also demonstrated that

reovirus inclusions are structurally similar to aggresomes, and that reovirus inclusions, impair the normal functioning of the UPP resulting in inhibition of Ub-dependent proteolysis and possibly contributing to cell death. The data also suggests that the control of the rate of reovirus inclusion formation by μ2 protein could in part be due to its interactions with the UPP.

5.2 Materials and Methods

5.2.1 Cells and viruses

Human embryonic kidney (HEK) 293 cells stably expressing the reporter protein GFP^u, with the short degron CL1 fused to the C-terminus of green fluorescent protein (GFP) were a kind gift from R. Kopito (Stanford University, CA). The A549 cell lines, A549-wtUb and A549-K48R, expressing wild type Ub and K48R mutant Ub were a kind gift from D. Gray (University of Ottawa). The Indiana serotype of VSV used in this study was obtained from Y. Kang.

5.2.2 Indirect immunofluorescence

To enable staining for γ-tubulin, cells were extracted for 2 min in 0.25% Triton X-100 in PEM buffer (80 mM PIPES, 5 mM EGTA and 1 mM $MgCl_2$) and fixed for 15 min in a 4:1 (v/v) mixture of methanol and acetone at - 20^{0}C. Cells to be stained for hsp-70 were fixed in Fix-Extract solution (PEM buffer, 3.7% formaldehyde, 0.5% Triton X-100 and 0.25% glutaraldehyde). After rinsing in PBS the cells were soaked in fresh solution of 1 mg/ml sodium borohydrate in PBS to reduce the free aldehyde groups followed by a further rinse in PBS. All cells were stained as described in section 2.3.

5.2.3 Proteasome inhibitor experiments

Parallel monolayer cultures of HeLa cells grown in 6-well plates or on 22x22 mm glass coverslips (Corning Inc.) in 6-well plates were mock-infected or infected with T1L or T3D at an MOI of 10 PFU/cell for various intervals. This was followed by incubation for 4 h with either medium alone, medium plus the proteasome inhibitor, PSI (Calbiochem-Novabiochem Corp.) at 50 μM or medium plus PSI and cycloheximide (CHX) at 100 μg/ml. Where indicated the cells were allowed a period of recovery by a further 2 h incubation in fresh medium. The samples were either harvested in SDS sample buffer for immunoblot analysis, by three cycles of freeze-thaw for plaque assay or fixed in acetone for immunofluorescence staining.

5.2.4 *In vitro* translation and protein degradation assays

The T3D M1 gene subcloned into pGEM vector under a T7 bacteriophage promoter (clone T3-18) (Zou and Brown, 1996b) was digested with HindIII to create run-off transcripts and purified using QIAquick Gel Extraction Kit (Qiagen). The digested and purified M1 cDNAs were transcribed and translated using the TnT T7 coupled reticulocyte lysate system (Promega) in the presence of [^{35}S]met, [^{35}S]cys (NEN, Boston, MA) and T7 RNA polymerase for 90 min at 30^{0}C in 50 μl final volume. Conjugation and degradation assays contained 10 μl of translation reaction, 25 μl of crude reticulocyte lysate and was made up to 50 μl with either 50 μM PSI , or 15 μg Ub (Sigma) plus 2 mM ATP, or 15 μg Ub plus 5 mM ATP-γ-S (Sigma), or dH20. Degradation and conjugation assays were carried out at 37^{0}C for 2 h and the reactions were terminated by the addition of an equal volume of 2X SDS sample buffer and resolved by SDS-PAGE. The gel was then fixed and processed for autoradiography.

5.2.5 Flow cytometry and intracellular staining

GFP^u-expressing HEK cells were grown in adherent culture to a monolayer in 6-well plates and were either treated with PSI, mock-infected or infected with reovirus or VSV at an MOI of 10 PFU/cell. The cells were harvested by treatment with 1 ml PBS containing 0.5 mM EDTA and transferred to 5 ml FACS analysis tubes. The cells were washed twice in 1 ml FACS buffer (1% BSA and 0.1% sodium azide in PBS) by centrifugation at 300g for 5 min at 4^{0}C. After the final wash the pellet was resuspended in 0.5 ml FACS analysis buffer and either stored at 4^{0}C for a maximum of 24 h or immediately analyzed by flow cytometry with EXPO32 v1.2 analysis software (Beckman Coulter, Inc.) for a total of 30,000 events gated on viable cells by forward/side scatter. For intracellular staining, the cells were permeabilized and fixed using the IntraPrep™ Permeabilization Reagent kit (Immunotech) and stained following the manufacturer's procedure for staining using unconjugated primary antibody. The secondary antibody used was PE-conjugated goat anti-mouse IgG Fc (Immunotech, Marseille, France).

5.3 Results

5.3.1 Degradation of reovirus μ2 protein via the Ub-proteasome pathway

Experiments in the previous chapter showed that reovirus T3D μ2 protein is degraded faster than reovirus T1L μ2 protein. During chase experiments, the appearance of evenly spaced, μ2 antibody reactive bands that migrated slower than μ2 protein were observed suggesting that the protein might be polyubiquitinated. To investigate whether μ2 protein is ubiquitinated and degraded by the 26S proteasome, parallel cultures of T3D-infected HeLa cells at 20 h p.i. were either left untreated or treated with PSI, a peptidyl aldehyde inhibitor of the proteasome, for 4

h, resolved by SDS-PAGE and analyzed by immunoblot. The treatment of HeLa cells with PSI resulted in the accumulation of polyubiquitinated proteins seen as a heavy smear of high molecular weight proteins compared to untreated cells in both mock- and T3D-infected cells when detected by immunoblot using a Ub-specific polyclonal antibody (Fig. 5.1 A; Wojcik *et al.*, 1996). The treatment of cells with cycloheximide (CHX), which blocks protein synthesis, resulted in a decrease in the accumulation of polyubiquitinated proteins, in cells simultaneously treated with PSI (Fig. 5.1 A). Immunoblotting of the same samples with a μ2-specific rabbit polyclonal antibody showed that in addition to the main μ2 protein band (~80 kDa) there were slower migrating, evenly spaced bands of approximately 8.5 kDa increments in T3D-infected cells treated with PSI (Fig. 5.1 B). These bands were not detected in T3D-infected cells without treatment with PSI or cells treated with PSI and CHX, suggesting that μ2 protein is polyubiquitinated. Several μ2-specific peptides of smaller apparent molecular weight were also seen consistent with proteolytic degradation.

Degradation of μ2 protein by the 26S proteasome was confirmed further using a cell free reticulocyte lysate-based proteolysis system. Ub-dependent proteolysis occurs in reticulocyte lysates when supplemented with Ub and ATP, because they contain all the enzymes required for ubiquitination as well as proteasomes (Orian *et al.*, 1995; Abu-Hatoum *et al.*, 1998). Following μ2 protein translation in reticulocyte lysates for 90 min, the sample was divided into four aliquots and supplemented with either PSI, Ub plus ATP, Ub plus ATP-γ-S, or dH_20 and incubated for a further 2 h. ATP-γ-S has been shown to support the activity of E1 enzyme but not that of the 26S proteasome resulting in inhibition of protein degradation and accumulation of

Figure 5.1 *In vivo* and *in vitro* ubiquitination and degradation of reovirus μ2 protein.

Parallel monolayer cultures of HeLa cells were mock infected or infected with T3D for 20 h. This was followed by incubation for 4 h with either medium alone, medium plus PSI or medium plus PSI and CHX. The samples were resolved by SDS-PAGE and immunoblotted using polyclonal rabbit anti-Ub (A), polyclonal rabbit anti-μ2 (B), polyclonal rabbit anti-σNS (C), polyclonal rabbit anti-μNS (D), or polyclonal rabbit anti-T3D (E) followed by a goat anti-rabbit-alkaline phosphatase. The blots were then reacted with Attophos. (F) μ2 protein was expressed in an *in vitro* coupled transcription and translation system using T3D M1 cDNA run off transcripts for 90 min. The sample was then divided into equal parts and supplemented with either PSI, Ub plus ATP, Ub plus ATP-γ-S or dH_2O and incubated for 2 h. The samples were resolved by SDS-PAGE, and processed for autoradiography. The bands were quantified by densitometry and the values shown at the bottom of each lane expressed as a fraction of the control sample (dH_2O).

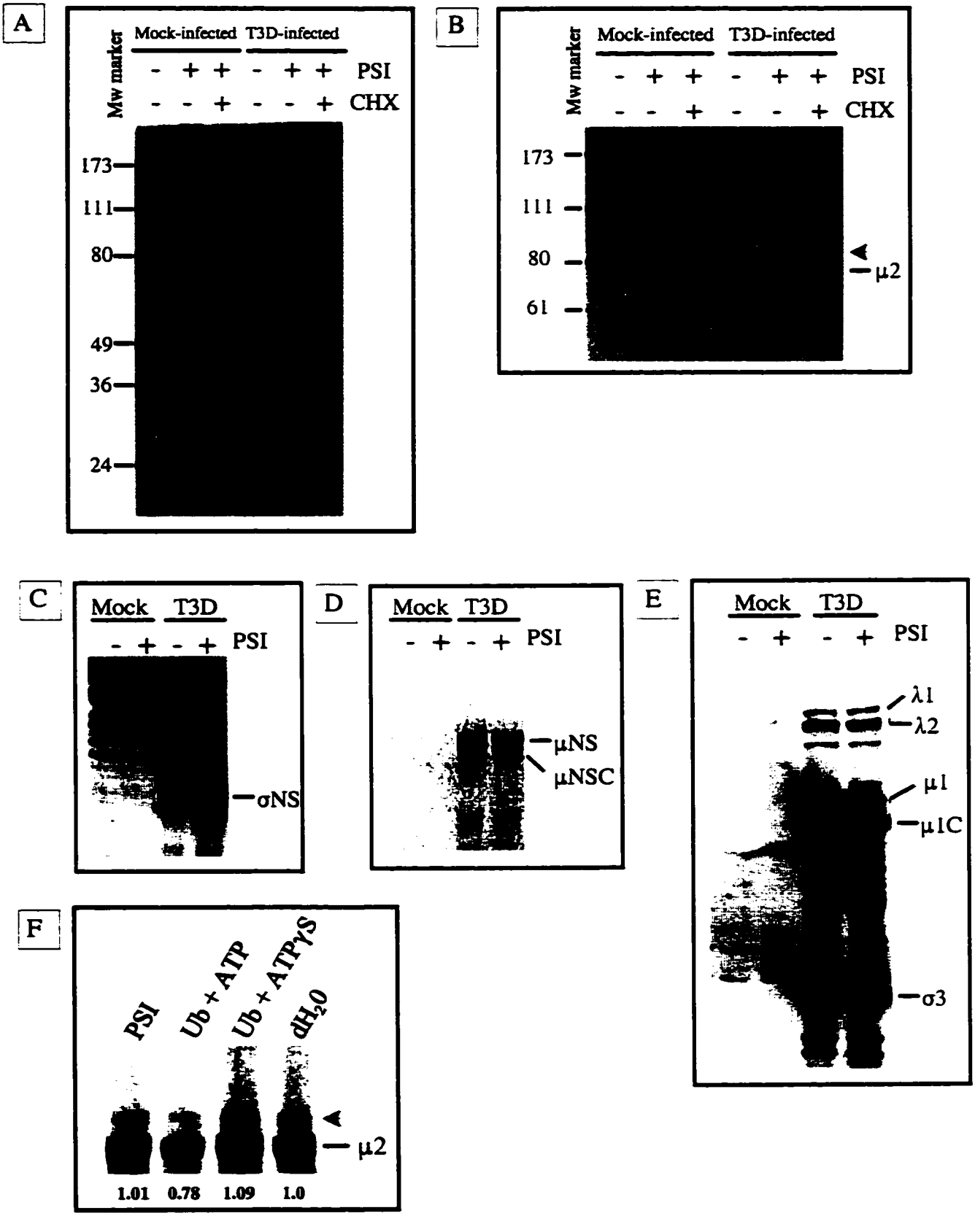
A
Mock-infected
T3D-infected
Mw marker
- + + - + + PSI
- - + - - + CHX
173
111
80
49
36
24
B
Mock-infected
T3D-infected
Mw marker
- + + - + + PSI
- - + - - + CHX
173
111
80
61
μ2
C
Mock
T3D
- + - + PSI
σNS
D
Mock
T3D
- + - + PSI
μNS
μNSC
E
Mock
T3D
- + - + PSI
λ1
λ2
μ1
μ1C
σ3
F
PSI
Ub + ATP
Ub + ATPγS
dH2O
μ2
1.01
0.78
1.09
1.0

polyubiquitinated proteins. The amount of μ2 protein was reduced by more than 20% in the sample supplemented with Ub plus ATP compared to the other three samples indicating that μ2 protein is degraded by the 26S proteasome (Fig. 5.1 F). It is worth noting that the fastest migrating modified μ2 protein band was the most abundant species both *in vivo* and *in vitro* (Fig. 5.1 B and F, arrow), suggesting that a major fraction of ubiquitinated μ2 protein exists in the mono-ubiquitinated form. Immunoblot analysis of T3D-infected cells treated with PSI using a rabbit polyclonal antibody against reovirus structural proteins or rabbit polyclonal antibodies against nonstructural proteins σNS and μNS did not detect additional bands resulting from polyubiquitination of other reovirus proteins (Fig. 5.1 C, D and E), suggesting that this process is primarily μ2 protein-specific.

5.3.2 Ubiquitinated μ2 protein is present in the insoluble fraction

In Chapter three it was shown that μ2 protein localizes to viral inclusions with other reovirus proteins during infection. Reovirus inclusions are insoluble to nonionic detergent treatment, as are accumulations of polyubiquitinated proteins in cells treated with proteasome inhibitor (Anton *et al.*, 1999). This prompted the investigation of the cellular localization of ubiquitinated μ2 protein in infected cells. Parallel cultures of T1L- and T3D-infected cells were either treated with PSI at 20 h p.i. or left untreated for an additional 4 h, followed by lysis with Triton X-100 and sedimentation to separate the soluble fraction (supernatant) from the insoluble fraction (pellet) which includes the nucleus and intermediate filament matrix to which reovirus inclusions are attached (He *et al.*, 1990). These fractions were resolved by SDS-PAGE and immunoblotted using rabbit polyclonal anti-μ2 antibody. This showed that in the presence or

absence of PSI, ubiquitinated μ2 protein is detectable and accumulates in the insoluble fraction (Fig. 5.2 A and B), suggesting that it might be located in either the reovirus inclusions or the nucleus, since μ2 protein also localizes to the nucleus during infection (see Chapter three).

To further investigate the localization of ubiquitinated μ2 protein the cellular localization of Ub and μ2 protein was examined by confocal laser scanning microscopy in infected cells. Double-immunofluorescence staining of T3D-infected cells at 24 h p.i. showed that Ub colocalized with μ2 protein in the viral inclusions compared to mock-infected cells in which the Ub had a generalized nuclear and cytoplasmic staining (Fig. 5.3). This is consistent with the association of ubiquitinated μ2 protein with reovirus inclusions.

5.3.3 Reovirus inclusions are virus-induced aggresomes

Cytoplasmic viral inclusions of some large DNA viruses which are situated close to the MTOC, have been shown to resemble aggresomes and to be enriched in Ub, proteasomal antigens, vimentin and molecular chaperones (Heath *et al.*, 2001). To investigate whether reovirus inclusions resemble aggresomes they were investigated for the presence of proteasomes, the molecular chaperone heat shock protein-70 (hsp-70) and γ-tubulin, a component of the MTOC, by immunofluorescent staining using μ2 protein as a marker for reovirus inclusions. Confocal laser scanning microscopy revealed that proteasomes and hsp-70 localize specifically to reovirus inclusions (Fig. 5.4 A-F). Hsp-70 was present inside reovirus inclusions as well as outside suggesting that its relationship with the inclusions may involve shuttling between these locations. However, γ-tubulin is not present in reovirus inclusions although some μ2 protein

Figure 5.2 Ubiquitinated μ2 protein is present in the insoluble fraction of reovirus-infected cells.

Parallel monolayer cultures of HeLa cells were either mock-infected or infected with T1L or T3D for 20 h. This was followed by incubation with medium alone or with medium plus PSI for 4 h. The monolayers were fractionated into soluble and insoluble fraction by Triton X-100 treatment and sedimentation. The samples were resolved by SDS-PAGE and immunoblotted using a polyclonal rabbit anti-μ2 followed by a goat anti-rabbit-alkaline phosphatase and then reacted with Attophos. (A) Soluble fraction, (B) Insoluble fraction.

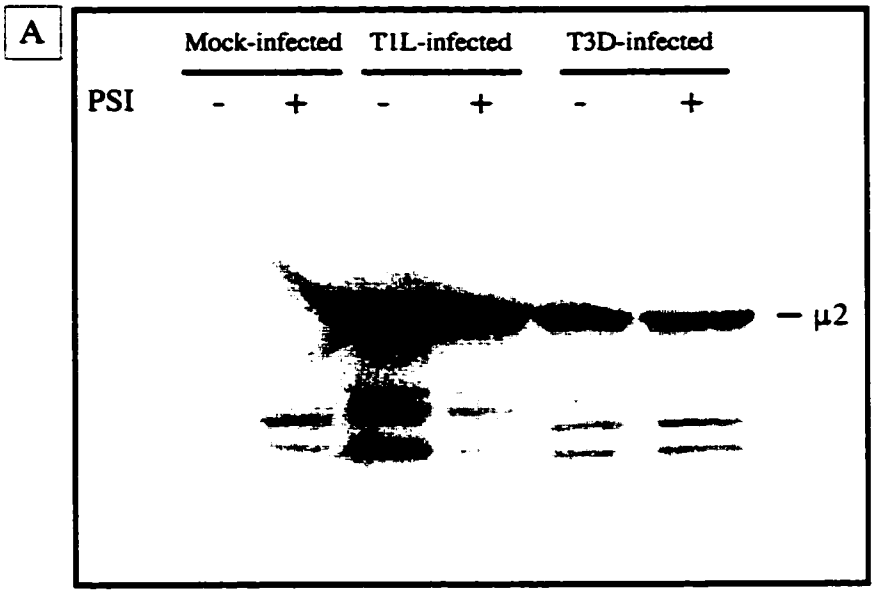
A
Mock-infected
T1L-infected
T3D-infected
PSI
- + - + - +
— μ2

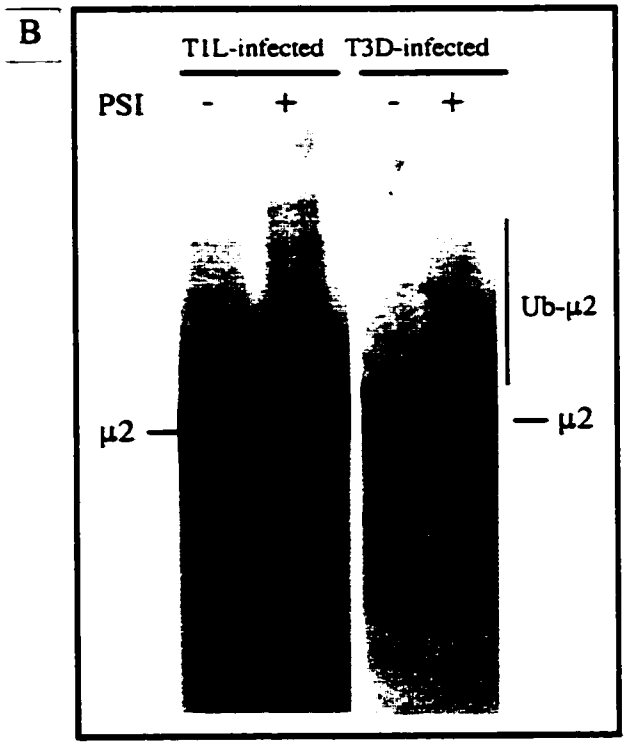
B
T1L-infected
T3D-infected
PSI
- + - +
Ub-μ2
μ2
— μ2

Figure 5.3 μ2 protein colocalizes with Ub in reovirus-infected cells.

HeLa cells were either infected with T3D (A-C) or mock-infected (D-F) for 24 h. Cells were stained for Ub using a polyclonal rabbit anti-Ub (B and E) followed by a Cy3-conjugated donkey anti-rabbit and for μ2 using a polyclonal rabbit anti-μ2 directly conjugated to FITC (A and D). Nuclei were stained with DAPI. Images were obtained using a confocal laser scanning microscope. In the overlay pictures (C and F), colocalization of μ2 and Ub is indicated by the yellow colour. The bar represents 10 μm.

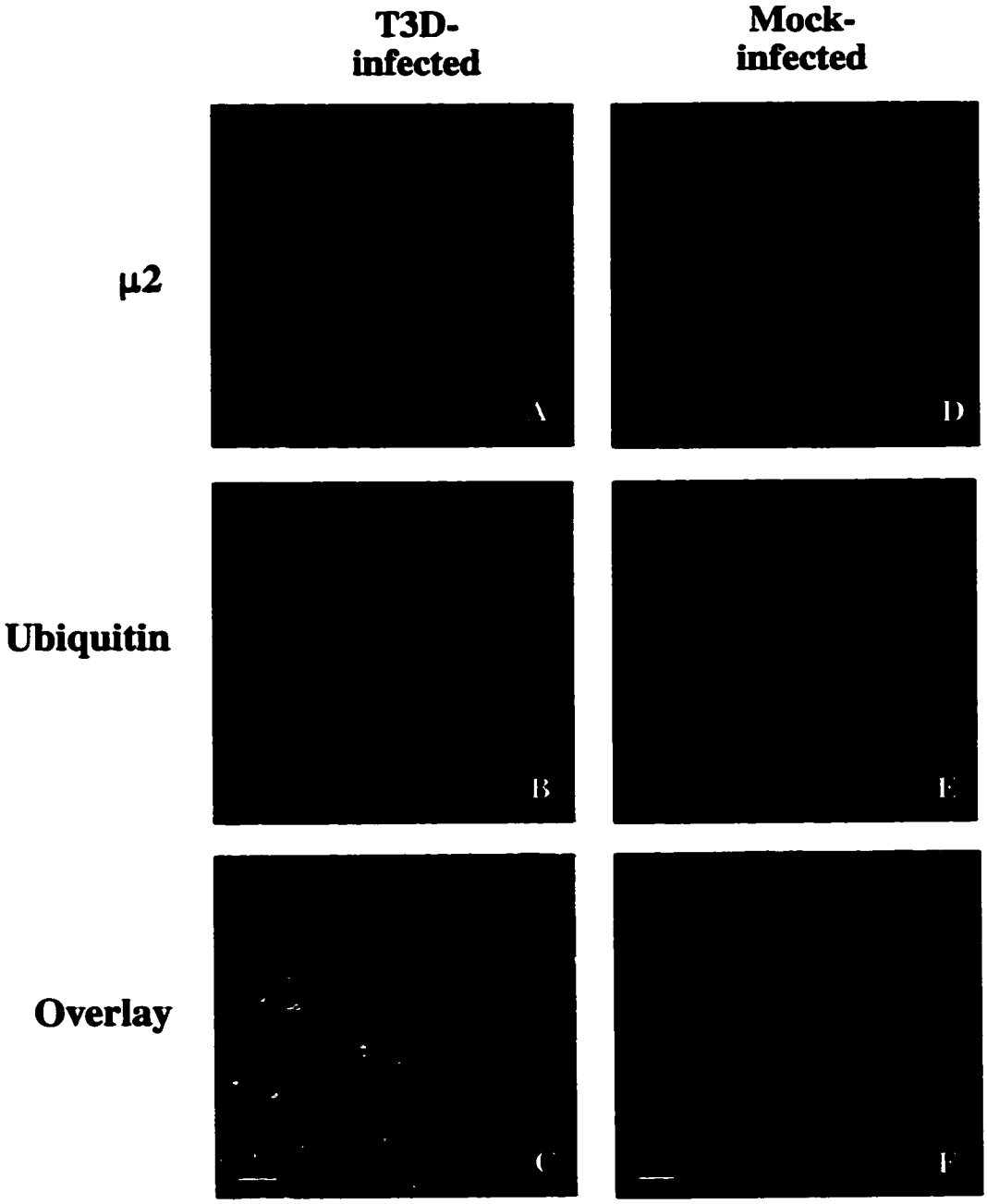
T3D-infected
Mock-infected
μ2
Ubiquitin
Overlay
A
B
C
D
E
F

Figure 5.4 Association of μ2 protein with UPP components in reovirus-infected cells.

HeLa cells were infected with T3D for 24 h. Cells were stained for either proteasomes using a polyclonal rabbit antisera to α-subunit of 20S proteasome (B), or hsp-70 using a hsp-70-specific mAb (E) or γ-tubulin using a γ-tubulin-specific mAb (H) and double-stained for μ2 using a polyclonal rabbit anti-μ2 directly conjugated to FITC (A, D and G). The secondary antibodies used were Cy3-conjugated donkey anti-rabbit (B) and Cy3-conjugated donkey anti-mouse (E and H). Nuclei were stained with DAPI. Images were obtained using a confocal laser scanning microscope. In the overlay pictures (C, F and I), colocalization of μ2 and proteasomes or hsp-70 or γ-tubulin is indicated by the yellow colour. The arrows point to the MTOC. The bar represents 10 μm.

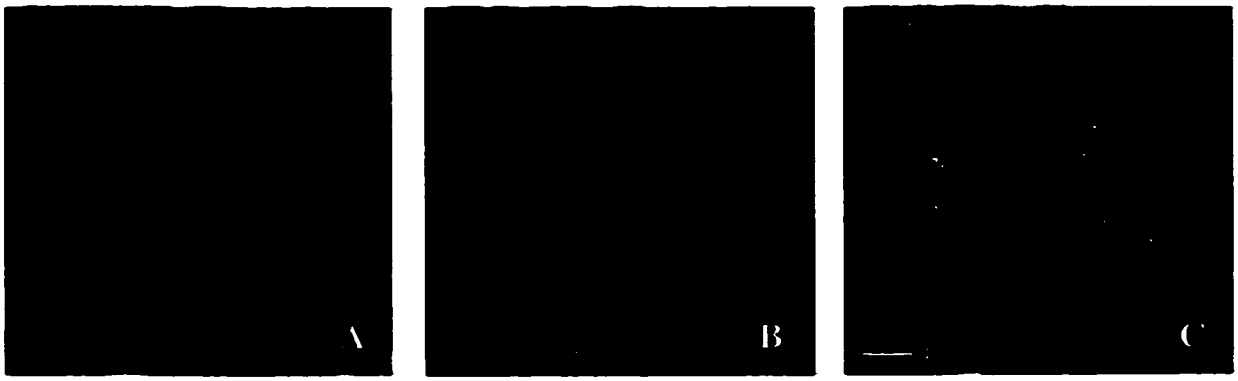

μ2 Proteasome Overlay

μ2 hsp-70 Overlay

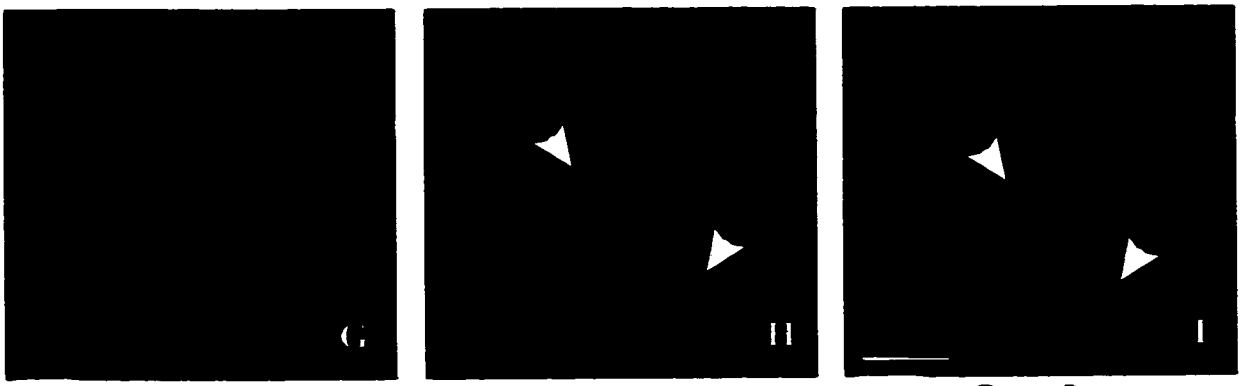

μ2 γ-tubulin Overlay

does localize to the MTOC (Fig. 5.4 G-I). This experiment shows that UPP components are recruited to the reovirus inclusions during infection. Thus reovirus inclusions resemble modified aggresomes, since like aggresomes, they not only contain Ub, proteasomal antigens and molecular chaperones but are also enclosed by a vimentin cage and depend on microtubules for their formation (Sharpe *et al.*, 1982; Spendlove *et al.*, 1964).

5.3.4 Inhibition of the Ub-proteasome pathway by reovirus

Aggresome formation has been shown to deregulate the UPP resulting in accumulation of proteins that are normally degraded through this pathway (Bence *et al.*, 2001). This is similar to the accumulation of polyubiquitinated proteins following treatment of cells with proteasome inhibitor. To further test the hypothesis that reovirus inclusions are virus-induced aggresomes, the effect of reovirus infection on degradation of proteins by the 26S proteasome was examined. To this end, a human embryonic kidney (HEK) 293 cell line stably expressing a short degron, CL1, fused to the C-terminus of green fluorescent protein (GFP^u) was used (Bence *et al.*, 2001). This fusion reporter protein is rapidly ubiquitinated and degraded by the 26S proteasome. Treatment of this cell line with proteasome inhibitor or transfection with an aggregation-prone protein has been shown to result in accumulation of GFP^u as quantified by flow cytometry. This cell line was infected with T1L or T3D for 24 or 48 h followed by monitoring of the GFP^u fluorescence intensity by flow cytometry. This showed that similar to cells treated with PSI, a large fraction of the cells infected with either T1L or T3D had substantially increased GFP^u fluorescence intensity compared to mock-infected cells (Fig. 5.5 and Table 5.1). In fact the percentage of cells showing increased GFP^u fluorescence intensity in T3D-infected cells was

Figure 5.5 Reovirus infection inhibits Ub-dependent proteolysis.

HEK (293) cells expressing an unstable GFP construct (GFP^u) that is rapidly degraded by the UPP were either mock-infected or infected with reovirus T1L, reovirus T3D, VSV or treated with PSI. The cells were then analyzed by flow cytometry to detect GFP fluorescence that results from inhibition of the UPP. Mock-infected GFP^u-expressing HEK cells are used as the control in all panels and are indicated by the red histogram. (A-D) Histograms showing changes in GFP^u fluorescence intensity (FL1 axis) in GFP^u-expressing HEK cells treated with PSI for 4 h (A), infected with VSV for 8 h (B), infected with reovirus T1L for 24 h (C), or infected with reovirus T3D for 24 h (D) all indicated by the black line. (E-F) are fluorescence density plots depicting the cell populations showing fluorescence changes (FL1 axis - GFP^u; FL2 axis - PE). (E) GFP^u-expressing HEK cells infected with T3D for 24 h. (F) GFP^u-expressing HEK cells infected with T3D for 24 h and stained for reovirus using a mAb to the nonstructural protein σNS (3E10) followed by a goat anti-mouse-PE and analyzed by two colour flow cytometry.

A

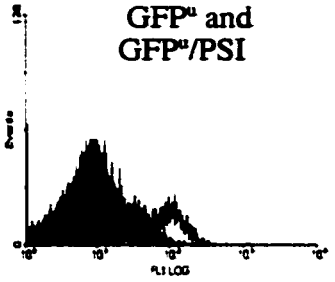

B

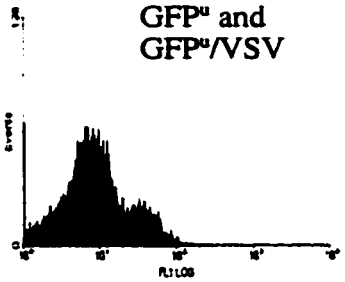

C

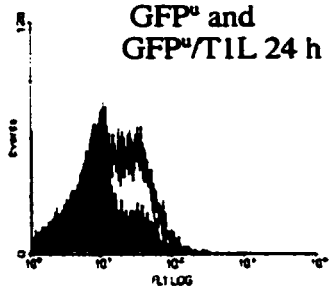

D

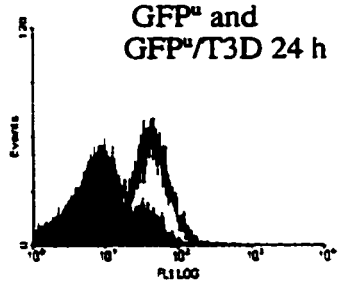

E

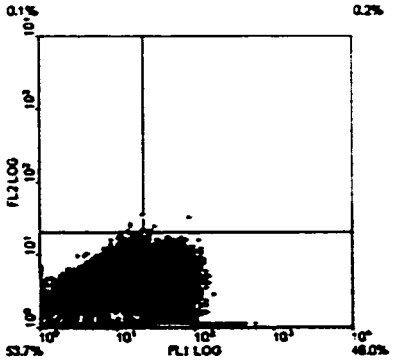

T3D 24 h

F

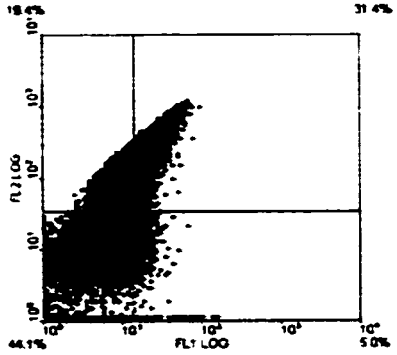

T3D 24 h stained
for virus

higher than in PSI-treated cells (Table 5.1). In addition, the percentage of cells showing increased GFP^u fluorescence intensity at 24 h p.i. was much higher in T3D-infected cells than T1L-infected cells (Fig. 5.5 C and D, and Table 5.1). This correlates with the rate of viral inclusion formation which is faster in T3D- than T1L-infected cells and suggests that inclusion formation is the basis for inhibition of Ub-dependent proteolysis.

Table 5.1 Percentage of cells in the viable cell population gate showing increased GFP^u fluorescence intensity

Sample	Percentage of cells showing increased GFP^u fluorescence intensity
HEK (-ve control)	0.1
HEK-GFP^u (+ve control)	17.2
PSI (4 h)	34.4
VSV (8 h p.i.)	4.7
T1L (24 h p.i.)	30.3 ± 6.8
T1L (48 h p.i.)	32.8
T3D (24 h p.i.)	51.9 ± 2.5
T3D (48 h p.i.)	40.7

Intracellular staining of reovirus-infected cells with a monoclonal antibody against the nonstructural protein, σNS, confirmed that the cells showing increased GFP^u fluorescence intensity were infected with reovirus (Fig. 5.5 E and F). The percentage of viral antigen-positive T3D-infected cells that showed increased GFP^u fluorescence intensity due to inhibition of Ub-

dependent proteolysis was similar to the percentage of viral antigen-positive T3D-infected L929 cells showing inclusion formation as determined previously by immunofluorescence microscopy *i.e.* 61.8% (Fig. 5 F) vs 66% (Table 3.1) respectively. Infection of GFP^u-expressing HEK cells with VSV did not result in increased GFP^u fluorescence intensity indicating that inhibition of Ub-dependent proteolysis is virus-specific. Infection of the cells by VSV was confirmed by immunofluorescence staining with a rabbit polyclonal antibody to VSV G protein (data not shown) indicating that the failure of VSV to inhibit Ub-dependent proteolysis was not due to inability to infect the cells. In summary, these results show that reovirus inclusions are not only structurally but also functionally similar to aggresomes because they inhibit Ub-dependent proteolysis.

5.3.5 Ub and proteasomal antigen expression during reovirus infection

Indirect immunofluorescent staining of T3D- and mock-infected cells for Ub and proteasomes suggested that there might be an increase in their expression during reovirus infection (Fig. 5.3 and 5.4). The expression levels of Ub and the α-subunit of the proteasome were therefore assessed during reovirus infection by immunoblot analysis. This showed that the amount of Ub did not change significantly but that the expression of a Ub cross reactive protein of approximately 13 kDa increased significantly during reovirus infection compared to mock-infected cells (Fig. 5.6 A, arrow). This protein is probably the interferon-inducible Ub-like protein, ISG15 (Haas *et al.*, 1987) or a tandem diubiquitin polypeptide (Bates *et al.*, 1997). Similarly, the expression of the α-subunit of the proteasome did not change significantly, however, there was expression of a higher molecular weight band of approximately 70 kDa that

Figure 5.6 Expression of UPP proteins in reovirus-infected cells.

HeLa cells were either mock-infected or infected with T1L or T3D for 6 or 24 h. The cell lysates were resolved by SDS-PAGE and immunoblotted using a polyclonal rabbit anti-Ub (A) or a polyclonal rabbit antibody to the α-subunit of the 20S proteasome (B) followed by a goat anti-rabbit-alkaline phosphatase. The blots were then reacted with Attophos. The arrows point to the higher molecular weight bands that are overexpressed or induced by reovirus infection and react with the anti-Ub (A) or anti-α-subunit 20S proteasome antibodies (B).

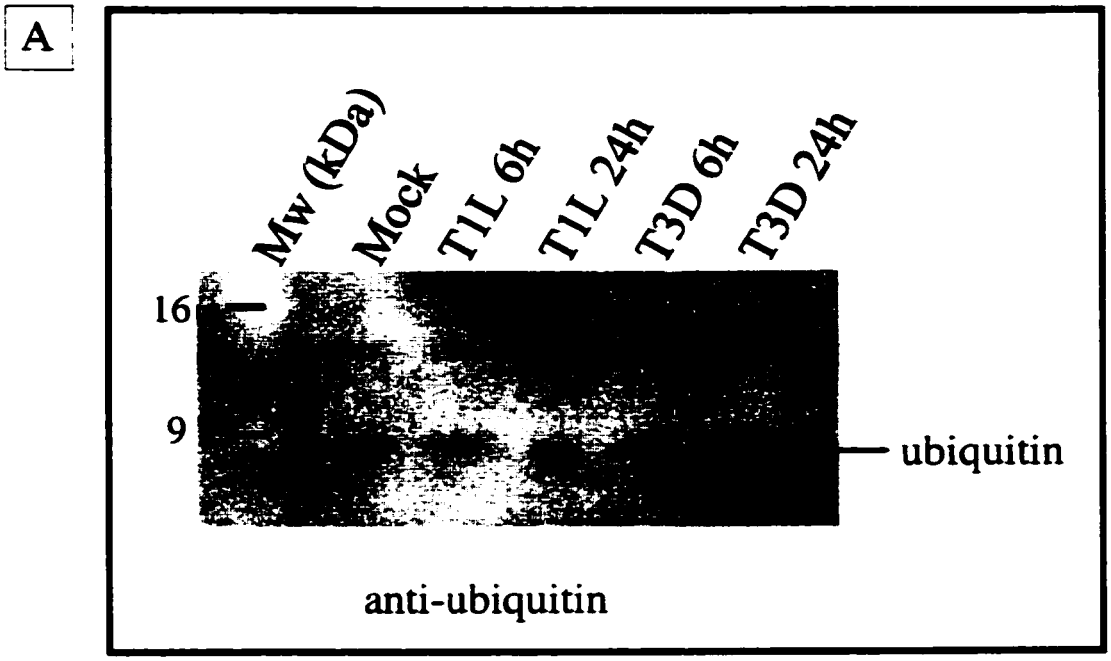
A
Mw (kDa)
Mock
T1L 6h
T1L 24h
T3D 6h
T3D 24h
16
9
ubiquitin
anti-ubiquitin

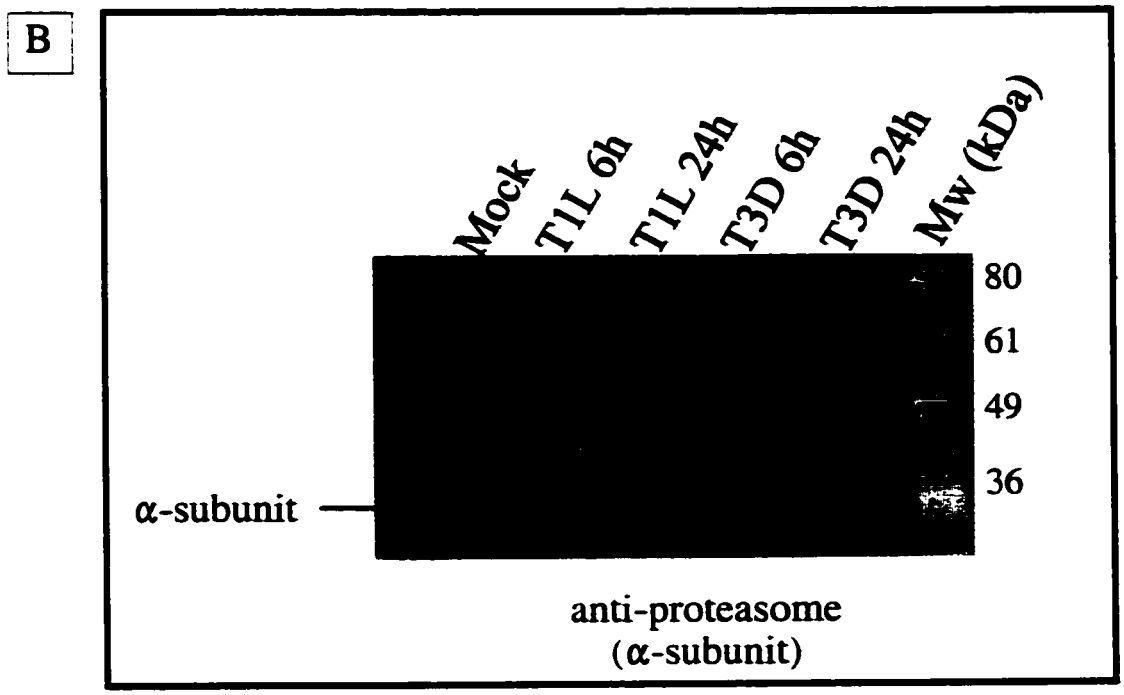
B
Mock
T1L 6h
T1L 24h
T3D 6h
T3D 24h
Mw (kDa)
80
61
49
36
α-subunit
anti-proteasome
(α-subunit)

reacts with anti-α-subunit antibody in the infected cells at 24 h p.i. (Fig. 5.6 B, arrow). These data suggest that reovirus infection induces the expression of, or modifies some UPP components.

5.3.6 Effect of Ub overexpression on reovirus growth

The observation that the UPP components localize to reovirus inclusions and that expression of some of these components is induced by reovirus infection suggests that reovirus could be using the UPP for replication or assembly. It is also possible that the localization of the UPP components to the inclusions could be a defence mechanism by the cell to rid itself of unwanted viral proteins. This prompted examination of the effect of Ub overexpression on reovirus growth. The first approach was to assess the growth of reovirus in a lung cancer cell line, A549, stably overexpressing wild-type Ub (A549-wtUb) compared to the original A549 cell line. Parallel cultures of the two cell lines were infected with T3D for 72 h and the yield of infectious virus was quantified by plaque assay. This showed no difference in the amount of virus produced by the two cell lines suggesting that overexpression of Ub is not deleterious to reovirus growth (Fig. 5.7).

To investigate whether inhibition of K48-linked polyubiquitination of a viral or cellular protein has an effect on reovirus growth, viral production in A549 cells stably overexpressing a mutant Ub with K48 changed to R (A549-Ub-K48R) was examined. The covalent linkage of this mutant Ub to the target protein prevents the formation of a K48-linked polyubiquitin chain. Growth of T3D reovirus in this cell line was significantly higher (3-fold; *t* test p=0.0003) than

Figure 5.7 Effect on reovirus growth of overexpressing Ub or a Ub K48R mutant.

The lung cancer cell line, A549, or A549 cells stably expressing wild-type Ub (A549-wtUb) or a K48R Ub mutant (A549-K48R) were infected with T3D at an MOI of 10 PFU/cell. Virus was harvested at 72 h p.i. and titrated in L929 cells. Bar graph showing growth titer of reovirus T3D in A549, A549-wtUb (wtUb) and A549-K48R (K48R) cell lines. Error bars denote the standard error of the mean of three different experiments (* = *t* test p=0.0003). Insert immunoblot shows the amount of reovirus outer capsid protein μ1C expressed during T3D infection of A549, A549-wtUb and A549-K48R cells. Cell lysates were collected at 48 h p.i., resolved by SDS-PAGE and immunoblotted with a polyclonal rabbit anti-T3D antibody and goat anti-rabbit-alkaline phosphatase followed by reaction with Attophos.

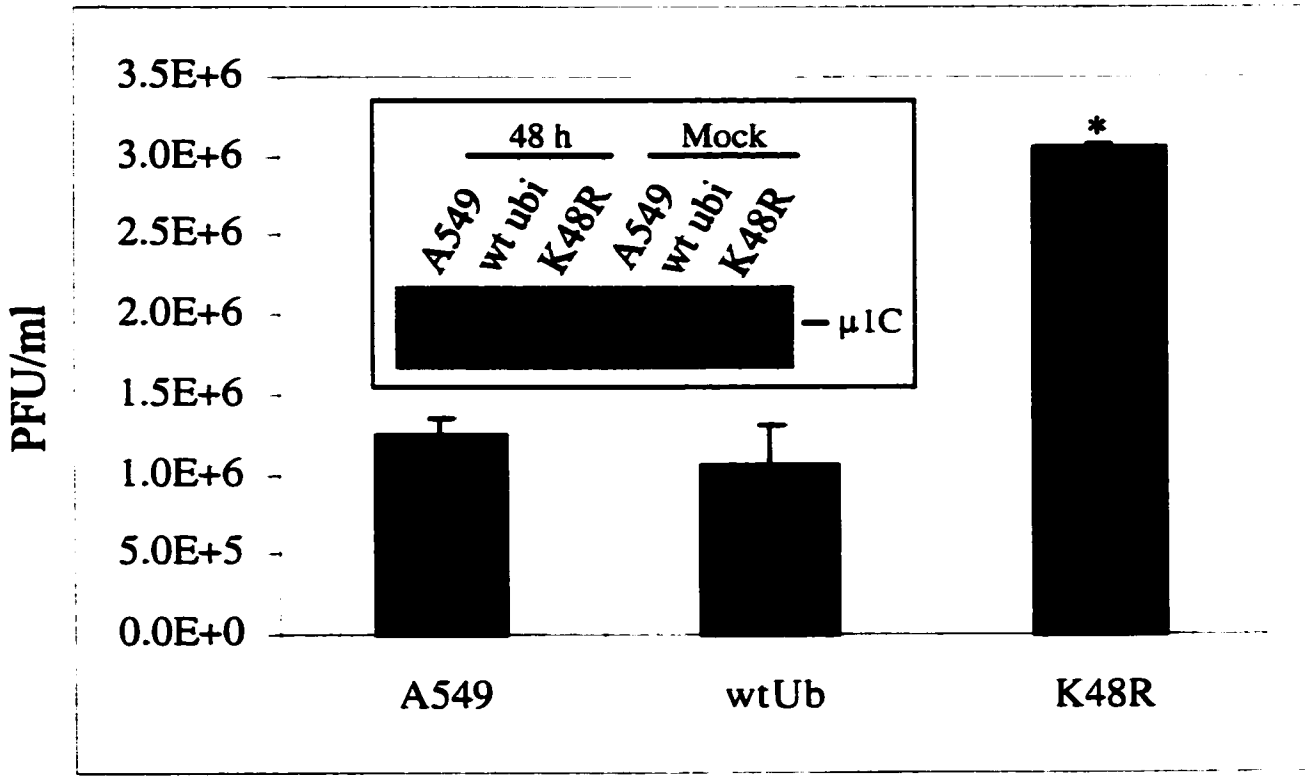
3.5E+6
3.0E+6
2.5E+6
2.0E+6
1.5E+6
1.0E+6
5.0E+5
0.0E+0
PFU/ml
48 h
Mock
A549
wt ubi
K48R
A549
wt ubi
K48R
μ1C
*
A549
wtUb
K48R

in normal A549 cells (Fig. 5.7) suggesting that either preventing K48-linked polyubiquitination and therefore degradation, or the addition of a limited number of Ubs (*e.g.* mono- or di-ubiquitination) to viral or cellular protein is advantageous for reovirus growth. The difference in growth of reovirus in Ub-K48R-A549 compared to normal A549 or wtUb-A549 was shown not to be due to a difference in viral protein synthesis because the amount of viral protein produced in the three cell lines was similar during infection (Fig 5.7, insert immunoblot). This suggests that the role played by the UPP in reovirus replication probably involves a stage in reovirus replication downstream of viral gene expression.

5.3.7 Effect of depleting the cellular pool of free Ub on reovirus growth and inclusion formation

Although ubiquitination is mostly linked with protein degradation in general and of μ2 protein in particular, overexpression of Ub did not result in reduced reovirus growth as would be expected if it accelerated the destruction of μ2 protein. These results therefore suggest that reovirus might be using the UPP for viral assembly rather than protein degradation. To test this hypothesis further, the effect of depleting the cellular pool of free Ub on reovirus growth and viral assembly was examined. Treatment of cells with proteasome inhibitor has been shown to decrease the cellular pool of free Ub and results in the aggregation of polyubiquitinated proteins and proteasomes (Mimnaugh *et al.*, 1997). The production of infectious virus in parallel cultures of T3D-infected HeLa cells with respect to PSI treatment was quantified by plaque assay. The cells were infected for 10 h followed by 4 h treatment with PSI and a further 2 h chase period without PSI. The amount of virus produced in cells treated with PSI decreased significantly (10-

fold; *t* test p=0.004) compared to untreated cells (Fig. 5.8 A). This difference may have been due to a defect in viral assembly because immunofluorescence staining of PSI-treated cells for reovirus inclusions using μ2 and σNS antibodies showed generalized staining and inhibition of reovirus inclusion formation (Fig. 5.8 B), even though the PSI-treated cells produced comparable amounts of viral protein (Fig. 5.8 A, insert immunoblot). These data suggest that reovirus uses the UPP to transport viral macromolecules to sites of viral assembly.

5.4 Discussion

The data presented in this chapter show that reovirus inclusions are virus-induced, modified aggresomes and that reovirus replication initially usurps the UPP for inclusion formation but ultimately inhibits Ub-dependent proteolysis. This has several implications with respect to viral infection. Specifically, reovirus inclusions are shown to be structurally similar to aggresomes containing UPP components: proteasomal antigens, Ub, vimentin and the molecular chaperone hsp-70. This is the first time that host proteins, other than vimentin filaments, have been shown to be present in reovirus inclusions. In addition, the formation of reovirus inclusions and aggresomes is blocked by treatment of cells with drugs that depolymerize microtubules indicating that both processes are microtubule-dependent (Garcia-Mata *et al.*, 1999; Babiss *et al.*, 1979; Spendlove *et al.*, 1964).

Interestingly, the assembly of some large cytoplasmic DNA viruses such as poxviruses, iridoviruses and ASFV occurs at an inclusion body that is located close to the MTOC and which also structurally resembles aggresomes (Heath *et al.*, 2001). In particular it was shown that the

Figure 5.8 Treatment of T3D-infected HeLa cells with proteasome inhibitor perturbs reovirus growth and inclusion formation.

Parallel cultures of HeLa cells were infected with T3D for 10 h. The cells were then either incubated with or without PSI for 4 h followed by an additional 2 h in medium alone. (A) Bar graph showing growth titer of reovirus T3D in PSI-treated (PSI) or untreated cells (No PSI). Error bars denote the standard error of the mean of three different experiments (* = *t* test p=0.004). Insert immunoblot shows the amount of reovirus outer capsid protein μ1 and μ1C expressed in T3D-infected cells treated with PSI or left untreated. Cells were infected as indicated above and the cell lysates were collected and resolved by SDS-PAGE and immunoblotted with a polyclonal rabbit anti-T3D antibody and goat anti-rabbit-alkaline phosphatase followed by reaction with Attophos. (B) Cellular localization of μ2 and σNS proteins in T3D-infected cells treated with PSI or left untreated. Cells were infected as indicated above, fixed in acetone and stained with either a polyclonal rabbit anti-μ2 antibody or a polyclonal rabbit anti-σNS antibody followed by a Cy3-conjugated donkey anti-rabbit. Images were obtained using a confocal laser scanning microscope. The bar represents 10 μm.

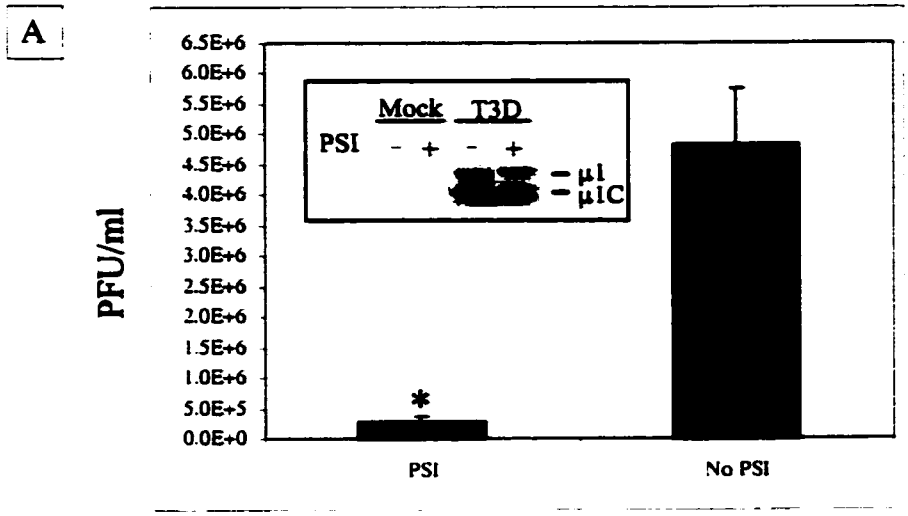
A
PFU/ml
6.5E+6
6.0E+6
5.5E+6
5.0E+6
4.5E+6
4.0E+6
3.5E+6
3.0E+6
2.5E+6
2.0E+6
1.5E+6
1.0E+6
5.0E+5
0.0E+0
Mock T3D
PSI - + - +
μ1
μ1C
*
PSI
No PSI

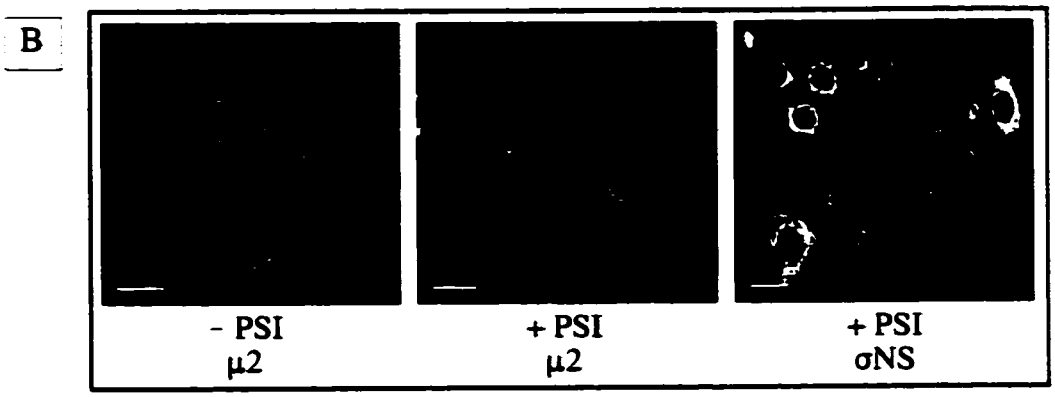
B
- PSI
μ2
+ PSI
μ2
+ PSI
σNS

transport of viral proteins to these viral inclusions and aggregated proteins to aggresomes is by a dynein-dependent retrograde transport system on microtubules (Heath *et al.*, 2001; Garcia-Mata *et al.*, 1999). Given these similarities it has been proposed that assembly of these viruses exploits the aggresome formation pathway to concentrate their structural proteins at the site of viral assembly.

Reovirus possibly utilizes the same pathway for transportation of its macromolecules, the difference being that in reovirus the final destination is not the MTOC but multiple perinuclear sites. It is possible that a viral protein or another host protein, other than γ-tubulin, acts as a nucleating protein for reovirus inclusions resulting in the accumulation of UPP components along with viral proteins and RNA. The reovirus nonstructural protein σNS, which plays a secondary role in the rate of inclusion formation (see Chapter three), has been reported to accumulate at reovirus inclusions earlier than other reovirus proteins suggesting that it might be the reovirus inclusion-nucleating protein (Becker *et al.*, 2001). However, the involvement of other reovirus or host proteins can not be ruled out.

The treatment of cells with proteasome inhibitor results in the accumulation of polyubiquitinated proteins, aggresome formation and depletion of the cellular pool of free Ub (Wojcik *et al.*, 1996; Wigley *et al.*, 1999). The treatment of reovirus-infected cells with proteasome inhibitor resulted in a 10-fold reduction in virus growth. Infected cells treated with PSI showed lack of inclusion formation suggesting that the reduced viral growth was due to inhibition of the transport of viral macromolecules to the sites of viral assembly. Infected cells

treated with PSI produced significant amounts of viral protein suggesting that the effect on virus growth is not due to decreased viral protein synthesis. The amount of viral protein was slightly lower in PSI-treated cells than untreated cells possibly due to reduced secondary transcription from progeny viral particles which is the major source of mRNA transcripts during infection (Skup *et al.*, 1981; Watanabe *et al.*, 1968). This is consistent with an involvement of the UPP or its components in the transport of reovirus macromolecules to reovirus inclusions for viral assembly. Another contributing factor to reduced reovirus replication in PSI-treated cells could be the competitive formation of cellular aggresomes that presumably utilizes the same pathway as reovirus macromolecules.

It has been reported that mRNA in the nontranslated state is in complex with the 20S subunit of the proteasome forming a subset of proteasomes called prosomes which are distributed preferentially on intermediate and actin filaments (Grossi de Sa *et al.*, 1988; Arcangeletti *et al.*, 1992; Olink-Coux *et al.*, 1992; De Conto *et al.*, 1997). Prosomes have also been shown to play a role in regulation and cytodistribution of viral mRNA during infection (Arcangeletti *et al.*, 1997). Thus, it is possible that the presence of proteasomal antigens in reovirus inclusions serves to deliver reovirus mRNA to the site of viral assembly which is then packaged into nascent virions for genome replication. Another possibility is that recruiting UPP components creates an environment conducive to the formation of viral ribonucleoprotein and multi-protein complexes required for viral assembly. Identification of the UPP components that are induced or overexpressed during reovirus infection will be important in clarifying the role played by the UPP in reovirus inclusion formation and assembly.

Experiments in this chapter also show that the reovirus μ2 protein, which controls the rate of reovirus inclusion formation, is ubiquitinated and degraded by the 26S proteasome. The treatment of reovirus-infected cells with PSI resulted in the accumulation of polyubiquitinated μ2 protein that was detected by immunoblot analysis. The degradation of μ2 protein by the UPP was confirmed *in vitro* using a reticulocyte lysate-based proteolysis system. Furthermore, μ2 protein is present at the MTOC which is considered a proteolysis center in the cytoplasm containing UPP components (Wojcik *et al.*, 1996; Wigley *et al.*, 1999; Fabunmi *et al.*, 2000). The most abundant ubiquitinated μ2 protein species was shown to be mono-ubiquitinated suggesting that physiologically, mono-ubiquitination of μ2 protein is preferred over polyubiquitination and that this could play a role in inclusion formation or viral assembly. Interestingly, reovirus growth was significantly increased (3-fold) in cells overexpressing a K48R mutant Ub. Elongation of K48-linked polyubiquitin chains is inhibited once this mutant Ub is ligated to the substrate or the growing Ub chain. This results in the formation of subthreshold length chains, or chains assembled through alternative linkages resulting in inhibition of Ub-dependent proteolysis (Tsirigotis *et al.*, 2001). The increase in reovirus growth in this cell line could be a result of inhibition of the degradation of a viral or cellular protein required for viral assembly or it could suggest that mono-ubiquitination of a viral or cellular protein is essential for viral assembly. This is consistent with a role for mono-ubiquitinated μ2 protein in inclusion formation and viral assembly. The polyubiquitinated μ2 protein species could also result from a series of mono-ubiquitinations at any of the 35 lysine residues in the same μ2 molecule forming Ub conjugates not recognized for proteolysis (Hicke, 2001). Conversely, μ2 protein polyubiquitination could occur through other lysines on Ub and that the K48R mutation would

tip the balance in favour of such linkages that do not result in proteolysis.

Recent studies suggest that mono-ubiquitination is involved in cellular localization and sorting of proteins as well as budding of retroviruses (Hicke, 2001; Garcia-Higuera *et al.*, 2001). For example, mono-ubiquitination of cell surface receptors which results in their down regulation is often coupled with protein sorting in the multivesicular body pathway (Katzmann et al., 2001). On the other hand, the budding of retroviruses has been shown to be promoted by the mono-ubiquitination of their Gag polyproteins and involves the recruitment of a Ub-ligase activity to the site of virus release (Ott *et al.*, 1998; Strack *et al.*, 2000). The identification of the E2 or E3 enzymes used for μ2 protein ubiquitination and analysis of the μ2 and Ub residues used in this process would be an important step in elucidating the mechanism and importance of μ2 protein ubiquitination in reovirus morphogenesis.

Finally, the data in this chapter shows that reovirus infection results in inhibition of Ub-dependent proteolysis because infection of a cell line stably expressing a GFP fusion reporter protein, GFP^u, that is rapidly degraded by the UPP resulted in significant accumulation of GFP^u in the cell. Transfection of this cell line with an aggregation-prone protein or treatment with proteasome inhibitor has previously been shown to have the same effect (Bence *et al.*, 2001). Interestingly, T3D caused an accumulation of GFP in a higher percentage of cells than T1L at 24 h p.i. (51.9% vs 30.3% respectively) which correlates with the rate of inclusion formation by these viruses. This further confirms the similarity between reovirus inclusions and aggresomes, in that not only are they structurally similar but that they also have the same effect on Ub-

dependent proteolysis.

It has been reported that the formation of aggresomes in neurodegenerative diseases may contribute to the underlying pathology in these conditions because inhibition of the UPP leads to deregulation of cellular metabolism and cell death (Bence *et al.*, 2001). Reovirus infection results in CPE, which involves the induction of apoptosis, that presumably contributes to the pathogenesis in infected animals. The utilization by reovirus of the UPP for inclusion formation and possibly viral assembly resulting in inhibition of Ub-dependent proteolysis would be expected to induce apoptosis due to accumulation of proapoptotic agents that are normally degraded by the UPP such as p53 (Lopes *et al.*, 1997). Another possibility is that degradation of μ2 protein by the 26S proteasome would lead to μ2-specific peptide presentation by the MHC Class I molecules at the host cell surface resulting in cytolytic T-cell activity. The ability of reovirus to cause CPE has been mapped to the μ2-encoding M1 gene (Moody and Joklik, 1989; Baty and Sherry, 1993) while the ability to induce apoptosis is linked to the S1 gene encoding the receptor binding protein, σ1 (Tyler *et al.*, 1995; Tyler *et al.*, 1996; Rodgers *et al.*, 1998). The M1 gene also segregates with strain-specific differences in the ability of reovirus to cause hepatic injury (Haller *et al.*, 1995) and myocarditis which correlates with induction and sensitivity of reovirus to interferon (Sherry and Fields, 1989; Sherry and Blum, 1994; Sherry *et al.*, 1998). Thus the role of ubiquitinated μ2 protein in viral replication may also involve interferon effects since interferon induces the expression of UPP components including subunits of the 26S proteasome required for MHC class I peptide presentation (Fruh *et al.*, 1994; Ahn *et al.*, 1995; Realini *et al.*, 1994).

Reovirus T3D is being developed as an oncolytic agent (Coffey *et al.*, 1998; Norman and Lee, 2000; Wilcox *et al.*, 2001), therefore understanding the events that control CPE during reovirus infection will provide novel strategies not only for antiviral therapeutics but also for the application of reovirus as a therapeutic agent. In addition, since reovirus has the ability to infect neurons (Tyler, 1998), analyzing the role that reovirus inclusions play in inducing CPE might shed light on the effects of aggresome formation in neurodegenerative diseases which, like reovirus inclusions, can be present at multiple sites in a host cell.

CHAPTER SIX

ANALYSIS OF RECOMBINANT μ2 PROTEIN NUCLEAR LOCALIZATION AND PROTEIN COMPLEX FORMATION

6.1 Introduction

The data presented to this point suggests that the μ2 protein could be playing a direct role in reovirus inclusion formation. The strain-dependent formation of protein complexes by recombinant μ2 protein with kinetics that paralleled the rate of inclusion formation during infection suggests that expression of recombinant μ2 protein alone could be used to analyze the role the protein plays in reovirus inclusion formation, as well as further the knowledge on μ2 protein biology. To that end, this chapter addresses nuclear localization and protein complex formation of recombinant μ2 protein.

Nucleocytoplasmic shuttling occurs through multi-protein channels called nuclear pore complexes (NPC) which have a passive diffusion channel of about 9nm. This allows the passage of small proteins but the nuclear localization of large proteins (>60 kDa) requires active transport. This is mediated by specific domains on the protein called nuclear localization signals (NLS) which interact with shuttling carriers. A NLS is generally characterized by the presence of basic residues in either one (monopartite) or two (bipartite) clusters (reviewed by Nigg, 1997; Gorlich and Mattaj, 1996). Conversely, export of a protein out of the nucleus is mediated by a nuclear export signal (NES) which, prototypically, is short and hydrophobic and has a high

leucine content. Nucleocytoplasmic transport is essential for the replication of many DNA and RNA viruses, especially those that require the host DNA/RNA synthesis machinery for replication and expression of their genomes (Nakielny *et al.*, 1997). In addition to importing and exporting their genomes into the nucleus, viruses also need to export their mRNA out of the nucleus and import proteins required for assembly of viral ribonucleoproteins into the nucleus. Hence, viruses with nuclear involvement have proteins which possess nuclear import and export signals that play a role in import and export of viral RNA and DNA. Examples include the HIV-1 Rev protein which is one of the first proteins identified to have an NES and is implicated in export of viral RNA (Fischer *et al.*, 1995), and the SV40 large T antigen which has a 7 aa long monopartite NLS (Lanford and Butel, 1984). However, the need for such protein shuttling between the cytoplasm and the nucleus in reovirus still remains unclear since it appears not to require host cell nuclear functions.

Further analysis of the nuclear localization of recombinant μ2 protein could provide insight into the reason for μ2 protein nuclear localization. The nucleus, although appearing uniform under the light microscope, is compartmentalized into substructures specializing in different functions. One such substructure is the PML body which was discovered using autoimmune sera and immunofluorescence and is tightly associated with the nuclear matrix such that it is insoluble to detergent extraction (reviewed by Sternsdorf *et al.*, 1997; Hodges *et al.*, 1998). These bodies are also alternatively referred to as nuclear domain 10 (ND 10), PML oncogenic domains (PODs), nuclear dots (NDs), multiple nuclear dots (MNDs) or Kr-bodies. More than 15 proteins have been shown to localize to PML bodies and by far the best

characterized is the PML protein, which has been reported to not only have antiviral properties but also to suppress growth and transformation as well as exhibiting proapoptotic activity (Chelbi-Alix *et al.*, 1998; Regad *et al.*, 2001; Wang *et al.*, 1998a; Wang *et al.*, 1998b; Quignon *et al.*, 1998). Fusion of PML protein with the retinoic acid receptor α (RAR), due to reciprocal chromosomal translocation of chromosome 15 and 17, is believed to be the cause of acute promyelocytic leukemia (APL) since the fusion protein is sufficient for transformation of cells (De The *et al.*, 1991; Goddard *et al.*, 1991; Kakizuka *et al.*, 1991). As discussed in section 1.7.5, the function of PML bodies remains controversial. However, the recent report that the PML body functions as a proteolysis center in the nucleus has changed how these structures are viewed (Anton *et al.*, 1999). This could also explain the autoantigenicity of proteins that localize to these bodies since Ub-dependent proteolysis plays a role in the production of antigenic peptides for presentation by the class I MHC complex.

In this chapter, μ2 protein is demonstrated to possess a specific bipartite nuclear localization signal and that the protein localizes to PML bodies during transient transfection. Preliminary data from studies mapping the regions involved in μ2 protein complex formation or PML body localization is also presented and the significance of these findings in relation to the role of μ2 protein in reovirus inclusion formation is discussed.

6.2 Materials and Methods

6.2.1 Construction of M1 gene deletion mutants

M1 gene deletion mutants were generated by PCR of pGEM-M1 clone T1-15 using *Taq* DNA polymerase (MBI Fermentas, Burlington, ON). The primers used to generate the specific deletions are listed in Table 6.1. The cycling parameters were as follows: an initial denaturation step of 94^{0}C for 5 min followed by an initial 3 cycles of 94^{0}C for 1 min; 33^{0}C for 30 sec; 72^{0}C for 5 min followed by 30 cycles of 94^{0}C for 30 sec; 45^{0}C for 30 sec; 72^{0}C for 5 min and a final incubation of 7 min at 72^{0}C. The PCR products were then purified from agarose gels using the QIAquick Gel Extraction Kit (Qiagen) and subjected to end-repair in a 8 µl reaction mix containing Klenow buffer (50 mM Tris-HCl pH 7.6, 10 mM $MgCl_2$), 0.1 mM of each of the 4 dNTPs and 1.2 U of DNA polymerase I Klenow fragment for 30 min at room temperature. This was followed by phosphorylation of the 5' termini by supplementing the reaction with Blunt supplement buffer (5% polyethylene glycol 8000, 1 mM DTT and 0.2 mg/ml BSA), 1 mM ATP and 2 U of T4 polynucleotide kinase and incubated at 37^{0}C for 30 min. The reaction was

Table 6.1 Primers used in making M1 gene deletion mutants

Plasmid	Forward primers[a]	Reverse primers[a]	Region deleted
T1-NH-710-10	M1+710	M1 - 19	aa3-232 (20-709bp)
T1-NH-266-8	M1+266	M1 - 19	aa3-84 (20-265bp)
T1-NLS-del-9	M1+806	M1 - 790	aa261-264 (791-805bp)
T1-NH-806-2	M1+806	M1 - 19	aa3-264 (20-805bp)
T1-NH-1133-1	M1+1133	M1 - 19	aa3-373 (20-1132bp)

[a] see Appendix two for sequence data.

stopped by deactivating the enzyme at 70°C for 5 min. The dsDNA was recircularized by blunt end ligation by adding 1 U of T4 DNA ligase to the above mix and incubating overnight at room temperature. 1 µl of the ligation mix was used to transform *Escherichia coli* DH5α cells by electroporation using a BRL microelectroporation chamber at 2000 V. The cells were diluted in 2 ml of LB Broth and allowed to recover for 1 hr on a shaker at 37°C before plating on LB plates (LB broth plus 1.5% Bacto agar) containing ampicillin. Minipreps of DNA were made from individual colonies and screened by restriction digestion. The positive clones of expected size were sequenced using the Big Dye terminator kit (Applied BioSystems, Foster City, CA) to verify the presence and position of the deletions and to check for any mutations that may have occurred during PCR. The T1L M1 gene expressing construct, 8BK44, and M1 deletion mutants 8BK34, 5X23P, 5X23I, 9B23B, 9B23M and 7E23F were obtained from B. Sherry (North Carolina State University, Raleigh, NC) and were constructed as described in Appendix one. All transfections in this chapter were carried out using Effectene reagent (Qiagen) as described in section 2.5.

6.3 Results

6.3.1 Nuclear localization of recombinant µ2 protein

The presence of recombinant µ2 protein in the nucleus by epifluorescence microscopy was reported in Chapter three. To confirm this finding confocal laser scanning microscopy following dual staining for µ2 and DNA to detect the nucleus in M1 gene-transfected cells was performed. This showed the presence of µ2 protein complexes in the nucleus (Fig. 6.1 A-C). To further assess the nuclear localization of recombinant µ2 protein, transfected cells were

fractionated into soluble (cytoplasmic) and pellet (nuclear) fractions by detergent extraction and sedimentation. The resulting samples were analyzed by immunoblot using a rabbit polyclonal anti-T1L μ2 antiserum. Both T1L and T3D μ2 proteins were found in the soluble and pellet fractions (Fig. 6.1 D). Quantification by phosphorimaging showed that 61% of T3D μ2 protein compared to 49% of T1L μ2 protein had accumulated in the pellet by 24 h post-transfection. The integrity of the fractionation procedure was verified by staining the same samples for tubulin, a cytoplasmic protein, which was shown to be present only in the soluble fraction (Fig. 6.1 D). This observation is consistent with the nuclear localization of T3D and T1L μ2 proteins as seen by immunofluorescence in infected cells and also suggests that recombinant μ2 protein is nuclear matrix-associated since the detergent treatment solubilizes all proteins except those tightly associated with the nuclear matrix.

6.3.2 μ2 protein nuclear localization signal (NLS)

Sequence analysis of μ2 protein revealed a prototypical nuclear localization signal (NLS) motif at positions 261 to 264 (KRLR) that fits a consensus sequence. K R/K X R/K (Garcia-Bustos *et al.*, 1991; Mukaigawa and Nayak, 1991), required for the nuclear localization of several other proteins including the PB1 and PB2 subunits of the influenza virus RNA polymerase (Nath and Nayak, 1990; Mukaigawa and Nayak, 1991). Nuclear localization signals have also been shown to consist of a single stretch of basic amino acids (Chelsky *et al.*, 1989; Garcia-Bustos *et al.*, 1991) and one such region is present in the μ2 protein from position 100 to 114 (RRLRKRLMLKKDLRK). Deletion of both regions were constructed by PCR directed-mutagenesis. The plasmid constructs were then transfected into L929 cells and the localization

Figure 6.1 Nuclear localization of recombinant μ2 protein in transfected cells.

L929 cells were transfected with pGEM-M1 clone T3-18 expressing the T3D M1 gene for 24 h. The cells were fixed in acetone and stained for μ2 protein (A) using a rabbit polyclonal anti-μ2 antibody followed by a Cy3-conjugated donkey anti-rabbit. The cells were then incubated with the dsDNA-specific fluorescent dye, pico green, to stain for the nuclei (B). The μ2 protein is coloured red and the nuclei are coloured green. The overlay image is shown in (C). The images were obtained using a confocal laser scanning microscope. The bar represents 10 μm. (D) Immunoblot analysis of recombinant μ2 protein in the soluble (cytoplasmic) and pellet (nuclear) fractions of L929 cells transfected with either T1L or T3D M1 gene. The cell lysates were collected and fractionated at 24 h post-transfection, resolved by SDS-PAGE and immunoblotted with rabbit polyclonal anti-μ2 antibody followed by PAAP. The blot was then reacted with Attophos. The middle panel shows an immunoblot of the same samples stained for tubulin, a cytoplasmic protein that is present only in the soluble fraction. The bottom panel shows the same samples stained with coomassie blue showing a protein in the pellet fractions of 67 kDa in molecular weight corresponding to lamin and unidentified proteins in the soluble fractions, as loading controls. M = mock-infected; S = soluble fraction; P = pellet fraction.

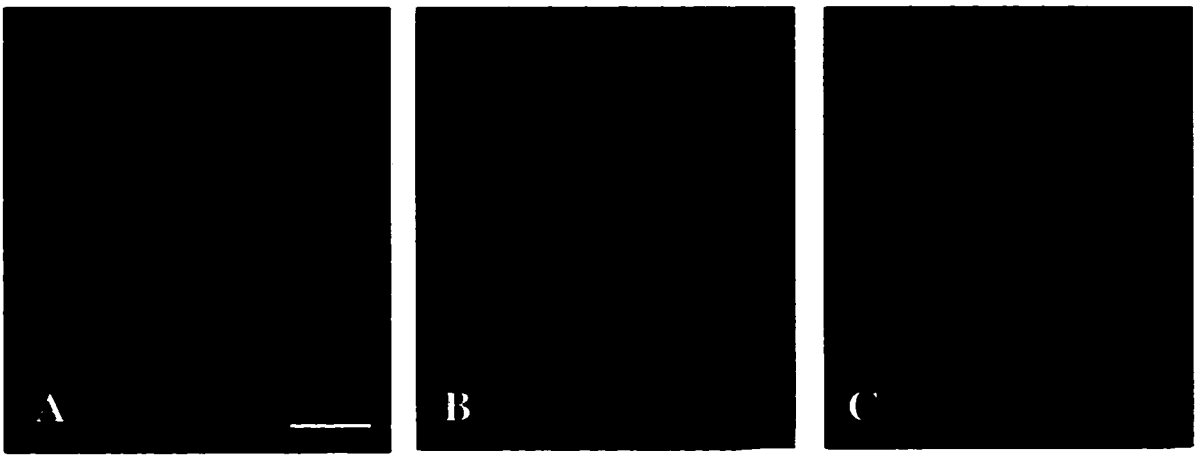
A
B
C
μ2
nuclei
overlay

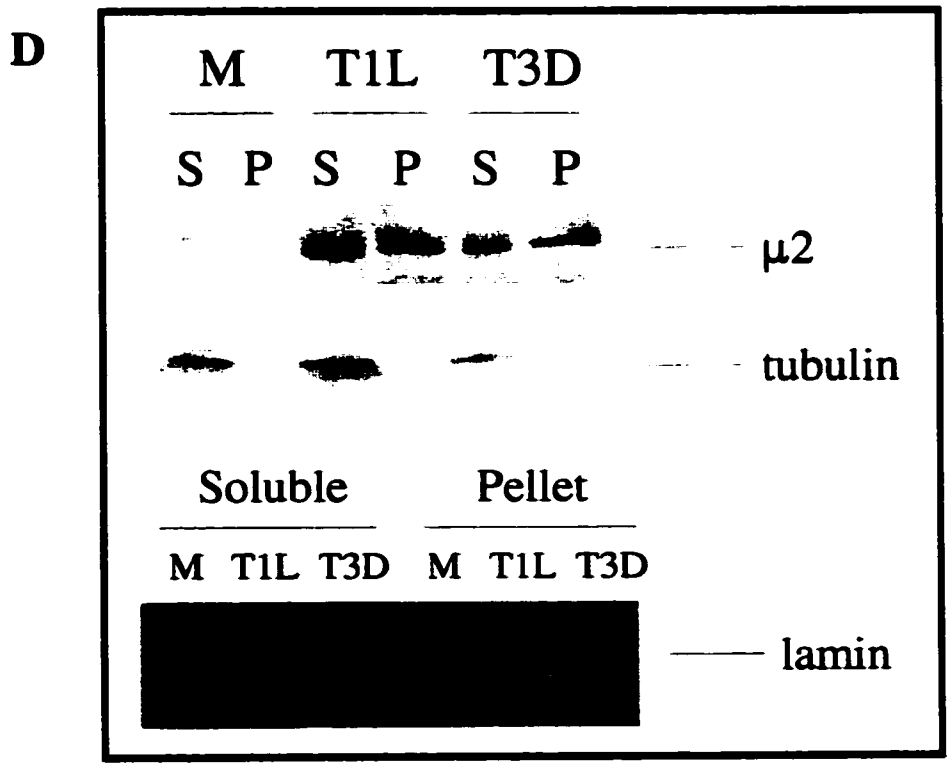
D
M
T1L
T3D
S P S P S P
μ2
tubulin
Soluble
Pellet
M T1L T3D M T1L T3D
lamin

of the mutant recombinant μ2 protein determined by double immunofluorescence staining for μ2 protein and the nucleus. This showed that deletion of either region resulted in the recombinant μ2 protein localizing mostly to the cytoplasm compared to cells transfected with wt μ2 protein (Fig. 6.2). Deletion of aa261-264 resulted in a generalized cytoplasmic distribution whereas deletion of aa95-127 resulted in a perinuclear distribution of μ2 protein. This indicates that reovirus μ2 protein has a bipartite nuclear localization signal similar to that of the influenza PB2 protein.

6.3.3 Recombinant μ2 protein localizes to PML bodies

PML bodies are nuclear matrix-associated structures that have been described to be proteolysis centers in the nucleus that recruit UPP components when a misfolded nuclear protein is overexpressed (Anton *et al.*, 1999). Since μ2 protein may be nuclear matrix-associated and is ubiquitinated and degraded by the 26S proteasome, association of recombinant μ2 protein complexes with PML bodies in the nucleus during transfection was investigated. To determine the localization of μ2 protein relative to PML bodies, double immunofluorescence labeling for μ2 and PML proteins in HeLa cells transfected with T3D M1 gene for 24 h was performed using confocal laser scanning microscopy. This showed that μ2 protein colocalized with PML protein in PML bodies in the nucleus as well as the cytoplasm (fig 6.3 A-C). This suggested that μ2 protein could be interacting with PML protein during infection. However, double immunofluorescent staining of infected HeLa cells for μ2 and PML proteins showed that the two proteins do not colocalize in the nucleus during reovirus infection (Fig. 6.3 D-F). Interestingly, small foci of PML protein were present within reovirus inclusions in the cytoplasm suggesting

Figure 6.2 Mapping of μ2 protein nuclear localization signal (NLS).

L929 cells were transfected with either the T1L M1 gene-expressing plasmid vector 8BK44 (A-C) or plasmid vectors expressing M1 gene deletion mutants 5X23P (Δ95-127) (D-F) or T1-NLS-del-9 (Δ261-264) (G-I) for 24 h. The cells were fixed in acetone and stained for μ2 protein using a rabbit polyclonal anti-μ2 antibody followed by a Cy3-conjugated donkey anti-rabbit (A, D and G). Nuclei were stained with DAPI (B, E and H). The images were obtained using an epifluorescence microscope. The μ2 protein is coloured red and the nuclei are coloured blue. In the overlay images (C, F and I) the colocalization of μ2 protein and the nucleus is indicated by the pink colour. The bar represents 20 μm.

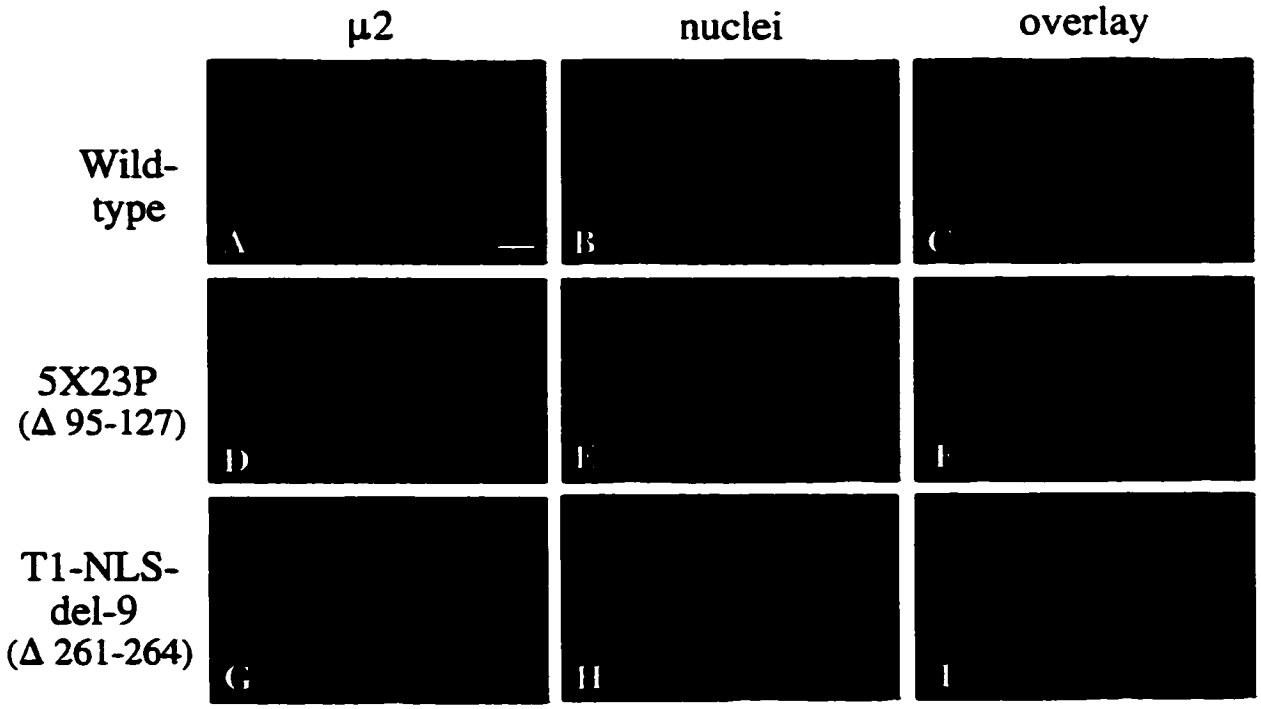
μ2
nuclei
overlay
Wild-type
5X23P (Δ 95-127)
T1-NLS-del-9 (Δ 261-264)
A
B
C
D
E
F
G
H
I

Figure 6.3 Localization of recombinant μ2 protein to PML bodies.

HeLa cells were either transfected with the plasmid vector pGEM-M1 clone T3-18 expressing the T3D M1 gene (A-C) or infected with T3D (D-F) for 24 h. The cells were fixed in acetone and stained for μ2 protein using a rabbit polyclonal anti-μ2 antibody (A and D) and for PML protein using a mAb to PML protein (B and E). The secondary antibodies used were FITC-conjugated goat anti-rabbit and Cy3-conjugated donkey anti-mouse. Nuclei were stained with DAPI. The images were obtained using a confocal laser scanning microscope. The μ2 protein is coloured green and the PML protein is coloured red. In the overlay images (C and F), colocalization of μ2 and PML proteins is indicated by the yellow colour. The bars represent 10 μm.

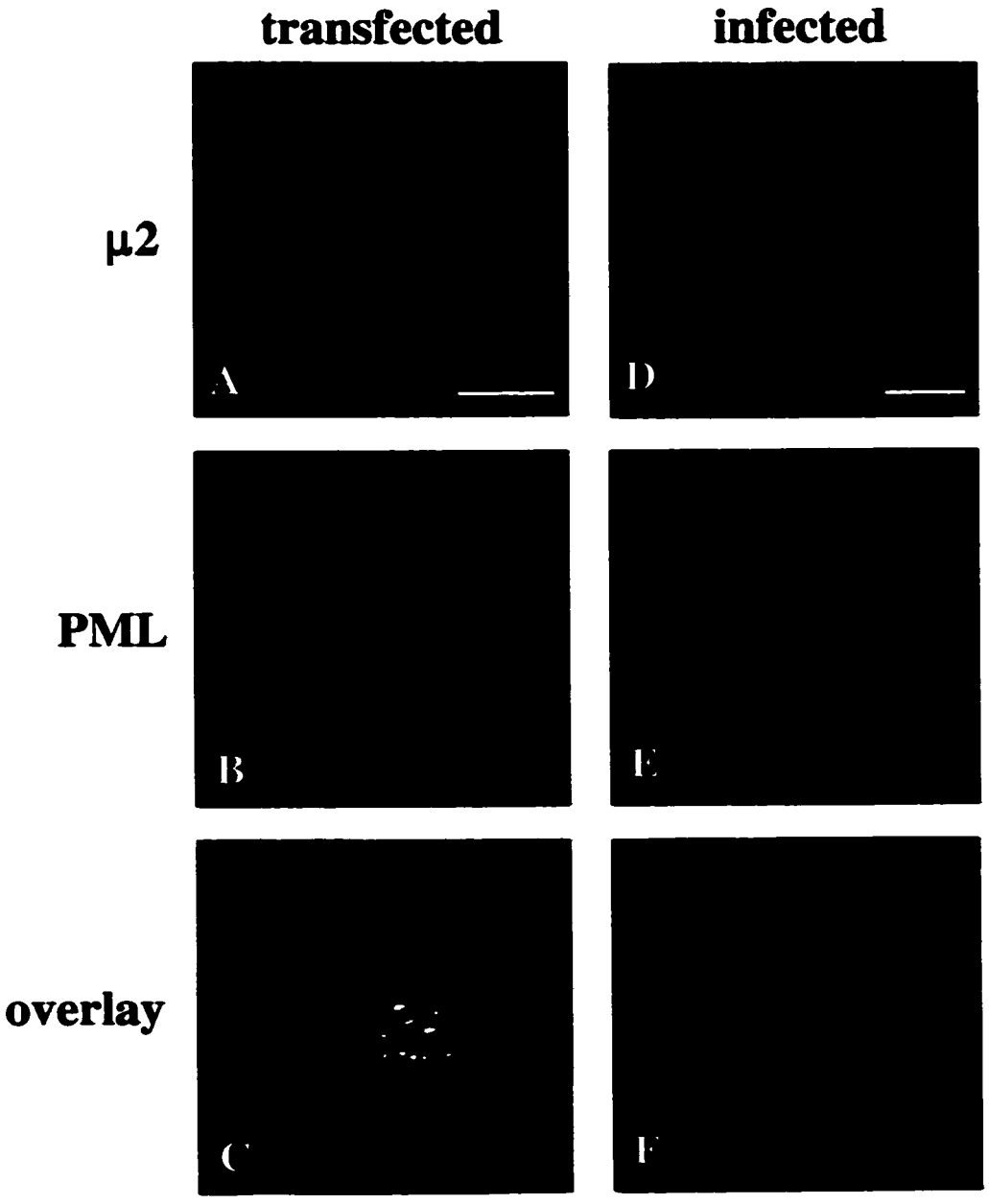
transfected
infected
μ2
PML
overlay
A
B
C
D
E
F

relocalization of PML protein and possible interaction with μ2 protein. However, some PML foci were located elsewhere in the cytoplasm apart from reovirus inclusions and *in vitro* co-expression of μ2 and the PML protein isoform VI (Borden *et al.*, 1998) in reticulocyte lysate followed by immunoprecipitation with rabbit polyclonal anti-μ2 antiserum showed that the two proteins did not directly interact (data not shown).

6.3.4 Mapping of μ2 protein region(s) involved in localization to PML bodies and protein complex formation

The localization of recombinant μ2 protein to PML bodies and formation of protein complexes could be a result of μ2 protein interactions with constituents of PML bodies such as components of the UPP, and therefore could be similar to interactions during reovirus inclusion formation. To gain insight into the kind of interaction(s) leading to the localization of μ2 protein to PML bodies or the formation of μ2 protein complexes it was decided to map the region(s) involved using M1 gene deletion mutants. M1 gene deletion mutants were constructed by PCR-directed mutagenesis. The deletion mutants were then transfected into HeLa cells and localization of the μ2 proteins determined by costaining for μ2, PML and the nucleus.

Expression of the C-terminal end deletion mutant, 8BK34 (Δ239-736), of T1L μ2 protein, resulted in a faster rate of μ2 protein complex formation and PML body localization at 24 h post-transfection when compared to wt T1L μ2, 8BK44, which forms protein complexes at a slower rate than T3D μ2 protein (Fig. 6.4 and Table 3.3). This suggests that the amino-terminal end of μ2 protein is important for protein complex formation and localization to PML

Figure 6.4 Mapping of regions involved in recombinant μ2 protein complex formation and PML body localization.

Diagram showing μ2 protein deletion mutants used to map out regions involved in μ2 protein complex formation and PML body localization. The M1 gene deletion mutant constructs were transfected into HeLa cells and the cells were fixed in acetone and stained at 24 h post-transfection for μ2 protein using a polyclonal rabbit anti-μ2 antibody and for PML protein using a mAb to PML protein. The secondary antibodies used were FITC-conjugated goat anti-rabbit and Cy3-conjugated donkey anti-rabbit. Nuclei were stained with DAPI. The samples were then visualized using an epifluorescence microscope and assessed for μ2 protein complex formation. PML body and nuclear localization. Red circle = long basic NLS motif; red rectangle = short basic NLS motif; [a] the number of antigen-positive cells showing protein complex formation at 24 h post-transfection was counted using a fluorescence microscope and expressed as: + = 0 to 20%, ++ = 20 to 40% etc).

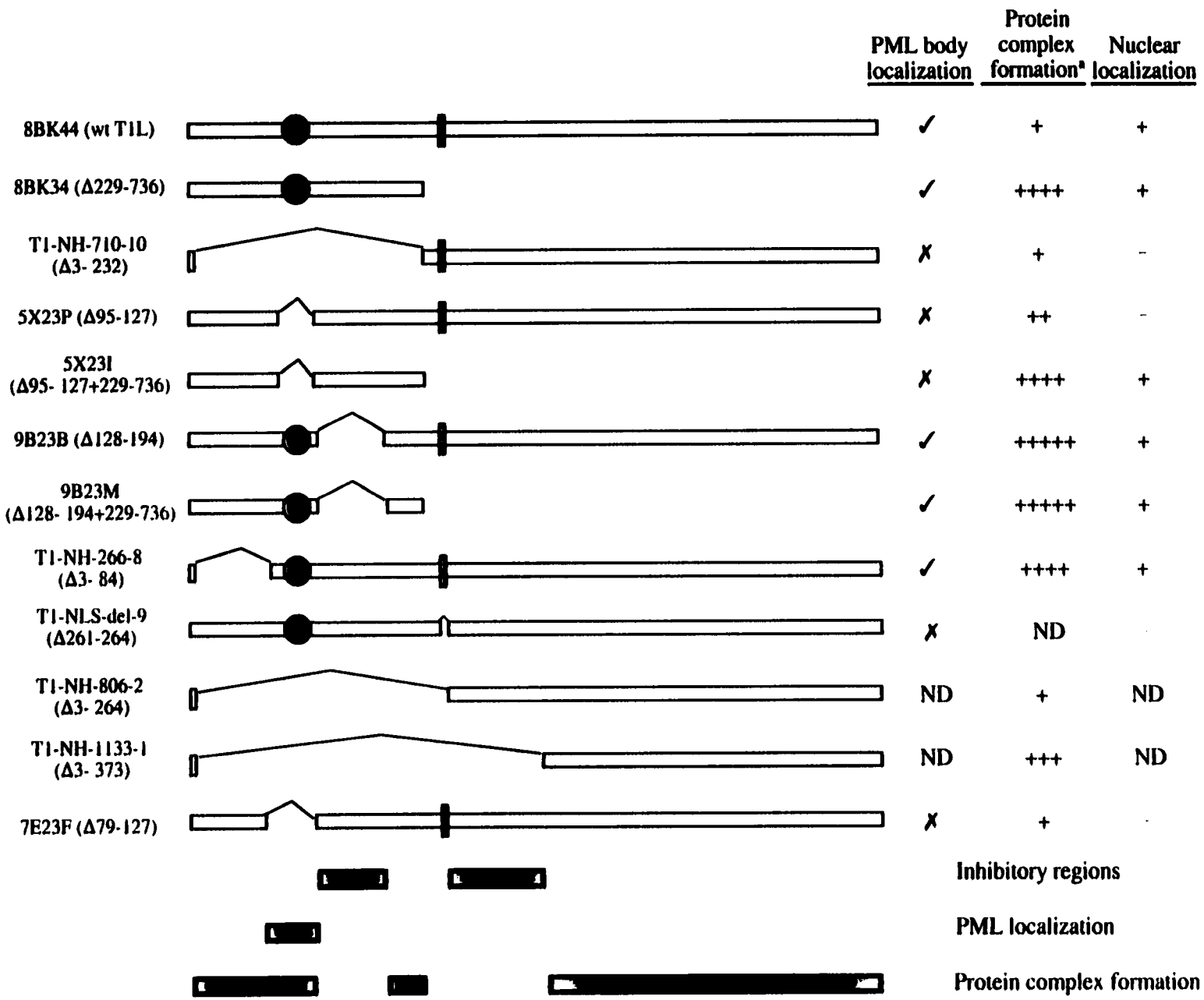
PML body localization
Protein complex formation[a]
Nuclear localization
8BK44 (wt T1L)
✓ + +
8BK34 (Δ229-736)
✓ ++++ +
T1-NH-710-10 (Δ3- 232)
✗ + -
5X23P (Δ95-127)
✗ ++ -
5X23I (Δ95- 127+229-736)
✗ ++++ +
9B23B (Δ128-194)
✓ +++++ +
9B23M (Δ128- 194+229-736)
✓ +++++ +
T1-NH-266-8 (Δ3- 84)
✓ ++++ +
T1-NLS-del-9 (Δ261-264)
✗ ND
T1-NH-806-2 (Δ3- 264)
ND + ND
T1-NH-1133-1 (Δ3- 373)
ND +++ ND
7E23F (Δ79-127)
✗ +
Inhibitory regions
PML localization
Protein complex formation

bodies and that the C-terminal end probably exerts inhibitory effects on this process. Consistent with this hypothesis the expression of the N-terminal end deletion mutant, T1-NH-710-10 (Δ3-232), resulted in a protein that did not localize to PML bodies and was similar to wt μ2 protein in protein complex formation. However, the loss of association with PML bodies is most likely due to the inability of the protein to localize to the nucleus since one of the NLS motifs is deleted in this mutant. Correspondingly, the deletion of either NLS motif, M1 mutants 5X23P (Δ95-127) and T1-NLS-del-9 (Δ261-264), resulted in a loss of association with PML bodies, an action most likely preempted by the inability of the protein to localize to the nucleus. However, it is possible that the long basic NLS motif (aa100-114) is important in localization of μ2 protein to PML bodies, as well as the nucleus, because its deletion from the amino-terminal mutant of μ2 protein, in M1 mutant 5X23I (Δ95-127+229-736) which is small enough not to require a NLS for nuclear localization, resulted in a decrease in the capability of μ2 protein to localize to PML bodies but not to form protein complexes. Thus μ2 protein complex formation and PML body localization could be a function of different but overlapping μ2 protein motifs.

Further analysis of the C-terminal end showed that it might also play a role in controlling protein complex formation. Deletion of the proximal region, M1 mutant T1-NH-1133-1 (Δ3-373), resulted in a protein that was more efficient in localizing into protein complexes compared to M1 mutant T1-NH-710-10 (Δ3-232). This suggests that the region between aa232-373 exerts inhibitory effects on protein complex formation. In addition, deleting aa128-194 from the amino-terminal end (M1 mutant 9B23B) accelerates protein complex formation by T1L μ2 protein suggesting the presence of another inhibitory region. In summary, these data suggest that the

amino-terminal end of μ2 protein, aa1-228, and possibly C-terminal end, aa373-736, are important for protein complex formation or PML body localization. Specifically, PML body localization appears to require the region spanning from aa95-127 which includes the long basic NLS motif. The data also suggests the existence of protein complex formation inhibitory regions between aa128-194 and 232-373.

6.3.5 Comparison of recombinant μ2 protein complexes to aggresomes

The observation that recombinant μ2 protein is capable of accumulating in protein complexes independent of other reovirus proteins and that it accumulates in PML bodies in the nucleus which have been shown to be capable of recruiting UPP components led to the examination of whether μ2 protein complexes, like reovirus inclusions, are similar to aggresomes. Localization of μ2 protein complexes relative to the UPP components, Ub, proteasomal antigens, and the MTOC nucleating protein γ-tubulin was examined in M1 gene-transfected HeLa cells by confocal laser scanning microscopy. Unlike reovirus inclusions, recombinant μ2 protein complexes only partially colocalized with proteasomal antigens and Ub (Fig. 6.5 A-F compared to Fig.5.3). However, the MTOC nucleating protein γ-tubulin colocalized with μ2 protein complexes at multiple locations (Fig. 6.5 G-I). This suggests that recombinant μ2 protein complexes share some similarities with aggresomes because additionally they also partially colocalize with vimentin (Fig. 3.6 A-C).

To further investigate the interactions of recombinant μ2 protein and the UPP in transfected cells, M1 gene-transfected cells at 16 h post-transfection were treated with PSI for

Figure 6.5 Association of recombinant μ2 protein with UPP components in M1 gene-transfected HeLa cells.

HeLa cells were transfected with a T3D M1 gene construct (pGEM-M1 clone T3-18). Cells were stained at 24 h post-transfection for either proteasomes using a rabbit polyclonal antiserum to α-subunit of 20S proteasome (B), or Ub using a rabbit polyclonal antiserum to Ub (E) or γ-tubulin using a γ-tubulin-specific mAb (H) and double-stained for μ2 using a rabbit polyclonal anti-μ2 directly conjugated to FITC (A, D and G). The secondary antibodies used were Cy3-conjugated donkey anti-rabbit (B and E) and Cy3-conjugated donkey anti-mouse (H). Nuclei were stained with DAPI. Images were obtained using a confocal laser scanning microscope. In the overlay pictures (C, F and I), colocalization of μ2 and proteasomes or Ub or γ-tubulin is indicated by the yellow colour. The bar represents 10 μm.

(J) Immunoblot of M1 gene- or M1 gene deletion mutants-transfected HeLa cells showing polyubiquitination of recombinant μ2 protein. HeLa cells were either transfected with the wt M1 gene construct pGEM-M1 clone T3-18 (wt), NLS deletion mutants 5X23P (5X23P) or T1-NLS-del-9 (del-9) or mock-transfected with pGEM vector (mock). At 16 h post-transfection, cells were treated with PSI for 4 h or left untreated. Cell lysates were collected and resolved by SDS-PAGE and immunoblotted using a rabbit polyclonal anti-μ2 antibody, followed by goat anti-rabbit conjugated to alkaline phosphatase. The blot was then reacted with Attophos. * = probable ubiquitinated μ2 protein species.

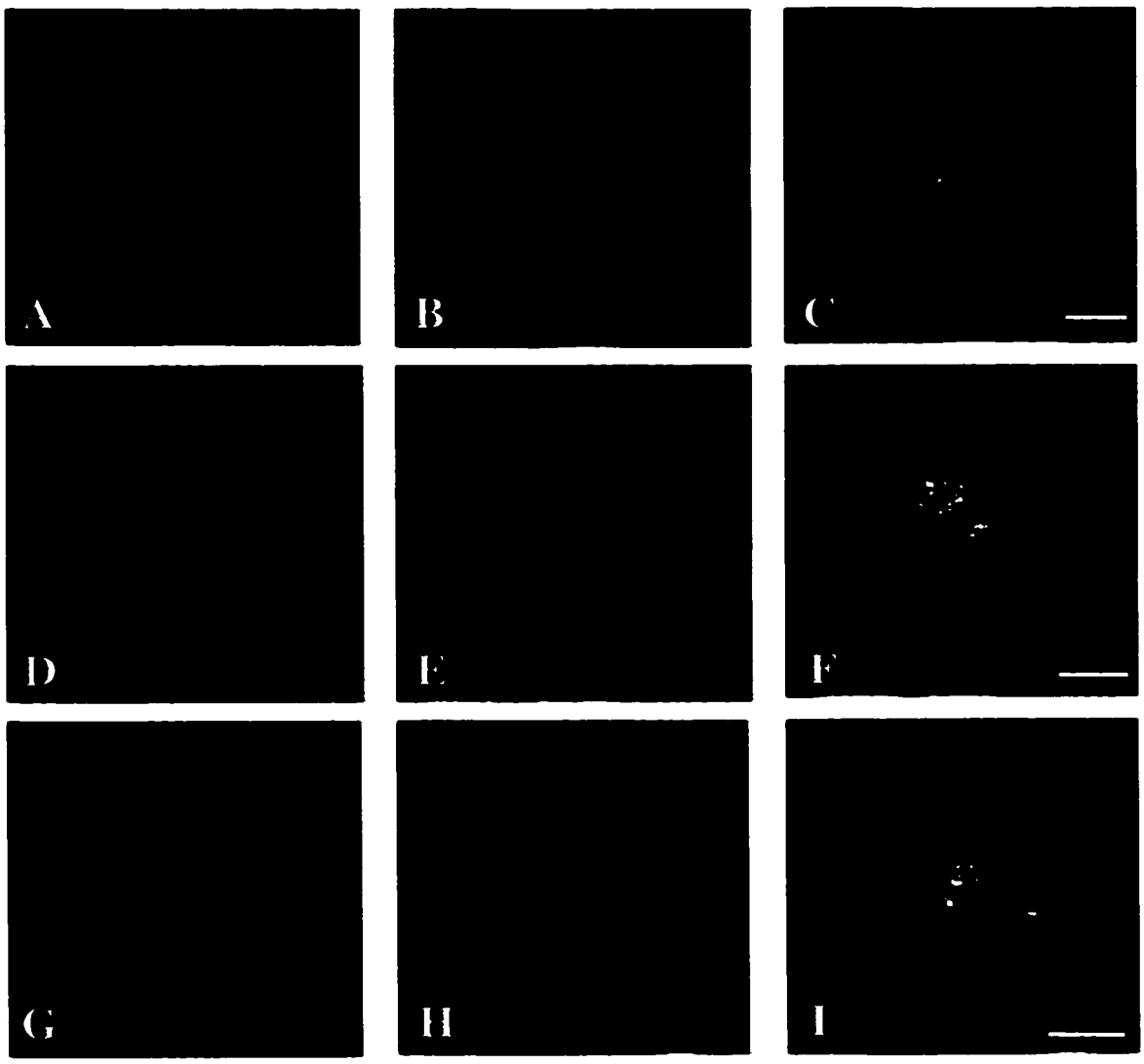
A
B
C
D
E
F
G
H
I

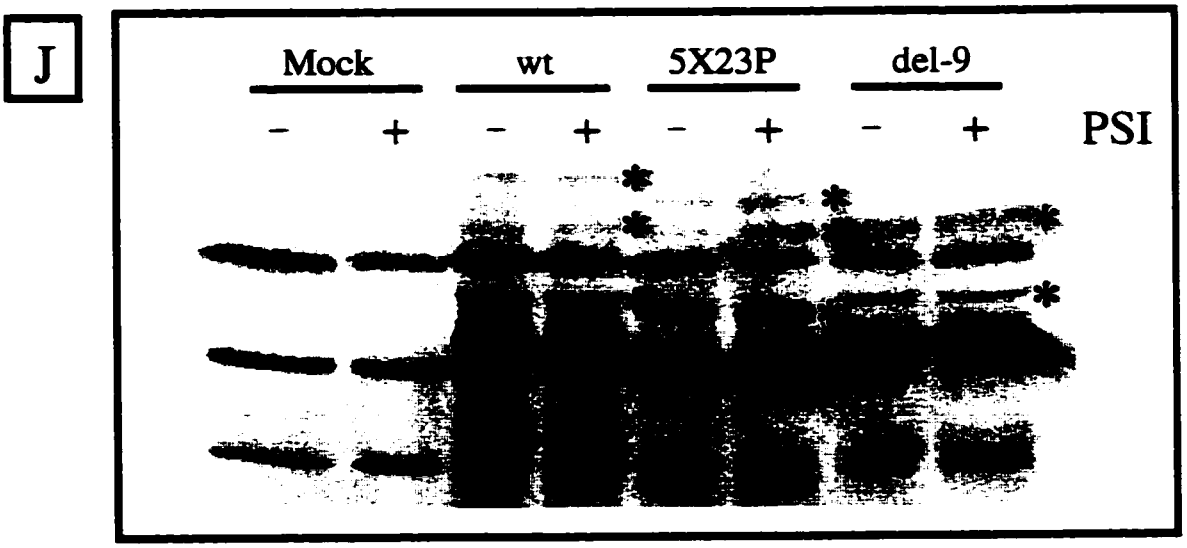
J
Mock
wt
5X23P
del-9
- + - + - + - +
PSI

4 h or left untreated and the samples were resolved by SDS-PAGE and analyzed by immunoblot using a rabbit polyclonal anti-μ2 antiserum. This showed that in both PSI-treated and untreated cells there were higher molecular weight μ2-specific bands that could represent Ub-modified μ2 protein species that were not present in mock-transfected cells (Fig 6.5 J). The same results were obtained when the cells were transfected with NLS-deleted μ2 proteins except that the bands were more intense in PSI-treated cells especially for 5X23P. This suggests that recombinant μ2 protein is possibly polyubiquitinated and accumulates in cells even without PSI treatment.

6.3.6 Localization of recombinant μ2 protein in Cos-1 cells

Up to this point, in order to get high level expression of recombinant μ2 protein during transient transfection, expression of the M1 gene has been achieved using the bacteriophage T7 RNA polymerase promoter in conjunction with vaccinia virus infection to supply the T7 RNA polymerase. However, vaccinia virus, a poxvirus, forms viral inclusions at the MTOC that resemble aggresomes and accumulate UPP components (described in Chapter one). It is therefore possible that this would compete or interfere with the normal functioning or localization of recombinant μ2 protein. To address this point, the localization of recombinant μ2 protein was examined in Cos-1 cells transfected with a pcDNA3 construct expressing the M1 gene under the eukaryotic CMV promoter. The pcDNA3 vector also contains an SV40 origin of replication that ensures high copy number due to replication of the plasmid construct in Cos-1 cells, which express the SV40 large T antigen. Localization of μ2 protein relative to the UPP components, Ub and proteasomal antigens, was examined by confocal laser scanning microscopy. μ2 protein complexes were shown to colocalize with Ub (Fig. 6.6 D-F), as well as

proteasomal antigens (Fig. 6.6 A-C). The μ2 protein complexes in Cos-1 cells were also shown to be entirely located in the cytoplasm and to be mostly perinuclear. This confirms that recombinant μ2 protein has the capability to accumulate in protein complexes which similar to reovirus inclusions are located around the nucleus and contain UPP components. This also suggests that the ability of μ2 protein to form complexes is probably linked to its interactions with the UPP and indicates that the Cos-1 expression system may be better suited for analyzing the role of μ2 protein in inclusion formation compared to the vaccinia virus expression system.

6.4 Discussion

In this chapter, the nuclear localization and protein complex formation of recombinant μ2 protein was examined to gain insight into the role played by μ2 protein in reovirus inclusion formation. The experiments demonstrate that μ2 protein has a well defined bipartite nuclear localization signal containing two basic regions separated by 147 aa, and is thus similar to that of a number of viral and host proteins. The μ2 protein NLS may function in a similar fashion to that described for the influenza PB2 protein where the short, four basic residue-motif, with the consensus sequence K R/K X R/K, is involved in targeting the protein to the perinuclear region while the longer basic region is involved in translocation of the protein across the nuclear envelope (Mukaigawa and Nayak, 1991). In μ2 protein, deletion of the short region ($K^{261}RLR$) resulted in a generalized cytoplasmic distribution while deletion of the long basic region ($R^{100}RLRKRLMLKKDLRK$) resulted in accumulation of μ2 protein around the nucleus. This is in keeping with the behaviour of the influenza PB2 protein. Possession of a distinct and highly organized nuclear localization signal by μ2 protein suggests that localization of the protein

Figure 6.6 Association of recombinant μ2 protein with UPP components in M1 gene-transfected Cos-1 cells.

Cos-1 cells were transfected with a T3D M1 gene construct (pCMV-M1CN clone T3-13). Cells were stained at 24 h post-transfection for either proteasomes using a rabbit polyclonal antiserum to α-subunit of 20S proteasome (B), or Ub using a rabbit polyclonal antiserum to Ub (E) and double-stained for μ2 using a rabbit polyclonal anti-μ2 directly conjugated to FITC (A and D). The secondary antibody used was Cy3-conjugated donkey anti-rabbit (B and E). Nuclei were stained with DAPI. Images were obtained using a confocal laser scanning microscope. In the overlay pictures (C and F), colocalization of μ2 and proteasomes or Ub is indicated by the yellow colour. The bar represents 10 μm.

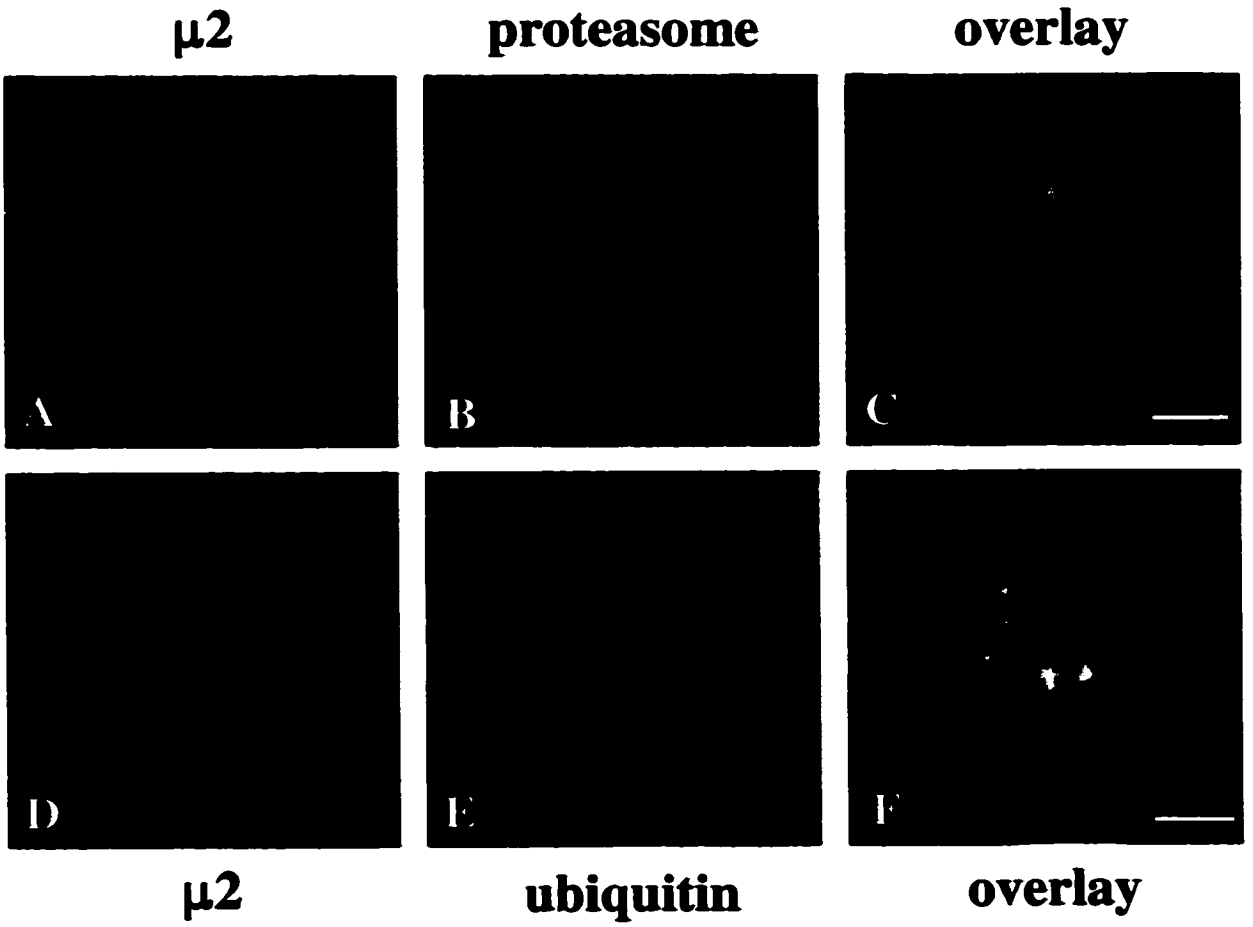
μ2
proteasome
overlay
A
B
C
D
E
F
μ2
ubiquitin
overlay

to the nucleus could play an important role in reovirus replication. It is also possible that the NLS motif is important for a function unrelated to nuclear localization, such as interaction with another viral protein, which would be competitive with nuclear localization. This could explain the decrease in amount of μ2 protein localizing to the nucleus during infection compared to transfection as observed by immunofluorescence. The nuclear localization of reovirus σ3 protein is inhibited by coexpression and interaction with μ1C protein (Yue and Shatkin, 1996).

Further analysis of recombinant μ2 protein nuclear localization showed that it specifically localizes to PML bodies, which are proposed to play a role in host antiviral defence and contain interferon-inducible proteins including PML. PML protein is present in at least seven different isoforms due to alternative splicing in the C-terminal end. The PML isoform III has been shown to play a direct role in inhibiting replication of influenza, VSV and HFV (Chelbi-Alix *et al.*, 1998; Regad *et al.*, 2001). It is therefore possible that μ2 protein could be localizing to the nucleus to inhibit a nuclear process directed by PML protein that down regulates viral replication. However, μ2 protein does not localize with PML protein in the nucleus during infection. Instead, PML protein is present as distinct punctate foci in reovirus cytoplasmic inclusions suggesting a direct interaction of PML with viral or host proteins present in the inclusions. The possibility of μ2 protein-PML protein interaction was explored using an *in vitro* reticulocyte lysate assay with PML isoform VI. This showed no direct interaction between the two proteins. It is possible that μ2 protein could interact with a different PML isoform since they have been shown to perform different functions and interact with different proteins (Jensen *et al.*, 2001). Other possibilities could be that μ2 protein interacts with another component of PML bodies that is not present or

is displaced from these bodies during infection. Further experiments are needed to resolve these possibilities.

It has recently been reported that overexpression of an unstable influenza NP protein results in its localization to PML bodies and the recruitment of UPP components (Anton *et al.*, 1999). Thus μ2 protein localization to PML bodies could be similar to localization to reovirus inclusions, which also recruit UPP components. It was therefore reasoned that mapping of a region(s) required for μ2 protein localization to PML bodies would help in understanding the type of interactions or mechanisms involved not only in μ2 protein localization to PML bodies but also to reovirus inclusions. Preliminary data suggests that the amino-terminal end of μ2 protein, including the long basic region involved in nuclear localization, could be important for PML body localization and protein complex formation. The removal of the C-terminal end from T1L μ2 protein accelerated the formation of protein complexes by the T1L μ2 protein suggesting that a region within the C-terminal end could have inhibitory effects on protein complex formation by the protein. Further deletion analysis indicated that the inhibitory region could reside between aa232-373. Another potential inhibitory region was found between aa128-194, since deletion of this region also resulted in accelerated protein complex formation. Deletion of the long basic NLS motif from the amino-terminal end mutant of μ2 protein (mutant, 5X23I : Δ95-127) blocked the localization of the protein to PML bodies suggesting that this region could be important for PML body localization. This region includes four lysine residues that could be used for ubiquitination of μ2 protein which could be involved in PML body localization. Sequence analysis also revealed a potential E3 Ub-ligase binding motif, P^{91}SAIP, that is partly

deleted in the M1 mutant, 5X23I. This motif resembles the consensus sequence P (T/S) A P, that can act as an E3 Ub-ligase interaction motif (Strack *et al.*, 2000). Furthermore, expression of an M1 mutant with the whole motif deleted (7E23F : Δ79-127) does not enhance protein complex formation. The deletion of this region in T3D μ2 protein is required to further assess its importance in protein complex formation. Interestingly, the residue A^{93} is mutated to V in T1L μ2 protein (P^{91}SAIP →P^{91}SVIP) which could explain the difference in protein degradation and inclusion formation rates between the two proteins. Identification of the E3 Ub-ligase involved in μ2 protein ubiquitination will also be important in pinpointing if this region plays any role in μ2 protein ubiquitination and protein complex formation.

The localization of μ2 protein to PML bodies during transfection using the vaccinia virus system seems to resemble localization of μ2 protein to reovirus inclusions in that it is strain-dependent. However, μ2 protein does not detectably localize to PML bodies during infection even though the protein translocates to the nucleus, and most importantly it does not form protein complexes in the nucleus when transfection is performed in Cos-1 cells which do not require the use of vaccinia virus. In addition, colocalization of recombinant μ2 protein and the UPP components, Ub or proteasomal antigens, was partial in M1 gene-transfected cells using vaccinia virus and did not occur to the same extent as in infected cells. This suggests that vaccinia virus, which forms viral inclusions at the MTOC that recruits UPP components could be affecting the normal interactions and localization of μ2 protein during transfection. In contrast, the expression of μ2 protein using the Cos-1 expression system resulted in protein complex formation that, similar to reovirus inclusions, were perinuclear and contained Ub and

proteasomal antigens. This suggests that the protein complexes formed using the Cos-1 cell expression system more closely resemble reovirus inclusions and would be better suited for analysis of the role played by μ2 protein in reovirus inclusion formation and the elucidation of the mechanism behind it. This data also suggests that the interaction of μ2 protein and the UPP could be critical to this process. To gain further knowledge of the region(s) and the mechanism involved in μ2 protein complex formation, the M1 gene deletion mutants constructed so far need to be transferred into a pcDNA3 vector that can be used in the Cos-1 cell expression system. In addition, specific point mutations need to be developed by site directed mutagenesis to address lysine residues that are used for μ2 protein ubiquitination and other interactions important for ubiquitination, protein complex formation or inclusion formation. These mutants would also have the added advantage of maintaining the protein secondary structure, a likely shortcoming of deletion mutants.

CHAPTER SEVEN

SUMMARY AND CONCLUSION

The initial focus of our laboratory was to develop reovirus as an expression vector for *in vitro* expression of foreign genes or for use in gene therapy. However, early attempts to introduce a foreign gene into reovirus were unsuccessful and it was reasoned that an understanding of the reovirus assembly process might help in this endeavour. This study was aimed at identifying virus-host cell interactions involved in the formation of reovirus inclusions which are believed to be the major sites of reovirus assembly. The data reported in this thesis represents ground breaking work on the characterization of the mechanism behind reovirus inclusion formation and includes novel findings that will be the basis for detailed molecular characterization of this process.

7.1 The players and the mechanism behind reovirus inclusion formation

Using reovirus genetics, the reovirus M1 gene, which encodes the minor core protein μ2, was identified as the primary determinant of the rate of inclusion formation in reovirus-infected cells. Reassortant reoviruses containing the T3D M1 gene formed inclusions at a faster rate than those with T1L M1 gene. The S3 gene encoding the nonstructural protein σNS was shown to play a secondary role in the process. To date, the intermediate filament protein, vimentin, and microtubules are the only host proteins implicated in reovirus inclusion formation. In this study, it was shown for the first time that the UPP components namely, Ub, proteasomal antigens and

the molecular chaperone hsp-70, are recruited to reovirus inclusions. This makes reovirus inclusions structurally similar to aggresomes. Furthermore, it was demonstrated that inhibition of the UPP by depletion of the cellular pool of free Ub using proteasome inhibitor perturbs inclusion formation and reovirus growth. This suggests that reovirus uses the UPP and possibly the aggresome formation pathway to concentrate its viral macromolecules at sites of viral assembly. However, unlike aggresomes reovirus inclusions do not form at the MTOC suggesting that it uses a modified aggresome formation pathway and that another host or a viral protein initiates the nucleation of these sites at other cytoplasmic locations.

Evidence presented in this study also suggests that the μ2 protein could play a direct role in inclusion formation. Recombinant μ2 protein accumulates in protein complexes in a strain-dependent manner with kinetics that resemble inclusion formation in reovirus-infected cells. μ2 protein complexes partially colocalize with Ub, vimentin and proteasomal antigens. Furthermore, it is shown that μ2 protein is ubiquitinated with mono-ubiquitinated μ2 protein being the most abundant μ2-ubiquitinated species. Since mono-ubiquitination of cellular proteins has been shown to function in subcellular localization and sorting of tagged proteins in the multivesicular body pathway it is possible that ubiquitination of μ2 protein accomplishes a similar task resulting in μ2 protein or μ2 protein-containing complexes localizing to reovirus inclusions for viral assembly. The potential role for mono-ubiquitination in reovirus morphogenesis is made more appealing by the increase in reovirus growth in A549 cells expressing a mutant Ub with K48R mutation which results in mostly mono-ubiquitination of target proteins. Thus the control of the rate of inclusion formation by μ2 protein could in part be due to its interactions with the UPP.

However, the role played by μ2 protein and especially μ2 protein ubiquitination in reovirus inclusion formation and viral assembly will require further investigation. One way of gaining further insight into the role of μ2 protein ubiquitination in reovirus morphogenesis might be the identification of the E2 or E3 enzymes used for μ2 protein ubiquitination. This would allow the assessment of the ability of reovirus to grow in cell lines that have particular E2 or E3 enzymes mutated or knocked-out.

7.2 Model of reovirus viral assembly and inclusion formation

The data presented in this thesis suggests that reovirus assembly and/or inclusion body formation utilizes Ub and perhaps its protein sorting role in the endocytic pathway (Lemmon and Traub, 2000; Hicke, 2001). Protein sorting in the multivesicular body (MVB) of the endocytic system, that follows internalization and downregulation of surface proteins, is regulated by mono-ubiquitination. Evidence presented in this thesis shows that most of the Ub-modified μ2 protein is present in the mono-ubiquitinated state and that reovirus growth is enhanced in a cell line overexpressing a mutant Ub that results in conjugation of subthreshold length Ub chains e.g. monoubiquitination. This suggests that mono-ubiquitination could play an important role in reovirus assembly and allows me to propose a model for the assembly of reovirus particles and inclusion bodies based on the MVB pathway as shown in figure 7.1. The existence of the ssRNA complex containing σNS and other viral proteins (except μ2, λ3 and σ2) has been demonstrated (Antczak and Joklik, 1992). I propose that the ssRNA complex interacts with another complex containing μ2 protein in a body analogous to the MVB. Mono-ubiquitination, possibly of μ2 protein or host proteins, in this body facilitates protein sorting resulting in the assembly of

Figure 7.1 Model of reovirus viral assembly and inclusion formation.

Schematic representation of the endocytic pathway (on the left) and a model of reovirus viral assembly and inclusion formation based on the endocytic pathway (on the right). μ2 protein-containing complexes are indicated by the red ellipse, reovirus ssRNA-containing complexes are indicated by the green ellipse and mature reovirus particles are indicated by the yellow hexagon.

ENDOCYTIC PATHWAY

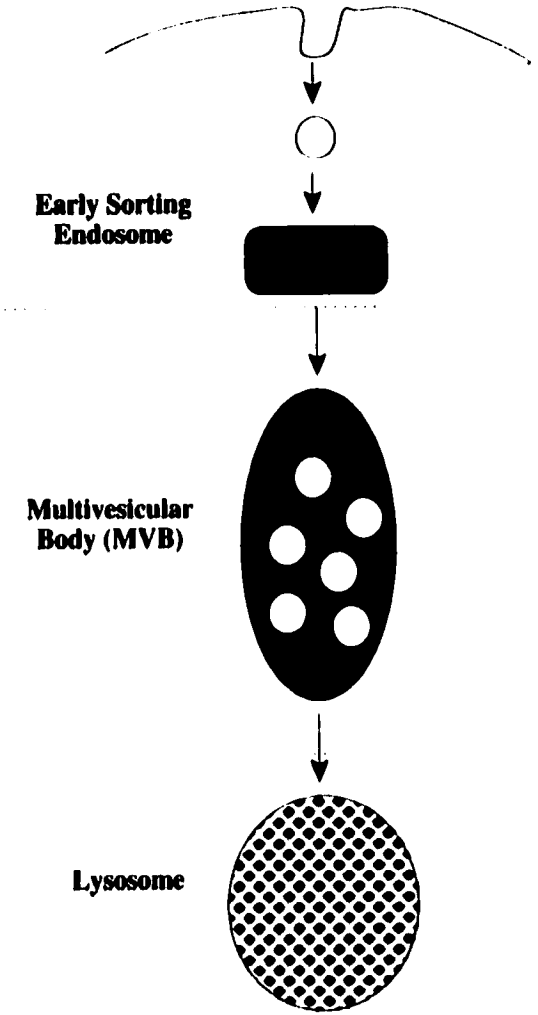

REOVIRUS VIRAL ASSEMBLY AND INCLUSION FORMATION

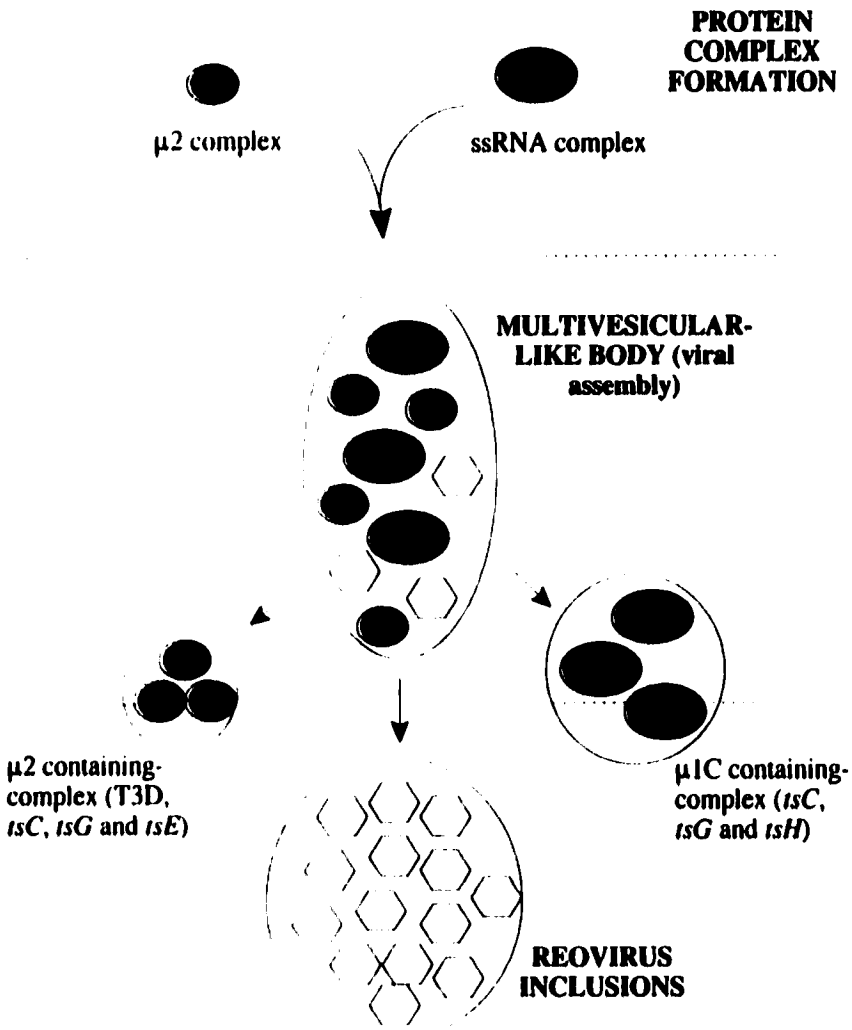

progeny viral particles.

Several key questions remain unanswered in this model and will require further detailed molecular studies. For example, if viral assembly occurs in inclusion bodies then why does T1L replicate to higher titers than T3D and with a time course that precedes T1L inclusion body formation? How does μ2 protein influence the process and how do T1L and T3D μ2 differ in this interaction? It is possible that a multivesicular-like body in which viral assembly is proposed to occur precedes the formation of the inclusion bodies. In this model inclusion bodies would be similar to lysosomes, the end-stage of the endocytic system, and would therefore be regarded as progeny virus storage depots or a response by the host cell to accumulating viral particles. The formation of inclusion bodies could also serve as a cell lysis mechanism by inhibiting cellular metabolism leading to release of progeny viral particles.

The ubiquitination of μ2 protein could be important for protein sorting, viral assembly or inclusion formation. Alternatively, the μ2 protein complex could promote the ubiquitination of other viral or host proteins required for the sorting of viral proteins into progeny viral particles. Other signals, in addition to ubiquitination, have been shown to contribute to protein sorting in the MVB including dileucine motifs that are present in the cytosolic portion of EGFR (Kil *et al.*, 1999). μ2 protein has 10 to 11 dileucine motifs which could play a similar role. It will be interesting to see if the two yeast hybrid experiments using μ2 protein as bait for a host cell library will show an interaction with host proteins involved in the MVB, for example TSG101, which is related to E2 enzymes (Babst *et al.*, 2000). The transition of the T3D μ2 protein

complex through the multivesicular-like body could be faster than that of T1L μ2 protein complex which may not allow sufficient interaction time with the ssRNA complex resulting in reduced T3D titers compared to T1L. Simply put, T3D μ2 protein could be described as being "fast and reckless" whilst T1L μ2 protein as being "slow and deliberate". Consistent with this idea, a recent study shows that μ2 protein could be a viral microtubule associated protein and that T1L μ2 protein is better at associating with microtubules than T3D μ2 protein which tends to accumulate in inclusion bodies (Parker *et al.*, 2002). The multivesicular-like body could be associated with the microtubules where viral assembly occurs before the progeny viral particles are transferred to inclusion bodies.

The faster transition of T3D μ2 complexes through the multivesicular-like body would result in the formation of some protein complexes containing μ2 protein but not the other viral proteins present in ssRNA complexes that were observed in T3D-infected cells (fig. 3.2 H). Mutations in μ2 protein that affect the localization of the protein to complexes would prevent μ2 protein complex formation and subsequent protein sorting in the multivesicular-like body resulting in no viral particle formation as seen in *tsH11.2*-infected cells even though the ssRNA complex is formed. Similarly, mutation in σNS would affect the formation of the ssRNA complex but not of the μ2 protein complex as seen in *tsE*-infected cells, thereby affecting μ2/Ub dependent-protein sorting because there would be no ssRNA complex proteins to sort. However, mutations in other viral proteins would have less severe effects on the formation of either μ2 protein complexes, ssRNA-containing complexes or protein sorting but would affect the finer detailed interactions in capsid formation. As a result a mutation in an outer capsid

protein would be detrimental to the formation of the outer capsid shell resulting in the formation of the core particle only and vice versa. Thus this model is consistent with the accumulation of core proteins (μ2) and outer capsid proteins (μ1C) in different protein complexes in *tsC447*- and *tsG453*-infected cells due to failure of either core or outer capsid formation (fig. 3.3).

A major shortcoming of this model is the comparison of reovirus inclusions, that are not enclosed by a membrane, to the membranous endocytic pathway. The transport of macromolecules in the endocytic pathway is achieved in membranous vesicles. However, except for the entry and uncoating stage, none of the reovirus replication stages have been shown to be associated with membranous vesicles. It is possible that the transport of reovirus macromolecules, similar to the transport of protein aggregates in the aggresome pathway, is achieved by the ability of the aggresome pathway to recognize large protein complexes which are then transported on microtubules to the various protein sorting compartments. These large protein complexes may also expose hydrophobic regions on the surface thereby mimicking the presence of a membrane.

7.3 Effects of reovirus inclusion formation on the host cell

The most compelling discovery in this study was the finding that the formation of reovirus inclusions results in the inhibition of Ub-dependent proteolysis, an effect also exerted by aggresomes. Given that Ub-dependent proteolysis is important in many cellular processes, the disruption of this pathway by reovirus would be detrimental to the host cell. It has been reported that inhibition of Ub-dependent proteolysis by aggresomes that form in neurodegenerative

diseases is the cause of neuronal cell death in these conditions. It is therefore likely that inhibition of this pathway by reovirus is the major cause of CPE in reovirus-infected cells which contributes to the pathology in reovirus disease. Undoubtedly, the mechanism leading to the formation of reovirus inclusions could be a very good target for antiviral therapy for members of the *Reoviridae* family, all of which form inclusion bodies, and include important human pathogens such as rotavirus. Studying reovirus inclusion formation could also prove insightful to the process of aggresome formation in neurodegenerative diseases and might provide possible targets for therapy in these conditions.

A lot of excitement has been generated recently with regards using reovirus as an oncolytic agent. Although it is thought that the basis for this effect is activation of the Ras signaling pathway in transformed and tumour cells which allows synthesis of viral proteins, the mechanism by which reovirus kills the cells has not been identified and it is likely that other cellular processes play a role in this effect. Cell division, the hallmark of cancerous cells, requires Ub-dependent proteolysis of cell cycle proteins in order for the cell to proceed through the different stages of mitosis. The use of the UPP by reovirus to form inclusion bodies leading to the inhibition of Ub-dependent proteolysis could represent a possible mechanism by which reovirus kills tumour cells where an active UPP could be optimal for reovirus growth. Analysis of reovirus inclusion formation could therefore help in understanding the oncolytic nature of reovirus and help in the development of better reovirus-based oncolytic agents.

7.4 M1 gene/interferon/UPP interrelationship

The data presented in this thesis shows that the control of the rate of inclusion formation by μ2 protein is probably due to its interactions with the UPP. The M1 gene has also been shown to control the induction and sensitivity of reovirus to interferon. Other studies have shown a requirement for the Ub-proteasome pathway in induction of the interferon antiviral response and the importance of interferon in the induction of UPP components. Taken together these data allow me to propose a three-point relationship with complex interactions that, depending on the balance of events, could either have positive or negative effects on reovirus replication (Fig. 7.2). T3D has been shown to readily induce interferon and is more sensitive to the antiviral effects of interferon than T1L, a phenotype that segregates with the M1 gene (Sherry *et al.*, 1998). Reciprocal regulation between the interferon and Ub-proteasome pathways has also been documented. Interferon has been shown to induce expression of genes that function in Ub conjugation and proteasomal degradation including the Ub-conjugating enzymes,UbcH5 and UbcH8 (Nyman *et al.*, 2000), as well as alternate proteasome β-subunits, LMP2 and LMP7 (Fruh *et al.*, 1994). On the other hand, the UPP is involved in regulating interferon-mediated signal transduction by degradation of components of the signaling pathway (Kim and Maniatis, 1996). A recent study also implicates the UPP in degradation of an interferon- or dsRNA-induced repressor of interferon-stimulated genes (Li and Hassel, 2001). The data in this thesis provides evidence for the third arm in this triangular relationship in that reovirus utilizes the UPP for inclusion formation and possibly viral assembly which then results in inhibition of Ub-dependent proteolysis. Conversely, reovirus μ2 protein is ubiquitinated and degraded by the 26S proteasome which could be involved in inclusion formation or could be part of antiviral defence

Figure 7.2 Interrelationship between reovirus (M1 gene), interferon and Ub-proteasome pathway that could influence the outcome of reovirus infection. Examples of the host and viral proteins that are involved are represented by the green circles. ? = no direct evidence available; Prot. = proteasomal antigens.

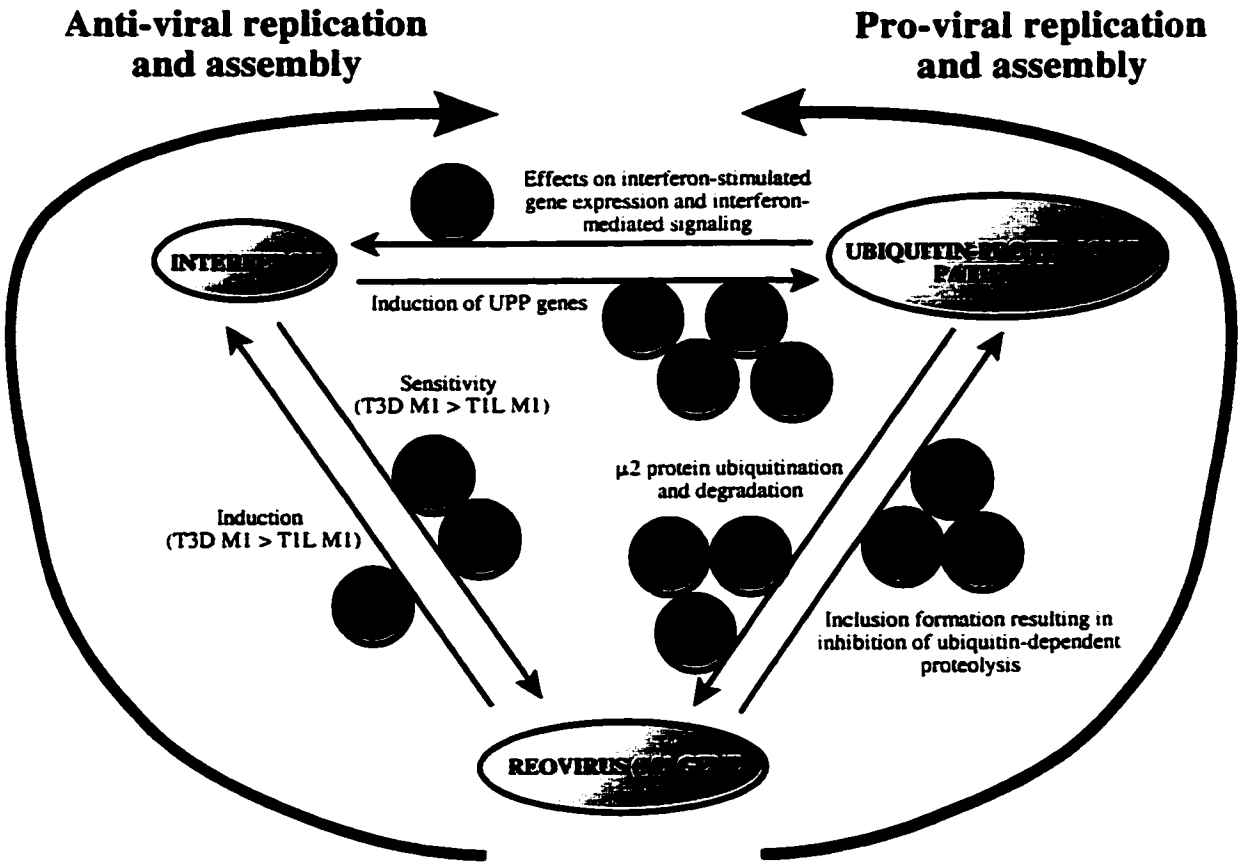
Anti-viral replication and assembly
Pro-viral replication and assembly
Effects on interferon-stimulated gene expression and interferon-mediated signaling
Induction of UPP genes
Sensitivity (T3D M1 > T1L M1)
Induction (T3D M1 > T1L M1)
μ2 protein ubiquitination and degradation
Inclusion formation resulting in inhibition of ubiquitin-dependent proteolysis

by the host cell. Consistent with this relationship is the fact that T3D, which induces interferon more readily, forms inclusions faster, has its μ2 protein ubiquitinated more efficiently and generally grows to lower titers than T1L. The interplay between these two systems and reovirus in general or μ2 protein in particular will definitely require further characterization at the molecular level to dissect the players and interactions involved. It is anticipated that this will create many avenues to be explored by succeeding members of the laboratory and revolutionize the study and understanding of reovirus replication and virus-host cell interactions.

In conclusion, this work has identified the major viral and host proteins involved in reovirus inclusion formation and has laid out the foundation for analysis of the mechanism behind reovirus inclusion formation at the molecular level. The impact of this work is very diverse, with the possibility of influencing such areas as antiviral therapy, development of reovirus as an expression vector and an oncolytic agent, as well as understanding the pathology of neurodegenerative diseases. After years of being considered a nonspecific event in reovirus replication, this work demonstrates that reovirus inclusion formation represents an important step in reovirus morphogenesis and pathogenesis, and that it is ready to take center stage as the main "act" in reovirus replication.

REFERENCES

[1] Abu, H.O., Gross-Mesilaty, S., Breitschopf, K., Hoffman, A., Gonen, H., Ciechanover, A., & Bengal, E. (1998) Degradation of myogenic transcription factor MyoD by the ubiquitin pathway in vivo and in vitro: regulation by specific DNA binding. *Mol. Cell Biol.*, **18,** 5670-5677.

[2] Ahn, J.Y., Tanahashi, N., Akiyama, K., Hisamatsu, H., Noda, C., Tanaka, K., Chung, C.H., Shibmara, N., Willy, P.J., Mott, J.D., Slaughter, C.A., & DeMartino, G.N. (1995) Primary structures of two homologous subunits of PA28, a gamma- interferon-inducible protein activator of the 20S proteasome. *FEBS Lett.*, **366,** 37-42.

[3] Antczak, J.B. & Joklik, W.K. (1992) Reovirus genome segment assortment into progeny genomes studied by the use of monoclonal antibodies directed against reovirus proteins. *Virology*, **187,** 760-776.

[4] Anton, L.C., Schubert, U., Bacik, I., Princiotta, M.F., Wearsch, P.A., Gibbs, J., Day, P.M., Realini, C., Rechsteiner, M.C., Bennink, J.R., & Yewdell, J.W. (1999) Intracellular localization of proteasomal degradation of a viral antigen. *J. Cell Biol.*, **146,** 113-124.

[5] Arcangeletti, C., Olink-Coux, M., Minisini, R., Huesca, M., Chezzi, C., & Scherrer, K. (1992) Patterns of cytodistribution of prosomal antigens on the vimentin and cytokeratin networks of monkey kidney cells. *Eur. J. Cell Biol.*, **59,** 464-476.

[6] Arcangeletti, M.C., Pinardi, F., Missorini, S., De Conto, F., Conti, G., Portincasa, P., Scherrer, K., & Chezzi, C. (1997) Modification of cytoskeleton and prosome networks in relation to protein synthesis in influenza A virus-infected LLC-MK2 cells. *Virus*

Research, **51**, 19-34.

[7] Aviel, S., Winberg, G., Massucci, M., & Ciechanover, A. (2000) Degradation of the epstein-barr virus latent membrane protein 1 (LMP1) by the ubiquitin-proteasome pathway. Targeting via ubiquitination of the N-terminal residue. *J. Biol. Chem.*, **275**, 23491-23499.

[8] Babiss, L.E., Luftig, R.B., Weatherbee, J.A., Weihing, R.R., Ray, U.R., & Fields, B.N. (1979) Reovirus serotypes 1 and 3 differ in their in vitro association with microtubules. *J. Virol.*, **30**, 863-874.

[9] Babst, M., Odorizzi, G., Estepa, E.J., & Emr, S.D. (2000) Mammalian tumor susceptibility gene 101 (TSG101) and the yeast homologue, Vps23p, both function in late endosomal trafficking. *Traffic*, **1**, 248-258.

[10] Bailly, J.E. & Brown, E.G. (1998) Interference by a non-defective variant of influenza A virus is due to enhanced RNA synthesis and assembly. *Virus Res.*, **57**, 81-100.

[11] Banerjea, A.C., Brechling, K.A., Ray, C.A., Erikson, H., Pickup, D.J., & Joklik, W.K. (1988) High-level synthesis of biologically active reovirus protein sigma 1 in a mammalian expression vector system. *Virology*, **167**, 601-612.

[12] Banerjee, A.K. & Shatkin, A.J. (1970) Transcription in vitro by reovirus-associated ribonucleic acid- dependent polymerase. *J. Virol.*, **6**, 1-11.

[13] Barton, E.S., Forrest, J.C., Connolly, J.L., Chappell, J.D., Liu, Y., Schnell, F.J., Nusrat, A., Parkos, C.A., & Dermody, T.S. (2001) Junction adhesion molecule is a receptor for reovirus. *Cell*, **104**, 441-451.

[14] Baty, C.J. & Sherry, B. (1993) Cytopathogenic effect in cardiac myocytes but not in cardiac fibroblasts is correlated with reovirus-induced acute myocarditis. *J. Virol.*, **67**, 6295-6298.

[15] Becker-Andre, M. & Hahlbrock, K. (1989) Absolute mRNA quantification using the polymerase chain reaction (PCR). A novel approach by a PCR aided transcript titration assay (PATTY). *Nucleic Acids Res.*, **17**, 9437-9446.

[16] Becker, M.M., Goral, M.I., Hazelton, P.R., Baer, G.S., Rodgers, S.E., Brown, E.G., Coombs, K.M., & Dermody, T.S. (2001) Reovirus sigmaNS protein is required for nucleation of viral assembly complexes and formation of viral inclusions. *J. Virol.*, **75**, 1459-1475.

[17] Bell, P., Brazas, R., Ganem, D., & Maul, G.G. (2000) Hepatitis delta virus replication generates complexes of large hepatitis delta antigen and antigenomic RNA that affiliate with and alter nuclear domain 10. *J. Virol.*, **74**, 5329-5336.

[18] Belli, B.A. & Samuel, C.E. (1991) Biosynthesis of reovirus-specified polypeptides: expression of reovirus S1-encoded sigma 1NS protein in transfected and infected cells as measured with serotype specific polyclonal antibody. *Virology*, **185**, 698-709.

[19] Belli, B.A. & Samuel, C.E. (1993) Biosynthesis of reovirus-specified polypeptides: identification of regions of the bicistronic reovirus S1 mRNA that affect the efficiency of translation in animal cells. *Virology*, **193**, 16-27.

[20] Bence, N.F., Sampat, R.M., & Kopito, R.R. (2001) Impairment of the ubiquitin-proteasome system by protein aggregation. *Science*, **292**, 1552-1555.

[21] Bisaillon, M., Bergeron, J., & Lemay, G. (1997) Characterization of the nucleoside triphosphate phosphohydrolase and helicase activities of the reovirus lambda1 protein. *J. Biol. Chem.*, **272,** 18298-18303.

[22] Bischoff, J.R. & Samuel, C.E. (1989) Mechanism of interferon action. Activation of the human P1/eIF-2 alpha protein kinase by individual reovirus s-class mRNAs: s1 mRNA is a potent activator relative to s4 mRNA. *Virology*, **172,** 106-115.

[23] Borden, K.L., Campbell Dwyer, E.J., & Salvato, M.S. (1998) An arenavirus RING (zinc-binding) protein binds the oncoprotein promyelocyte leukemia protein (PML) and relocates PML nuclear bodies to the cytoplasm. *J. Virol.*, **72,** 758-766.

[24] Breitschopf, K., Bengal, E., Ziv, T., Admon, A., & Ciechanover, A. (1998) A novel site for ubiquitination: the N-terminal residue, and not internal lysines of MyoD, is essential for conjugation and degradation of the protein. *EMBO J.*, **17,** 5964-5973.

[25] Brentano, L., Noah, D.L., Brown, E.G., & Sherry, B. (1998) The reovirus protein mu2, encoded by the M1 gene, is an RNA-binding protein. *J. Virol.*, **72,** 8354-8357.

[26] Brown, E.G., Nibert, M.L., & Fields, B.N. (1983) The L2 gene of reovirus serotype 3 controls the capacity to interfere, accumulate deletions and establish persistent infection. In *Double-stranded RNA viruses* (Compans, R.W. & Bishop, D.H.L., eds), pp. 275-287. Elsevier, Amsterdam.

[27] Brown, E.G. (1998) Reovirus M1 gene expression. *Curr. Top. Microbiol. Immunol*, **233 Reovir.i,** 197-213.

[28] Bruenn, J.A. (1991) Relationships among the positive strand and double-strand RNA viruses as viewed through their RNA-dependent RNA polymerases. *Nucleic Acids Res.*,

19, 217-226.

[29] Capco, D.G., Wan, K.M., & Penman, S. (1982) The nuclear matrix: three-dimensional architecture and protein composition. *Cell*, **29,** 847-858.

[30] Chandran, K., Walker, S.B., Chen, Y., Contreras, C.M., Schiff, L.A., Baker, T.S., & Nibert, M.L. (1999) In vitro recoating of reovirus cores with baculovirus-expressed outer- capsid proteins mu1 and sigma3. *J. Virol.*, **73,** 3941-3950.

[31] Chappell, J.D., Gunn, V.L., Wetzel, J.D., Baer, G.S., & Dermody, T.S. (1997) Mutations in type 3 reovirus that determine binding to sialic acid are contained in the fibrous tail domain of viral attachment protein sigma1. *J. Virol.*, **71,** 1834-1841.

[32] Chappell, J.D., Duong, J.L., Wright, B.W., & Dermody, T.S. (2000) Identification of carbohydrate-binding domains in the attachment proteins of type 1 and type 3 reoviruses. *J. Virol.*, **74,** 8472-8479.

[33] Chelbi-Alix, M.K., Quignon, F., Pelicano, L., Koken, M.H., & de The, H. (1998) Resistance to virus infection conferred by the interferon-induced promyelocytic leukemia protein. *J. Virol.*, **72,** 1043-1051.

[34] Chelsky, D., Ralph, R., & Jonak, G. (1989) Sequence requirements for synthetic peptide-mediated translocation to the nucleus. *Mol. Cell Biol.*, **9,** 2487-2492.

[35] Ciechanover, A. (1998) The ubiquitin-proteasome pathway: on protein death and cell life. *EMBO J.*, **17,** 7151-7160.

[36] Cleveland, D.R., Zarbl, H., & Millward, S. (1986) Reovirus guanylyltransferase is L2 gene product lambda 2. *J. Virol.*, **60,** 307-311.

[37] Coffey, M.C., Strong, J.E., Forsyth, P.A., & Lee, P.W. (1998) Reovirus therapy of tumors with activated Ras pathway. *Science*, **282,** 1332-1334.

[38] Cook, S.M., Glass, R.I., LeBaron, C.W., & Ho, M.S. (1990) Global seasonality of rotavirus infections. *Bull. World Health Organ.*, **68,** 171-177.

[39] Coombs, K.M. (1996) Identification and characterization of a double-stranded RNA-reovirus temperature-sensitive mutant defective in minor core protein mu2. *J. Virol.*, **70,** 4237-4245.

[40] Coombs, K.M. (1998) Stoichiometry of reovirus structural proteins in virus, ISVP, and core particles. *Virology* , **243,** 218-228.

[41] Coombs, K.M. (1998) Temperature-sensitive mutants of reovirus. *Curr. Top. Microbiol. Immunol.*, **233 Reovir.i,** 69-107.

[42] Cottrez, F., Auriault, C., Capron, A., & Groux, H. (1994) Quantitative PCR: validation of the use of a multispecific internal control. *Nucleic Acids Res.*, **22,** 2712-2713.

[43] Craven, R.C., Harty, R.N., Paragas, J., Palese, P., & Wills, J.W. (1999) Late domain function identified in the vesicular stomatitis virus M protein by use of rhabdovirus-retrovirus chimeras. *J. Virol.*, **73,** 3359-3365.

[44] Cross, R.K. & Fields, B.N. (1972) Temperature-sensitive mutants of reovirus type 3: studies on the synthesis of viral RNA. *Virology*, **50,** 799-809.

[45] Cudmore, S., Reckmann, I., & Way, M. (1997) Viral manipulations of the actin cytoskeleton. *Trends Microbiol.*, **5,** 142-148.

[46] Cummings, C.J., Mancini, M.A., Antalffy, B., DeFranco, D.B., Orr, H.T., & Zoghbi, H.Y. (1998) Chaperone suppression of aggregation and altered subcellular proteasome

localization imply protein misfolding in SCA1. *Nat. Genet.*, **19,** 148-154.

[47] Dales, S., Gomatos, P., & Hsu, K.C. (1965) The uptake and development of reovirus in strain L cells followed with labelled viral ribonucleic acid and ferritin-antibody conjugates. *Virology*, **25,** 193-211.

[48] De Conto, F., Missorini, S., Arcangeletti, C., Pinardi, F., Montarras, D., Pinset, C., Vassy, J., Geraud, G., Chezzi, C., & Scherrer, K. (1997) Prosome cytodistribution relative to desmin and actin filaments in dividing C2.7 myoblasts and during myotube formation in vitro. *Exp. Cell Res.*, **233,** 99-117.

[49] de Melker, A.A., van Der, H.G., Calafat, J., Jansen, H., & Borst, J. (2001) c-Cbl ubiquitinates the EGF receptor at the plasma membrane and remains receptor associated throughout the endocytic route. *J. Cell Sci.*, **114,** 2167-2178.

[50] de The, H., Lavau, C., Marchio, A., Chomienne, C., Degos, L., & Dejean, A. (1991) The PML-RAR alpha fusion mRNA generated by the t(15;17) translocation in acute promyelocytic leukemia encodes a functionally altered RAR. *Cell*, **66,** 675-684.

[51] DeMartino, G.N. & Slaughter, C.A. (1999) The proteasome, a novel protease regulated by multiple mechanisms. *J. Biol. Chem.*, **274,** 22123-22126.

[52] Dermody, T.S., Schiff, L.A., Nibert, M.L., Coombs, K.M., & Fields, B.N. (1991) The S2 gene nucleotide sequences of prototype strains of the three reovirus serotypes: characterization of reovirus core protein sigma 2. *J. Virol.*, **65,** 5721-5731.

[53] Doohan, J.P. & Samuel, C.E. (1992) Biosynthesis of reovirus-specified polypeptides: ribosome pausing during the translation of reovirus S1 mRNA. *Virology*, **186,** 409-425.

[54] Doucas, V., Ishov, A.M., Romo, A., Juguilon, H., Weitzman, M.D., Evans, R.M., & Maul, G.G. (1996) Adenovirus replication is coupled with the dynamic properties of the PML nuclear structure. *Genes Dev.*, **10,** 196-207.

[55] Drayna, D. & Fields, B.N. (1982) Activation and characterization of the reovirus transcriptase: genetic analysis. *J. Virol.*, **41,** 110-118.

[56] Dryden, K.A., Wang, G., Yeager, M., Nibert, M.L., Coombs, K.M., Furlong, D.B., Fields, B.N., & Baker, T.S. (1993) Early steps in reovirus infection are associated with dramatic changes in supramolecular structure and protein conformation: analysis of virions and subviral particles by cryoelectron microscopy and image reconstruction. *J. Cell Biol.*, **122,** 1023-1041.

[57] Dryden, K.A., Farsetta, D.L., Wang, G., Keegan, J.M., Fields, B.N., Baker, T.S., & Nibert, M.L. (1998) Internal/structures containing transcriptase-related proteins in top component particles of mammalian orthoreovirus. *Virology*, **245,** 33-46.

[58] Dubiel, W. & Gordon, C. (1999) Ubiquitin pathway: another link in the polyubiquitin chain? *Curr. Biol.*, **9,** R554-R557.

[59] Duncan, M.R., Stanish, S.M., & Cox, D.C. (1978) Differential sensitivity of normal and transformed human cells to reovirus infection. *J. Virol.*, **28,** 444-449.

[60] Ettenberg, S.A., Magnifico, A., Cuello, M., Nau, M.M., Rubinstein, Y.R., Yarden, Y., Weissman, A.M., & Lipkowitz, S. (2001) Cbl-b-dependent coordinated degradation of the epidermal growth factor receptor signaling complex. *J. Biol. Chem.*, **276,** 27677-27684.

[61] Everett, R.D., Meredith, M., Orr, A., Cross, A., Kathoria, M., & Parkinson, J. (1997) A novel ubiquitin-specific protease is dynamically associated with the PML nuclear domain and binds to a herpesvirus regulatory protein. *EMBO J.*, **16,** 1519-1530.

[62] Fabunmi, R.P., Wigley, W.C., Thomas, P.J., & DeMartino, G.N. (2000) Activity and regulation of the centrosome-associated proteasome. *J. Biol. Chem.*, **275,** 409-413.

[63] Farsetta, D.L., Chandran, K., & Nibert, M.L. (2000) Transcriptional activities of reovirus RNA polymerase in recoated cores. Initiation and elongation are regulated by separate mechanisms. *J. Biol. Chem.*, **275,** 39693-39701.

[64] Fields, B.N., Raine, C.S., & Baum, S.G. (1971) Temperature-sensitive mutants of reovirus type 3: defects in viral maturation as studied by immunofluorescence and electron microscopy. *Virology*, **43,** 569-578.

[65] Fischer, U., Huber, J., Boelens, W.C., Mattaj, I.W., & Luhrmann, R. (1995) The HIV-1 Rev activation domain is a nuclear export signal that accesses an export pathway used by specific cellular RNAs. *Cell*, **82,** 475-483.

[66] Francki, R.I.B. & Boccardo, G. (1983) The plant reoviridae. In *The Reoviridae* (Joklik, W.K., ed), pp. 505-563. Plenum Press, New York.

[67] Freemont, P.S. (2000) RING for destruction? *Curr. Biol.*, **10,** R84-R87.

[68] Fruh, K., Gossen, M., Wang, K., Bujard, H., Peterson, P.A., & Yang, Y. (1994) Displacement of housekeeping proteasome subunits by MHC-encoded LMPs: a newly discovered mechanism for modulating the multicatalytic proteinase complex. *EMBO J.*, **13,** 3236-3244.

[69] Furuichi, Y., LaFiandra, A., & Shatkin, A.J. (1977) 5'-Terminal structure and mRNA stability. *Nature*, **266**, 235-239.

[70] Gaillard, R.K., Jr. & Joklik, W.K. (1985) The relative translation efficiencies of reovirus messenger RNAs. *Virology*, **147**, 336-348.

[71] Garcia-Bustos, J., Heitman, J., & Hall, M.N. (1991) Nuclear protein localization. *Biochim. Biophys. Acta*, **1071**, 83-101.

[72] Garcia-Higuera, I., Taniguchi, T., Ganesan, S., Meyn, M.S., Timmers, C., Hejna, J., Grompe, M., & D'Andrea, A.D. (2001) Interaction of the Fanconi anemia proteins and BRCA1 in a common pathway. *Mol. Cell*, **7**, 249-262.

[73] Garcia-Mata, R., Bebok, Z., Sorscher, E.J., & Sztul, E.S. (1999) Characterization and dynamics of aggresome formation by a cytosolic GFP- chimera. *J. Cell Biol.*, **146**, 1239-1254.

[74] Goddard, A.D., Borrow, J., Freemont, P.S., & Solomon, E. (1991) Characterization of a zinc finger gene disrupted by the t(15;17) in acute promyelocytic leukemia. *Science*, **254**, 1371-1374.

[75] Gomatos, P.J., Tamm, I., Dales, S., & Franklin, R.M. (1962) Reovirus type 3: Physical characteristics and interactions with L cells. *Virology*, **17**, 441-454.

[76] Gorlich, D. & Mattaj, I.W. (1996) Nucleocytoplasmic transport. *Science*, **271**, 1513-1518.

[77] Grossi de Sa, M.F., Martins, d.S., Harper, F., Olink-Coux, M., Huesca, M., & Scherrer, K. (1988) The association of prosomes with some of the intermediate filament networks of the animal cell. *J. Cell Biol.*, **107**, 1517-1530.

[78] Haller, B.L., Barkon, M.L., Vogler, G.P., & Virgin, H.W. (1995) Genetic mapping of reovirus virulence and organ tropism in severe combined immunodeficient mice: organ-specific virulence genes. *J. Virol.*, **69,** 357-364.

[79] Hand, R. & Tamm, I. (1973) Reovirus: effect of noninfective viral components on cellular deoxyribonucleic acid synthesis. *J. Virol.*, **11,** 223-231.

[80] Harty, R.N., Paragas, J., Sudol, M., & Palese, P. (1999) A proline-rich motif within the matrix protein of vesicular stomatitis virus and rabies virus interacts with WW domains of cellular proteins: implications for viral budding. *J. Virol.*, **73,** 2921-2929.

[81] Harty, R.N., Brown, M.E., Wang, G., Huibregtse, J., & Hayes, F.P. (2000) A PPxY motif within the VP40 protein of Ebola virus interacts physically and functionally with a ubiquitin ligase: implications for filovirus budding. *Proc. Natl. Acad. Sci. U. S. A.*, **97,** 13871-13876.

[82] Harty, R.N., Brown, M.E., McGettigan, J.P., Wang, G., Jayakar, H.R., Huibregtse, J.M., Whitt, M.A., & Schnell, M.J. (2001) Rhabdoviruses and the cellular ubiquitin-proteasome system: a budding interaction. *J. Virol.*, **75,** 10623-10629.

[83] Hashiro, G., Loh, P.C., & Yau, J.T. (1977) The preferential cytotoxicity of reovirus for certain transformed cell lines. *Arch. Virol.*, **54,** 307-315.

[84] He, D.C., Nickerson, J.A., & Penman, S. (1990) Core filaments of the nuclear matrix. *J. Cell Biol.*, **110,** 569-580.

[85] Heath, C.M., Windsor, M., & Wileman, T. (2001) Aggresomes resemble sites specialized for virus assembly. *J. Cell Biol.*, **153,** 449-455.

[86] Hicke, L. (1999) Gettin' down with ubiquitin: turning off cell-surface receptors, transporters and channels. *Trends Cell Biol.*, **9,** 107-112.

[87] Hicke, L. (2001) Protein regulation by monoubiquitin. *Nat. Rev. Mol. Cell Biol.*, **2,** 195-201.

[88] Hochstrasser, M. (1996) Ubiquitin-dependent protein degradation. *Annu. Rev. Genet.*, **30,** 405-439.

[89] Hodges, M., Tissot, C., Howe, K., Grimwade, D., & Freemont, P.S. (1998) Structure, organization, and dynamics of promyelocytic leukemia protein nuclear bodies. *Am. J. Hum. Genet.*, **63,** 297-304.

[90] Holmes, D.S. & Quigley, M. (1981) A rapid boiling method for the preparation of bacterial plasmids. *Anal. Biochem.*, **114,** 193-197.

[91] Huibregtse, J.M., Scheffner, M., & Howley, P.M. (1991) A cellular protein mediates association of p53 with the E6 oncoprotein of human papillomavirus types 16 or 18. *EMBO J.*, **10,** 4129-4135.

[92] Hunter, E. (2001) Virus assembly. In *Fields Virology* (Knipe, D.M. & Howley, P.M., eds), pp. 171-197. Lippincott Williams & Wilkins, Philadephia.

[93] Ito, Y. & Joklik, W.K. (1972) Temperature-sensitive mutants of reovirus. I. Patterns of gene expression by mutants of groups C, D, and E. *Virology*, **50,** 189-201.

[94] Jensen, K., Shiels, C., & Freemont, P.S. (2001) PML protein isoforms and the RBCC/TRIM motif. *Oncogene*, **20,** 7223-7233.

[95] Johnston, J.A., Ward, C.L., & Kopito, R.R. (1998) Aggresomes: a cellular response to misfolded proteins. *J. Cell Biol.*, **143,** 1883-1898.

[96] Joklik, W.K. (1981) Structure and function of the reovirus genome. *Microbiol. Rev.*, **45,** 483-501.

[97] Joklik, W.K. (1983) The reovirus particle. In *The Reoviridae* (Joklik,W.K., ed), pp. 9-78. Plenum Press, New York.

[98] Kakizuka, A., Miller, W.H., Jr., Umesono, K., Warrell, R.P., Jr., Frankel, S.R., Murty, V.V., Dmitrovsky, E., & Evans, R.M. (1991) Chromosomal translocation t(15;17) in human acute promyelocytic leukemia fuses RAR alpha with a novel putative transcription factor, PML. *Cell*, **66,** 663-674.

[99] Katzmann, D.J., Babst, M., & Emr, S.D. (2001) Ubiquitin-dependent sorting into the multivesicular body pathway requires the function of a conserved endosomal protein sorting complex, ESCRT-I. *Cell*, **106,** 145-155.

[100] Kelly, C., Van Driel, R., & Wilkinson, G.W. (1995) Disruption of PML-associated nuclear bodies during human cytomegalovirus infection. *J. Gen. Virol.*, **76 (Pt 11),** 2887-2893.

[101] Khaustov, V.I., Korolev, M.B., & Reingold, V.N. (1987) The structure of the capsid inner layer of reoviruses. Brief report. *Arch. Virol.*, **93,** 163-167.

[102] Kil, S.J., Hobert, M., & Carlin, C. (1999) A leucine-based determinant in the epidermal growth factor receptor juxtamembrane domain is required for the efficient transport of ligand- receptor complexes to lysosomes. *J. Biol. Chem.*, **274,** 3141-3150.

[103] Kim, T.K. & Maniatis, T. (1996) Regulation of interferon-gamma-activated STAT1 by the ubiquitin- proteasome pathway. *Science*, **273,** 1717-1719.

[104] Knipe, D.M., Samuel, C.E., & Palese, P. (2001) Virus-host cell interactions. In *Fields Virology* (Knipe, D.M. & Howley, P.M., eds), pp. 133-170. Lippincott Williams & Wilkins, Philadephia.

[105] Kopito, R.R. & Sitia, R. (2000) Aggresomes and Russell bodies. Symptoms of cellular indigestion? *EMBO Rep.*, **1**, 225-231.

[106] Kopito, R.R. (2000) Aggresomes, inclusion bodies and protein aggregation. *Trends Cell Biol.*, **10**, 524-530.

[107] Kozak, M. (1981) Possible role of flanking nucleotides in recognition of the AUG initiator codon by eukaryotic ribosomes. *Nucleic Acids Res.*, **9**, 5233-5262.

[108] Kreis, T. & Vale, R. (1999) *Guidebook to the cytoskeletal and motor proteins*, 2 edn. Oxford University Press, Oxford.

[109] Lacaille, V.G. & Androlewicz, M.J. (2000) Targeting of HIV-1 Nef to the centrosome: implications for antigen processing. *Traffic.*, **1**, 884-891.

[110] Laemmli, U.K. (1970) Cleavage of structural proteins during the assembly of the head of bacteriophage T4. *Nature*, **227**, 680-685.

[111] Lanford, R.E. & Butel, J.S. (1984) Construction and characterization of an SV40 mutant defective in nuclear transport of T antigen. *Cell*, **37**, 801-813.

[112] Lemay, G. & Danis, C. (1994) Reovirus lambda 1 protein: affinity for double-stranded nucleic acids by a small amino-terminal region of the protein independent from the zinc finger motif. *J. Gen. Virol.*, **75 (Pt 11)**, 3261-3266.

[113] Lemmon, S.K. & Traub, L.M. (2000) Sorting in the endosomal system in yeast and animal cells. *Curr. Opin. Cell Biol.*, **12**, 457-466.

[114] Li, X.L. & Hassel, B.A. (2001) Involvement of proteasomes in gene induction by interferon and double- stranded RNA. *Cytokine*, **14,** 247-252.

[115] Lin, J.H., Grandchamp, B., & Abraham, N.G. (1991) Quantitation of human erythroid-specific porphobilinogen deaminase mRNA by the polymerase chain reaction. *Exp. Hematol.*, **19,** 817-822.

[116] Lopes, U.G., Erhardt, P., Yao, R., & Cooper, G.M. (1997) p53-dependent induction of apoptosis by proteasome inhibitors. *J. Biol. Chem.*, **272,** 12893-12896.

[117] Lucia-Jandris, P., Hooper, J.W., & Fields, B.N. (1993) Reovirus M2 gene is associated with chromium release from mouse L cells. *J. Virol.*, **67,** 5339-5345.

[118] Luftig, R.B., Kilham, S.S., Hay, A.J., Zweerink, H.J., & Joklik, W.K. (1972) An ultrastructural study of virions and cores of reovirus type 3. *Virology*, **48,** 170-181.

[119] Luftig, R.B. (1982) Does the cytoskeleton play a significant role in animal virus replication? *J. Theor. Biol.*, **99,** 173-191.

[120] Mao, Z.X. & Joklik, W.K. (1991) Isolation and enzymatic characterization of protein lambda 2, the reovirus guanylyltransferase. *Virology*, **185,** 377-386.

[121] Matoba, Y., Sherry, B., Fields, B.N., & Smith, T.W. (1991) Identification of the viral genes responsible for growth of strains of reovirus in cultured mouse heart cells. *J. Clin. Invest*, **87,** 1628-1633.

[122] Matoba, Y., Colucci, W.S., Fields, B.N., & Smith, T.W. (1993) The reovirus M1 gene determines the relative capacity of growth of reovirus in cultured bovine aortic endothelial cells. *J. Clin. Invest*, **92,** 2883-2888.

[123] Mayer, R.J., Lowe, J., Lennox, G., Doherty, F., & Landon, M. (1989) Intermediate filaments and ubiquitin: a new thread in the understanding of chronic neurodegenerative diseases. *Prog. Clin. Biol. Res.*, **317,** 809-818.

[124] Mayor, H.D., Jamison, R.M., Jordan, L.E., & Mitchell, M.V. (1965) Reoviruses. II. Structure and composition of the virion. *J. Bacteriol.*, **89,** 1548-1556.

[125] McCrae, M.A. & Joklik, W.K. (1978) The nature of the polypeptide encoded by each of the 10 double-stranded RNA segments of reovirus type 3. *Virology*, **89,** 578-593.

[126] Metcalf, P. (1982) The symmetry of the reovirus outer shell. *J. Ultrastruct. Res.*, **78,** 292-301.

[127] Metcalf, P., Cyrklaff, M., & Adrian, M. (1991) The three-dimensional structure of reovirus obtained by cryo-electron microscopy. *EMBO J.*, **10,** 3129-3136.

[128] Mimnaugh, E.G., Chen, H.Y., Davie, J.R., Celis, J.E., & Neckers, L. (1997) Rapid deubiquitination of nucleosomal histones in human tumor cells caused by proteasome inhibitors and stress response inducers: effects on replication, transcription, translation, and the cellular stress response. *Biochemistry*, **36,** 14418-14429.

[129] Moody, M.D. & Joklik, W.K. (1989) The function of reovirus proteins during the reovirus multiplication cycle: analysis using monoreassortants. *Virology*, **173,** 437-446.

[130] Mora, M., Partin, K., Bhatia, M., Partin, J., & Carter, C. (1987) Association of reovirus proteins with the structural matrix of infected cells. *Virology*, **159,** 265-277.

[131] Morgan, E.M. & Zweerink, H.J. (1975) Characterization of transcriptase and replicase particles isolated from reovirus-infected cells. *Virology*, **68,** 455-466.

[132] Morozov, S.Y. (1989) A possible relationship of reovirus putative RNA polymerase to polymerases of positive-strand RNA viruses. *Nucleic Acids Res.*, **17,** 5394.

[133] Mukaigawa, J. & Nayak, D.P. (1991) Two signals mediate nuclear localization of influenza virus (A/WSN/33) polymerase basic protein 2. *J. Virol.*, **65,** 245-253.

[134] Munemitsu, S.M. & Samuel, C.E. (1984) Biosynthesis of reovirus-specified polypeptides. Multiplication rate but not yield of reovirus serotypes 1 and 3 correlates with the level of virus-mediated inhibition of cellular protein synthesis. *Virology*, **136,** 133-143.

[135] Munemitsu, S.M. & Samuel, C.E. (1988) Biosynthesis of reovirus-specified polypeptides: effect of point mutation of the sequences flanking the 5'-proximal AUG initiator codons of the reovirus S1 and S4 genes on the efficiency of mRNA translation. *Virology*, **163,** 643-646.

[136] Nakielny, S., Fischer, U., Michael, W.M., & Dreyfuss, G. (1997) RNA transport. *Annu. Rev. Neurosci.*, **20,** 269-301.

[137] Nath, S.T. & Nayak, D.P. (1990) Function of two discrete regions is required for nuclear localization of polymerase basic protein 1 of A/WSN/33 influenza virus (H1 N1). *Mol. Cell Biol.*, **10,** 4139-4145.

[138] Negorev, D. & Maul, G.G. (2001) Cellular proteins localized at and interacting within ND10/PML nuclear bodies/PODs suggest functions of a nuclear depot. *Oncogene*, **20,** 7234-7242.

[139] Nibert, M.L., Schiff, L.A., & Fields, B.N. (1991) Mammalian reoviruses contain a myristoylated structural protein. *J. Virol.*, **65,** 1960-1967.

[140] Nibert, M.L. & Schiff, L.A. (2001) Reoviruses and their replication. In *Fields Virology* (Knipe, D.M. & Howley, P.M., eds), pp. 1679-1728. Lippincott Williams & Wilkins, Philadephia.

[141] Nigg, E.A. (1997) Nucleocytoplasmic transport: signals, mechanisms and regulation. *Nature*, **386,** 779-787.

[142] Noble, S. & Nibert, M.L. (1997) Core protein mu2 is a second determinant of nucleoside triphosphatase activities by reovirus cores. *J. Virol.*, **71,** 7728-7735.

[143] Norman, K.L. & Lee, P.W. (2000) Reovirus as a novel oncolytic agent. *J. Clin. Invest*, **105,** 1035-1038.

[144] Nothwang, H.G., Coux, O., Bey, F., & Scherrer, K. (1992) Prosomes and their multicatalytic proteinase activity. *Eur. J. Biochem.*, **207,** 621-630.

[145] Nyman, T.A., Matikainen, S., Sareneva, T., Julkunen, I., & Kalkkinen, N. (2000) Proteome analysis reveals ubiquitin-conjugating enzymes to be a new family of interferon-alpha-regulated genes. *Eur. J. Biochem.*, **267,** 4011-4019.

[146] Olink-Coux, M., Huesca, M., & Scherrer, K. (1992) Specific types of prosomes are associated to subnetworks of the intermediate filaments in PtK1 cells. *Eur. J. Cell Biol.*, **59,** 148-159.

[147] Orian, A., Whiteside, S., Israel, A., Stancovski, I., Schwartz, A.L., & Ciechanover, A. (1995) Ubiquitin-mediated processing of NF-kappa B transcriptional activator precursor p105. Reconstitution of a cell-free system and identification of the ubiquitin-carrier protein, E2, and a novel ubiquitin-protein ligase, E3, involved in conjugation. *J. Biol. Chem.*, **270,** 21707-21714.

[148] Ott, D.E., Coren, L.V., Copeland, T.D., Kane, B.P., Johnson, D.G., Sowder, R.C., Yoshinaka, Y., Oroszlan, S., Arthur, L.O., & Henderson, L.E. (1998) Ubiquitin is covalently attached to the p6Gag proteins of human immunodeficiency virus type 1 and simian immunodeficiency virus and to the p12Gag protein of Moloney murine leukemia virus. *J. Virol.*, **72,** 2962-2968.

[149] Palmer, A., Rivett, A.J., Thomson, S., Hendil, K.B., Butcher, G.W., Fuertes, G., & Knecht, E. (1996) Subpopulations of proteasomes in rat liver nuclei, microsomes and cytosol. *Biochem. J.*, **316 (Pt 2),** 401-407.

[150] Parker, J.S., Broering, T.J., Kim, J., Higgins, D.E., & Nibert, M.L. (2002) Reovirus core protein mu2 determines the filamentous morphology of viral inclusion bodies by interacting with and stabilizing microtubules. *J. Virol.*, **76,** 4483-4496.

[151] Patnaik, A., Chau, V., & Wills, J.W. (2000) Ubiquitin is part of the retrovirus budding machinery. *Proc. Natl. Acad. Sci. U. S. A*, **97,** 13069-13074.

[152] Payne, C.C. & Mertens, P.P.C. (1983) Cytoplasmic polyhedrosis viruses. In *The Reoviridae* (Joklik,W.K., ed), pp. 505-563. Plenum Press, New York.

[153] Petit, F., Jarrousse, A.S., Boissonnet, G., Dadet, M.H., Buri, J., Briand, Y., & Schmid, H.P. (1997) Proteasome (prosome) associated endonuclease activity. *Mol. Biol. Rep.*, **24,** 113-117.

[154] Pickart, C.M. (2000) Ubiquitin in chains. *Trends Biochem. Sci.*, **25,** 544-548.

[155] Pickart,C.M. (2001) Mechanisms underlying ubiquitination. *Annu. Rev. Biochem.*, **70,** 503-533.

[156] Ploubidou, A. & Way, M. (2001) Viral transport and the cytoskeleton. *Curr. Opin. Cell Biol.*, **13,** 97-105.

[157] Polymeropoulos, M.H., Lavedan, C., Leroy, E., Ide, S.E., Dehejia, A., Dutra, A., Pike, B., Root, H., Rubenstein, J., Boyer, R., Stenroos, E.S., Chandrasekharappa, S., Athanassiadou, A., Papapetropoulos, T., Johnson, W.G., Lazzarini, A.M., Duvoisin, R.C., Di Iorio, G., Golbe, L.I., & Nussbaum, R.L. (1997) Mutation in the alpha-synuclein gene identified in families with Parkinson's disease. *Science*, **276,** 2045-2047.

[158] Pouch, M.N., Petit, F., Buri, J., Briand, Y., & Schmid, H.P. (1995) Identification and initial characterization of a specific proteasome (prosome) associated RNase activity. *J. Biol. Chem.*, **270,** 22023-22028.

[159] Putterman, D., Pepinsky, R.B., & Vogt, V.M. (1990) Ubiquitin in avian leukosis virus particles. *Virology*, **176,** 633-637.

[160] Puvion-Dutilleul, F., Chelbi-Alix, M.K., Koken, M., Quignon, F., Puvion, E., & de The, H. (1995) Adenovirus infection induces rearrangements in the intranuclear distribution of the nuclear body-associated PML protein. *Exp. Cell Res.*, **218,** 9-16.

[161] Quignon, F., De Bels, F., Koken, M., Feunteun, J., Ameisen, J.C., & de The, H. (1998) PML induces a novel caspase-independent death process. *Nat. Genet.*, **20,** 259-265.

[162] Realini, C., Dubiel, W., Pratt, G., Ferrell, K., & Rechsteiner, M. (1994) Molecular cloning and expression of a gamma-interferon-inducible activator of the multicatalytic protease. *J. Biol. Chem.*, **269,** 20727-20732.

[163] Regad, T., Saib, A., Lallemand-Breitenbach, V., Pandolfi, P.P., de The, H., & Chelbi-Alix, M.K. (2001) PML mediates the interferon-induced antiviral state against a complex

retrovirus via its association with the viral transactivator. *EMBO J.*, **20,** 3495-3505.

[164] Reinisch, K.M., Nibert, M.L., & Harrison, S.C. (2000) Structure of the reovirus core at 3.6 A resolution. *Nature*, **404,** 960-967.

[165] Reinstein, E., Scheffner, M., Oren, M., Ciechanover, A., & Schwartz, A. (2000) Degradation of the E7 human papillomavirus oncoprotein by the ubiquitin- proteasome system: targeting via ubiquitination of the N-terminal residue. *Oncogene*, **19,** 5944-5950.

[166] Rhim, J.S., Jordan, L.E., & Mayor, H.D. (1962) Cytochemical, fluorescent-antibody and electron microscopic studies on the growth of reovirus (ECHO 10) in tissue culture. *Virology*, **17,** 342-355.

[167] Rodgers, S.E., Barton, E.S., Oberhaus, S.M., Pike, B., Gibson, C.A., Tyler, K.L., & Dermody, T.S. (1997) Reovirus-induced apoptosis of MDCK cells is not linked to viral yield and is blocked by Bcl-2. *J. Virol.*, **71,** 2540-2546.

[168] Rodgers, S.E., Connolly, J.L., Chappell, J.D., & Dermody, T.S. (1998) Reovirus growth in cell culture does not require the full complement of viral proteins: identification of a sigma1s-null mutant. *J. Virol.*, **72,** 8597-8604.

[169] Roner, M.R., Gaillard, R.K., Jr., & Joklik, W.K. (1989) Control of reovirus messenger RNA translation efficiency by the regions upstream of initiation codons. *Virology*, **168,** 292-301.

[170] Roner, M.R., Roner, L.A., & Joklik, W.K. (1993) Translation of reovirus RNA species m1 can initiate at either of the first two in-frame initiation codons. *Proc. Natl. Acad. Sci. U. S. A*, **90,** 8947-8951.

[171] Roner, M.R. & Joklik, W.K. (2001) Reovirus reverse genetics: Incorporation of the CAT gene into the reovirus genome. *Proc. Natl. Acad. Sci. U. S. A*, **98,** 8036-8041.

[172] Rosen, D.R., Siddique, T., Patterson, D., Figlewicz, D.A., Sapp, P., Hentati, A., Donaldson, D., Goto, J., O'Regan, J.P., Deng, H.X., *et al.* (1993) Mutations in Cu/Zn superoxide dismutase gene are associated with familial amyotrophic lateral sclerosis. *Nature*, **362,** 59-62.

[173] Samuel, C.E. & Brody, M.S. (1990) Biosynthesis of reovirus-specified polypeptides. 2-aminopurine increases the efficiency of translation of reovirus s1 mRNA but not s4 mRNA in transfected cells. *Virology*, **176,** 106-113.

[174] Saurin, A.J., Borden, K.L., Boddy, M.N., & Freemont, P.S. (1996) Does this have a familiar RING? *Trends Biochem. Sci.*, **21,** 208-214.

[175] Scherrer, K. & Bey, F. (1994) The prosomes (multicatalytic proteinases; proteasomes) and their relationship to the untranslated messenger ribonucleoproteins, the cytoskeleton, and cell differentiation. *Prog. Nucleic Acid Res. Mol. Biol.*, **49,** 1-64.

[176] Schmechel, S., Chute, M., Skinner, P., Anderson, R., & Schiff, L. (1997) Preferential translation of reovirus mRNA by a sigma3-dependent mechanism. *Virology*, **232,** 62-73.

[177] Schubert, U., Ott, D.E., Chertova, E.N., Welker, R., Tessmer, U., Princiotta, M.F., Bennink, J.R., Krausslich, H.G., & Yewdell, J.W. (2000) Proteasome inhibition interferes with gag polyprotein processing, release, and maturation of HIV-1 and HIV-2. *Proc. Natl. Acad. Sci. U. S. A*, **97,** 13057-13062.

[178] Seliger, L.S., Zheng, K., & Shatkin, A.J. (1987) Complete nucleotide sequence of reovirus L2 gene and deduced amino acid sequence of viral mRNA guanylyltransferase.

J. Biol. Chem., **262,** 16289-16293.

[179] Sharpe, A.H. & Fields, B.N. (1981) Reovirus inhibition of cellular DNA synthesis: role of the S1 gene. *J. Virol.*, **38,** 389-392.

[180] Sharpe, A.H., Chen, L.B., & Fields, B.N. (1982) The interaction of mammalian reoviruses with the cytoskeleton of monkey kidney CV-1 cells. *Virology*, **120,** 399-411.

[181] Shatkin, A.J., Furuichi, Y., LaFiandra, A.J., & Yamakawa, M. (1983) Initiation of mRNA synthesis and 5'-terminal modification of reovirus transcripts. In *Double-stranded RNA viruses* (Compans, R.W. & Bishop, D.H.L., eds), pp. 43-54. Elsevier, New York.

[182] Sherry, B. & Fields, B.N. (1989) The reovirus M1 gene, encoding a viral core protein, is associated with the myocarditic phenotype of a reovirus variant. *J. Virol.*, **63,** 4850-4856.

[183] Sherry, B. & Blum, M.A. (1994) Multiple viral core proteins are determinants of reovirus-induced acute myocarditis. *J. Virol.*, **68,** 8461-8465.

[184] Sherry, B., Torres, J., & Blum, M.A. (1998) Reovirus induction of and sensitivity to beta interferon in cardiac myocyte cultures correlate with induction of myocarditis and are determined by viral core proteins. *J. Virol.*, **72,** 1314-1323.

[185] Shmulevitz, M. & Duncan, R. (2000) A new class of fusion-associated small transmembrane (FAST) proteins encoded by the non-enveloped fusogenic reoviruses. *EMBO J.*, **19,** 902-912.

[186] Skinner, P.J., Koshy, B.T., Cummings, C.J., Klement, I.A., Helin, K., Servadio, A., Zoghbi, H.Y., & Orr, H.T. (1997) Ataxin-1 with an expanded glutamine tract alters nuclear matrix- associated structures. *Nature*, **389,** 971-974.

[187] Skup, D., Zarbl, H., & Millward, S. (1981) Regulation of translation in L-cells infected with reovirus. *J. Mol. Biol.*, **151,** 35-55.

[188] Spence, J., Sadis, S., Haas, A.L., & Finley, D. (1995) A ubiquitin mutant with specific defects in DNA repair and multiubiquitination. *Mol. Cell Biol.*, **15,** 1265-1273.

[189] Spendlove, R.S., Lennette, E.H., Knight, C.O., & Chin, J.N. (1963) Development of viral antigen and infectious virus on HeLa cells infected with reovirus. *J. Immunol*, **90,** 548-553.

[190] Spendlove, R.S., Lennette, E.H., Chin, J.N., & Knight, C.O. (1964) Effect of antimitotic agents on intracellular reovirus antigen. *Cancer Research*, **24,** 1826-1833.

[191] Starnes, M.C. & Joklik, W.K. (1993) Reovirus protein lambda 3 is a poly(C)-dependent poly(G) polymerase. *Virology*, **193,** 356-366.

[192] Staub, O., Abriel, H., Plant, P., Ishikawa, T., Kanelis, V., Saleki, R., Horisberger, J.D., Schild, L., & Rotin, D. (2000) Regulation of the epithelial Na+ channel by Nedd4 and ubiquitination. *Kidney Int.*, **57,** 809-815.

[193] Sternsdorf, T., Grotzinger, T., Jensen, K., & Will, H. (1997) Nuclear dots: actors on many stages. *Immunobiology* , **198,** 307-331.

[194] Strack, B., Calistri, A., Accola, M.A., Palu, G., & Gottlinger, H.G. (2000) A role for ubiquitin ligase recruitment in retrovirus release. *Proc. Natl. Acad. Sci. U. S. A*, **97,** 13063-13068.

[195] Strong, J.E., Coffey, M.C., Tang, D., Sabinin, P., & Lee, P.W. (1998) The molecular basis of viral oncolysis: usurpation of the Ras signaling pathway by reovirus. *EMBO J.*, **17,** 3351-3362.

[196] Szekely, L., Pokrovskaja, K., Jiang, W.Q., de The, H., Ringertz, N., & Klein, G. (1996) The Epstein-Barr virus-encoded nuclear antigen EBNA-5 accumulates in PML-containing bodies. *J. Virol.*, **70,** 2562-2568.

[197] Tsirigotis, M., Zhang, M., Chiu, R.K., Wouters, B.G., & Gray, D.A. (2001) Sensitivity of Mammalian Cells Expressing Mutant Ubiquitin to Protein-damaging Agents. *J. Biol. Chem.*, **276,** 46073-46078.

[198] Tyler, K.L., Squier, M.K., Rodgers, S.E., Schneider, B.E., Oberhaus, S.M., Grdina, T.A., Cohen, J.J., & Dermody, T.S. (1995) Differences in the capacity of reovirus strains to induce apoptosis are determined by the viral attachment protein sigma 1. *J. Virol.*, **69,** 6972-6979.

[199] Tyler, K.L., Squier, M.K., Brown, A.L., Pike, B., Willis, D., Oberhaus, S.M., Dermody, T.S., & Cohen, J.J. (1996) Linkage between reovirus-induced apoptosis and inhibition of cellular DNA synthesis: role of the S1 and M2 genes. *J. Virol.*, **70,** 7984-7991.

[200] Tyler, K.L. (1998) Pathogenesis of reovirus infections of the central nervous system. *Curr. Top. Microbiol. Immunol.*, **233 Reovir.ii,** 93-124.

[201] Vasquez, C. & Tournier, P. (1962) The morphology of reovirus. *Virology*, **17,** 503-510.

[202] Virgin, H.W., Mann, M.A., Fields, B.N., & Tyler, K.L. (1991) Monoclonal antibodies to reovirus reveal structure/function relationships between capsid proteins and genetics of susceptibility to antibody action. *J. Virol.*, **65,** 6772-6781.

[203] Wang, Z.G., Ruggero, D., Ronchetti, S., Zhong, S., Gaboli, M., Rivi, R., & Pandolfi, P.P. (1998) PML is essential for multiple apoptotic pathways. *Nat. Genet.*, **20,** 266-272.

[204] Wang, Z.G., Delva, L., Gaboli, M., Rivi, R., Giorgio, M., Cordon-Cardo, C., Grosveld, F., & Pandolfi, P.P. (1998) Role of PML in cell growth and the retinoic acid pathway. *Science*, **279,** 1547-1551.

[205] Watanabe, Y., Millward, S., & Graham, A.F. (1968) Regulation of transcription of the Reovirus genome. *J. Mol. Biol.*, **36,** 107-123.

[206] Weiner, H.L., Powers, M.L., & Fields, B.N. (1980) Absolute linkage of virulence and central nervous system cell tropism of reoviruses to viral hemagglutinin. *J. Infect. Dis.*, **141,** 609-616.

[207] Wiener, J.R., Bartlett, J.A., & Joklik, W.K. (1989) The sequences of reovirus serotype 3 genome segments M1 and M3 encoding the minor protein mu 2 and the major nonstructural protein mu NS, respectively. *Virology*, **169,** 293-304.

[208] Wigley, W.C., Fabunmi, R.P., Lee, M.G., Marino, C.R., Muallem, S., DeMartino, G.N., & Thomas, P.J. (1999) Dynamic association of proteasomal machinery with the centrosome. *J. Cell Biol.*, **145,** 481-490.

[209] Wilcox, M.E., Yang, W., Senger, D., Rewcastle, N.B., Morris, D.G., Brasher, P.M., Shi, Z.Q., Johnston, R.N., Nishikawa, S., Lee, P.W., & Forsyth, P.A. (2001) Reovirus as an oncolytic agent against experimental human malignant gliomas. *J. Natl. Cancer Inst.*, **93,** 903-912.

[210] Wojcik, C., Schroeter, D., Wilk, S., Lamprecht, J., & Paweletz, N. (1996) Ubiquitin-mediated proteolysis centers in HeLa cells: indication from studies of an inhibitor of the chymotrypsin-like activity of the proteasome. *Eur. J. Cell Biol.*, **71,** 311-318.

[211] Xu, P., Miller, S.E., & Joklik, W.K. (1993) Generation of reovirus core-like particles in cells infected with hybrid vaccinia viruses that express genome segments L1, L2, L3, and S2. *Virology*, **197**, 726-731.

[212] Yin, P., Cheang, M., & Coombs, K.M. (1996) The M1 gene is associated with differences in the temperature optimum of the transcriptase activity in reovirus core particles. *J. Virol.*, **70**, 1223-1227.

[213] Yue, Z. & Shatkin, A.J. (1996) Regulated, stable expression and nuclear presence of retrovirus double- stranded RNA-binding protein sigma3 in HeLa cells. *J. Virol.*, **70**, 3497-3501.

[214] Zarbl, H. & Millward, S. (1983) The reovirus multiplication cycle. In *The Reoviridae* (Joklik, W.K., ed), pp. 107-196. Plenum Press, New York.

[215] Zou, S. & Brown, E.G. (1992) Nucleotide sequence comparison of the M1 genome segment of reovirus type 1 Lang and type 3 Dearing. *Virus Res.*, **22**, 159-164.

[216] Zou, S. & Brown, E.G. (1996a) Stable expression of the reovirus mu2 protein in mouse L cells complements the growth of a reovirus ts mutant with a defect in its M1 gene. *Virology*, **217**, 42-48.

[217] Zou, S. & Brown, E.G. (1996b) Translation of the reovirus M1 gene initiates from the first AUG codon in both infected and transfected cells. *Virus Res.*, **40**, 75-89.

[218] Zweerink, H.J., Morgan, E.M., & Skyler, J.S. (1976) Reovirus morphogenesis: characterization of subviral particles in infected cells. *Virology*, **73**, 442-453.

APPENDIX ONE

ADDITIONAL MATERIALS AND METHODS

A1.1 Immunofluorescence staining of reovirus-infected cells (Fig. 3.2 and 3.3; by M.M. becker)

L cells (5 x 104) were grown on 12 mm glass coverslips (VWR Scientific Products, Atlanta, GA) for 24 h prior to infection with reovirus at an MOI of 10 PFU/cell. After adsorption at 4°C for 1 h, cells were incubated at either 37°C or 39.5°C for various intervals, washed two times with PBS, and fixed for 2 min in a 1:1 (v/v) mixture of methanol and acetone. Cells were kept in methanol at -20°C until stained. Cells were then washed two times in PBS and incubated for 15 min in PBS containing 5% BSA (Sigma). Nonspecific binding of antibody to cells was blocked by incubation for 10 min in PBS containing 1% BSA, 1% Triton X-100 (Bio-Rad Laboratories, Hercules, CA), and 2% normal goat serum (Vector Laboratories, Inc., Burlingame, CA). Cells were incubated with primary antibody for 1 to 1.5 h at a concentration of 10 μg/ml (mAb 8H6) or a dilution of 1:500 (polyclonal anti-μ2 antiserum) and then washed two times. All washes and dilutions were done in PBS/BSA (1%)/Triton X-100 (1%)/normal goat serum (2%). Cells were then incubated with goat anti-mouse Alexa488 and goat anti-rabbit Alexa546 (Molecular Probes) and ToPro3, a dsDNA-specific dye (Molecular Probes), at a dilution of 1:1000 for 1 to 1.5 h. Cells were washed two times for 15 min with PBS/BSA (1%)/Triton X-100 (1%) and then two times for 10 min with PBS. Coverslips were washed with deionized water and then mounted on glass slides using ProLong Antifade (Molecular Probes).

Cells were visualized using a Zeiss confocal fluorescence microscope (Carl Zeiss), and the images were processed and coloured using Adobe Photoshop (Adobe Systems, Inc., San Jose, CA).

A1.2 Construction of M1 deletion mutants (by L. Brentano and B. Sherry)

Plasmid constructs 8BK44, 8BK34, 5X23I, 5X23P, 9B23B, 9B23M and 7E23F, generated as follows, contained inserts in the EcoRI site of pBluescript II S/K- (pBII, Stratagene, La Jolla, CA). M1 clones were generated from a virus stock of 8B (Sherry *et al.*, 1989), whose M1 gene was derived after *in vivo* passage of T1L. Briefly, M1-specific primers (5' GCG GAA TTC GCT ATT CGC GGT CAT GGC TTA 3' and 5' GCG GAA TTC GAT GAA GCG CGT ACG T 3', corresponding to bases 1-21 and 2289-2304, respectively, with added EcoRI sites) were used for RT-PCR (using Vent polymerase with exonuclease function; Promega) and the gel-purified EcoRI-digested product was inserted into the EcoRI site of pBII. An internal EcoRI site in the M1 gene allowed the selection of two clones, both with M1 inserted in a positive orientation relative to the T7 promoter: pBII-8BK44, containing the 2304 bp M1 gene; and pBII-8BK34, containing the 5' terminal 698 bp of M1. The other plasmid constructs were generated by restriction digest of these two plasmids.

APPENDIX TWO

OLIGONUCLEOTIDE PRIMERS

1. M1(-)1697 (corresponding to bases 1697-1713 of M1 gene)

   5' AGC TCT CCA CCC TCA CG 3'

2. S4(-)1001 (corresponding to bases 1001-1118 of S4 gene)

   5' CCA TCC CGT CAT GCC ACC 3'

3. M1(+)1133 (corresponding to bases 1133-1150 of M1 gene)

   5' CCG TCA AGT GTG CCT CCT 3'

4. S4(+)174 (corresponding to bases 174-191 of S4 gene)

   5' GCC GTC GTT TGC ATG CAT 3'

5. M1(+)710 (corresponding to bases 710-727 of M1 gene)

   5' TTG TTT TAC CAG CGC GTC 3'

6. M1(-)19 (corresponding to bases 1-19 of M1 gene)

   5' AGC CAT GAC CGC GAA TAG C 3'

7. M1(+)266 (corresponding to bases 266-283 of M1 gene)

   5' GAG TAT TGG AAA AGT AAT 3'

8. M1(+)806 (corresponding to bases 806-823 of M1 gene)

   5' GTT CAT ACT CCA TCA GAT 3'

9. M1(-)790 (corresponding to bases 773-790 of M1 gene)

   5' GTT TAT CAT GTC AGA GAC 3'

APPENDIX THREE

PUBLICATIONS ORIGINATING FROM THESIS RESEARCH AND CONTRIBUTIONS OF COLLABORATORS

The work presented in this thesis was modified from manuscripts published, submitted or in preparation for publication as described below:

Mbisa J.L., M.M. Becker, S. Zou, T.S. Dermody, and E.G. Brown (2000). Reovirus μ2 Protein Determines Strain-Specific Differences in the Rate of Viral Inclusion Formation in L929 Cells. ***Virology 272,*** 16-26 *(Front cover feature)* - Chapter three.

Mbisa J.L., and E.G. Brown. A Role for Protein Stability in Strain-Dependent Differences of μ2 Protein Expression in Reovirus-Infected L929 Cells. Submitted to *Virology* - Chapter four.

Mbisa J.L., D.A. Gray, and E.G. Brown. Reovirus utilizes the ubiquitin-proteasome pathway for assembly of inclusion bodies resulting in inhibition of ubiquitin-dependent proteolysis. Submitted to *Journal of Virology* - Chapter five.

Mbisa J.L., L. Brentano, B. Sherry, and E.G. Brown. Formation of Aggresome-like Structures by Recombinant Reovirus μ2 Protein. In preparation - Chapter six.

The following people have contributed to the experimental work presented in this thesis: M.M. Becker performed indirect immunofluorescence experiments in figures 3.2 and 3.3. L. Brentano made the M1 gene deletion mutants 8BK44, 8BK34, 5X23I, 5X23P, 9B23B, 9B23M and 7E23F. Quan Ngo directly conjugated FITC to the rabbit polyclonal anti-μ2 antibody.

APPENDIX FOUR

CURRICULUM VITAE

Education:

1991	B.Sc. in Medical Sciences **St. Andrews University**, St. Andrews, Scotland.
1991-1993	Clinical Medicine **Royal Free Hospital School of Medicine, University of London**, London, England.
1992	MB,BS Part V (a) Pathology examinations **University of London**, London, England.
1994	M.Sc. (Immunology of Infectious Diseases) **London School of Hygiene and Tropical Medicine, University of London**, London, England.
1996-present	Ph.D. in Microbiology and Immunology **University of Ottawa**, Ottawa, Canada.

University of Ottawa activities:

Cosupervision (with Dr. E.G. Brown) of 4th year B.Sc. Honours and summer undergraduate students and volunteer scientists (Department of BMI, University of Ottawa, 1998-2001).

Student representative Dept. of BMI Space Committee (1997-2000)

Publications:

Mbisa J.L., M.M. Becker, S. Zou, T.S. Dermody, and E.G. Brown (2000). Reovirus μ2 Protein Determines Strain-Specific Differences in the Rate of Viral Inclusion Formation in L929 Cells. ***Virology 272,*** 16-26. *(Front cover feature)*

Mbisa J.L., D.A. Gray, and E.G. Brown. Reovirus utilizes the ubiquitin-proteasome pathway for assembly of inclusion bodies resulting in inhibition of ubiquitin-dependent proteolysis. Submitted to ***Journal of Virology***.

Mbisa J.L., and E.G. Brown. A Role for Protein Stability in Strain-Dependent Differences of μ2 Protein Expression in Reovirus-Infected L929 Cells. Submitted to *Virology*.

In preparation:

Mbisa J.L., L. Brentano, B. Sherry, and E.G. Brown. Formation of Aggresome-like Structures by Recombinant Reovirus μ2 Protein.

Published conference abstracts and oral presentations:

Mbisa J.L., D.A. Gray, and E.G. Brown. (2001). Strain- and Clone-Dependent Differences in Expression and Stability of Reovirus μ2 Protein. 20th Annual American Society for Virology (ASV) Conference, July 21-25, University of Wisconsin-Madison, Madison, Wisconsin.

Brown E.G., H. Li, J.C. Bell, and **J.L. Mbisa.** (2001). Fatal Systemic Reovirus Infection Following Intranasal Infection of Adult PKR-Knockout Mice. 20th Annual American Society for Virology (ASV) Conference, July 21-25, University of Wisconsin-Madison, Madison, Wisconsin.

Brown, E.G., H. Li, **J.L. Mbisa,** J.C. Bell, and D.F. Stojdl. (2000). Inhibition of Reovirus Replication by the Murine Double-Stranded RNA Dependent Protein Kinase, PKR, Segregates with the M1 Gene. 7th International Symposium on Double-Stranded RNA Viruses, December 2-7, Palm Beach, Aruba.

Mbisa, J.L., M.M. Becker, B. Sherry, T.S. Dermody, and E.G. Brown. (2000). Reovirus μ2 Protein Localizes to Promyelocytic Leukemia Protein Oncogenic Domains in the Nucleus. 19th Annual American Society for Virology (ASV) Conference, July 8-12, Colorado State University, Fort Collins, Colorado, USA.

Becker, M.M., M.I. Goral, **J.L. Mbisa,** P.R. Hazelton, K.M. Coombs, E.G. Brown, and T.S. Dermody. (2000). Reovirus σNS Protein Nucleates Sites of Viral Replication. 19th Annual American Society for Virology (ASV) Conference, July 8-12, Colorado State University, Fort Collins, Colorado, USA.

Mbisa, J.L., and E.G. Brown. (1999). Quantification of μ2 Protein and mRNA Expression in L929 Cells Infected with Reovirus Type 1 Strain Lang (T1L) or Type 3 Strain Dearing (T3D). 18th Annual American Society for Virology (ASV) Conference, July 10-14, University of

Massachusetts, Amherst, Massachusetts, USA.

Mbisa, J.L., and E.G. Brown. (1998). Reovirus μ2 Protein Forms Inclusions in Infected and Transfected Cells in a Type Specific Manner Due Solely to Differences in the M1 Gene. 17th Annual American Society for Virology (ASV) Conference, July 11-15, University of British Columbia, Vancouver, British Columbia, Canada.

Mbisa, J.L., and E.G. Brown. (1997). The Study of Reovirus μ2 Protein Expression and Cellular Localization in L929 Cells. 47th Annual Canadian Society of Microbiologists (CSM) Conference, June 15-19, Universite Laval, Quebec City, Quebec, Canada.

Awards:

1988-1993 Commonwealth Scholarship.

Other Contributions:

Patent submitted December 2000, by E.G. Brown, J.C. Bell, D.F. Stojdl and **J.L. Mbisa**. The invention provides for methods of reducing the viability of tumour cells by infecting them with reassortant reoviruses or other recombinant viruses expressing the reovirus M1 gene.